

Noureen Siraj

**Heterogeneous Electron Transfer Rates of  
Organic Redox Systems Measured in Ionic  
Liquids**

DISSERTATION

Zur Erlangung des akademischen Grades eines DoktorIn  
der Naturwissenschaften

erreicht an der

Technischen Universität Graz

O. Univ.-Prof. Dipl.-Ing. Dr. rer. nat. Günter Grampp  
Institut für Physikalische und Theoretische Chemie  
Technische Universität Graz

2011



To my parents



## ACKNOWLEDGMENTS

Before I start even a word ahead, I pray to Almighty Allah for His incalculable love and kindness and thank Him for His continuous blessings and guidance for which have been a light for me to accomplish my desired goals in life. His disguised love has always been a spiritual and world source and support for me, which has made me able and capable at reaching the level of accomplishment of my final work.

The first person, who became the deepest source of inspiration and aspirations for me in my entire course of studies, is Prof. Dr. Günter Grampp, and I am highly indebted to him for being so good. He is a gentle, caring, dedicated and devout person whose inspiring guidance, professional attitude and kind nature remained a solid tool for me till the completion of this research work and the entire phase of my studies. He is no doubt a great teacher with selfless passion of teaching and a great zeal of enhancing the skills and knowledge of the students. Mrs. Jutta Grampp is most loveable, graceful, knowledgeable, decent, humane, kind and very soft spoken. She is a remarkable human being with an enlightened heart and the brightest mind.

I am also highly indebted and obliged to my devout and great teacher Prof. Dr. Stephan Landgraf, the most proficient, sincere, and encouraging teacher whose significant teachings and words are most valuable for me.

It is just not over; I offer personal thanks to Kenneth Rasmussen for his proper guidance, special attention and incredible help throughout my studies. I am very thankful for discussions during the writing of this thesis, which helped me in the improvement of the presentation and final selection of the thesis. He is not only the expert of his field but the beautiful human being too who is a role model for me. He is a person of high dignity and sublime merits and I salute them to their dignity and their unending support and guidance.

I am also very thankful and indebted to our respected Anne Marie Kelterer for her spiritual and generous cooperation, helpful suggestions and encouragement in matters pertaining to theoretical calculations. It is with her generous support that I have been able to finalize my assigned task in time.

I also want to appreciate the support and cooperation of Marion Hofmeister, Hilde Frissmuth, Helmut Eisenkoelbl and Herbert Lang for providing indispensable assistance and all necessary facilities for pursuing the course of study.

The loveliest people behind my entire success and achievements are my proud parents who did all their best to make me the best. They are the special people of God who provided me the first hand love and incalculable support and guidance, which enshrined my intellect with piety and beautiful knowledge. My parents are more than Angels and they could be counted amongst the best of Almighty Allah in this world and hereinafter. I have no words to say thanks to them except saying aloud "I love you papa and mama for always being so good!". Though my father left this immortal world before I could accomplish this task but he is still with me as earlier and keeps reminding me "Hey, I am always with you".

My wonderful brothers (Mairaj & Muhammad Fahad), my sweet Aisha bhabi, my kind and caring sisters especially Erum and loving Mehreen form a beautiful family of mine. After my superb parents, they are the true support behind all my achievements and accomplishments. They are too good. May Almighty Allah keep them happy and gay till they breathe the last and they find a beautiful place in all the worlds.

The people behind my achievement and success who could never be paid for but always respected, well honoured, obeyed and obliged are Pakistani community in Graz, and friends (Asma, Waseem, Farah and Sadia) whose prayers are always with me. I owe a favour and feel deep love and for their unanimous support, momentous encouragement and utmost care.

I am also very thankful to Higher Education Commission of Pakistan.

Finally, I extend my best feelings and thanks to my esteemed colleagues (Asim, Bobby, Faiza, Kunal, Sadia, Tahir, Tajamal, and Zahid), cherished friends specially my closest Zeb, Erum, Binsih, Sir Sajid and my neighbour Sir Tahir for contributing advices, valuable suggestions and comments during the course of the research.





## ABSTRACT

Five different imidazolium based room temperature ionic liquids (RTILs) have been used as solvents in electrochemical investigations. These RTILs have been selected to understand the role of solvation in various ILs consisting of different cation and anions.

To probe the behaviour of ionic liquids as electrochemical solvents, the cyclic voltammetry technique has been employed. Two special electrochemical cells have been constructed in order to reduce the cost of the experiments, one for room temperature measurements and another for temperature dependence studies. Heterogeneous electron transfer reactions have been studied in ionic liquids by using nine different organic acceptor (A) and five donor (D) systems.

The values of the diffusion coefficient and the heterogeneous electron transfer rate constant have been determined in ionic liquids and these results are compared with data from organic solvents. It was found that the electron transfer reaction is slow in ionic liquids because of their high viscosities. The obtained results compare well to literature data on similar experiments in ionic liquids. A further elaboration of the results was achieved by means of measurements in binary mixtures of ionic liquids and acetonitrile, from which the effect of solvent viscosity was investigated.

Additionally, temperature dependence measurements have been carried out in undried (as received) and dried (in high vacuum for one day at 50-60°C) RTILs, arriving at the corresponding activation energies.

Furthermore, computational work has been done to get values of inner sphere reorganization energies. Theoretical values of the outer sphere reorganization energies have been calculated and these values have been compared with the experimental results. Based on the experimental result, it was suggested that role of solvent reorientation in ionic liquids is different from that seen in traditional solvents.



## Zusammenfassung

An fünf unterschiedlichen Raumtemperaturionenlösungen (RTILs) als Lösungsmittel wurden elektrochemische Untersuchungen durchgeführt. Diese RTILs wurden ausgewählt, um den Einfluss der Solvation in Ionenlösungen aus unterschiedlichen Kationen und Anionen besser zu verstehen.

Zur Untersuchung des Verhaltens von Ionenlösungen als elektrochemische Lösungsmittel, wurde die zyklische Voltammetrie angewendet. Es wurden zwei spezielle elektrochemische Zellen konstruiert, eine für Raumtemperaturmessungen, die andere für temperaturabhängige Untersuchungen. Heterogene Elektronentransferreaktionen in Ionenlösungen wurden unter Verwendung von neun unterschiedlichen organischen Akzeptor (A) und fünf Donor (D) –Systemen. untersucht.

Bestimmt wurden Diffusionskoeffizienten und heterogene Elektronenübergangskonstanten in Ionenlösung und mit organischen Lösungsmitteln verglichen. Dabei wurde festgestellt, dass der Elektronenübergang in Ionenlösungen aufgrund hoher Viskosität langsam ist. Die erhaltenen Ergebnisse sind in guter Übereinstimmung mit Literaturdaten aus ähnlichen Untersuchungen an Ionenlösungen. Weitere Bestätigung der Ergebnisse wurde anhand binärer Mischungen von Ionenlösungen und Acetonitril erhalten. Anhand dieser Mischungen wurde der Einfluss der Lösungsmittelviskosität untersucht.

Zusätzlich wurden anhand temperaturabhängiger Messungen an handelsüblichen und speziell getrockneten (Hochvakuum, 50-60°C für einen Tag) RTILs, die entsprechenden Aktivierungsenergien bestimmt. .

Weiters wurden theoretische Modelle zur Berechnungen von Reorganisationsenergien angewendet. Die berechneten Werte für Reorganisationsenergien der äußeren Solvationshülle wurden mit den experimentellen Daten in Beziehung gesetzt. Das unterschiedliche Verhalten der Lösungsmittelorientierung in Ionenlösungen im Vergleich zu traditionellen Lösungsmitteln wurde anhand der experimentellen Ergebnisse diskutiert.



## CONTENTS

CHAPTER 1	Outline of the Thesis	1
CHAPTER 2.	Introduction	5
2.1	Electrochemical Reactions in Organic Solvents	5
2.2	Electrochemical Reaction in Ionic Liquids	7
2.3	This Work	8
2.4	Aim of the Study	10
2.5	Scope of the Work	10
CHAPTER 3.	Theory of Electrochemical Electron Transfer	15
3.1	Types of Electron Transfer Reaction	16
3.1.1	Inner Sphere Mechanism	16
3.1.2	Outer Sphere Mechanism	17
3.2	Electrochemical Rate Constant	17
3.2.1	Pre Exponential Factor	18
3.3	Activation Energy	21
3.4	The Reorganization Energy	21
3.4.1	Inner-shell Reorganization Energy	21
3.4.2	Outer-shell Reorganization Energy	22
3.4.3	The Mean Spherical Approximation	25
CHAPTER 4.	Room Temperature Ionic Liquids (RTILs)	29
4.1	History of Ionic liquids	29
4.2	Classification of RTILs	31
4.2.1	First Generation	31
4.2.2	Second Generation	31
4.2.3	Third Generation	31
4.3	Impurities in RTILs	32
4.3.1	Color	32
4.3.2	Organic and Inorganic Impurity	32
4.3.3	Halide Impurities	33
4.3.4	Water	34
4.4	Physicochemical Properties of RTILs	36
4.4.1	Melting Point and Glass Transition	36
4.4.2	Electrochemical Windows	38
4.4.3	Vapor Pressure and Thermal Stability	41
4.4.4	Viscosity	42
4.4.5	Surface Tension	46
4.4.6	Density	47
4.4.7	Conductivity	49
4.5	Application	51
CHAPTER 5.	Experimental	57
5.1	Ionic Liquids	57

5.2	Reagents	62
5.3	Sample Handling	65
5.4	Apparatus	65
5.4.1	NIR Spectrometer	65
5.4.2	iR Drop Measurements	65
5.4.3	Room Temperature Electrochemical Cell	65
5.4.4	Temperature Controlled Electrochemical Cell	66
5.4.5	Potentiostat and Software	67
5.4.6	Computational Work	67
5.5	Procedure	67
5.5.1	NIR Spectrum	67
5.5.2	iR drop Measurements	68
5.5.3	Room Temperature Measurements	68
5.5.4	Temperature Dependent Measurements	68
5.5.5	Measurements in Binary Mixtures	68
CHAPTER 6. The iR Drop		71
6.1	Factors Affecting the iR Drop	71
6.2	The iR Drop in Ionic Liquids	72
6.3	Calculation of the iR Drop	72
6.3.1	Concentration Dependent Measurements	73
6.3.2	Determination of Uncompensated Resistance by Bode Plots	77
6.3.3	Theoretical Calculation	80
CHAPTER 7. Electrochemical Kinetics at Room Temperature		83
7.1	Diffusion Coefficients	89
7.2	Heterogeneous Electron Transfer Rate Constants	103
7.3	Formal Potential	108
7.4	Measurements in Binary Mixture of Ionic Liquids and Acetonitrile	110
CHAPTER 8. Theoretical Calculations of Reorganization Energies		115
8.1	Computational Study for the Inner Sphere Reorganization Energies	115
8.1.1	Molden Software	117
8.1.2	ORCA Program	117
8.1.3	Comparison of Ionization potential and Electron Affinity	119
8.1.4	Relation between Homogeneous And Heterogeneous $\lambda_i$ Values	119
8.1.5	Temperature Correction	120
8.1.6	Discussion	121
8.2	Theoretical Calculations of the Outer Sphere Reorganization Energy	124
8.2.1	Pekar Factor	126
8.2.2	Marcus Approach for Outer Sphere Reorganization Energy	126
8.2.3	Hush Approach for Outer Sphere Reorganization Energy	128
8.2.4	Experimental Outer Sphere Reorganization Energies	130
8.2.5	Discussion	133

CHAPTER 9. Temperature Dependent Measurements	139
9.1 Temperature Dependent Properties	141
9.1.1 Refractive Index	142
9.1.2 Pekar Factor	142
9.1.3 Viscosity	143
9.2 Diffusion Coefficient	145
9.3 The Heterogeneous Electron Transfer Rate Constant	151
9.4 Activation Energy	153
9.5 Co-relation with Radius	159
9.6 Temperature Dependent Measurement in Undried ILs	161
CHAPTER 10. Conclusions	163

## CHAPTER 1 OUTLINE OF THE THESIS

The goals and some other interesting points along with detail explanation are discussed in different chapter of this thesis. In the following, I present a brief outline of the thesis. These results are presented in several different international conferences. Details are also available here.

### *Chapter 2:*

A brief introduction on the electrochemical kinetics in organic solvent is presented. Afterwards, the utilization of ionic liquids in electrochemistry is described. Finally, a short introduction of the current work is given. The advantages of this study are mentioned here. Different questions which have not been answered yet for ionic liquids are raised. The future of ionic liquids as electrochemical solvent is going to be present in this chapter.

### *Chapter 3:*

The theory of electron transfer is presented and different existing models are given. From these entire presented model, we used collision model for ionic liquids in the present study. The others concepts could not be tried because of the unavailability of the necessary data of ionic liquids.

### *Chapter 4:*

This chapter consists of the historical background of ionic liquids, their physicochemical properties as well as how these properties are affected by the presence of impurities in ionic liquids. Application of ionic liquids in many different areas is also mentioned. One can realized that how different data for a same ionic liquids exists in literature. This is because of the presence of moisture and other impurities.

### *Chapter 5:*

In chapter 5, the experimental conditions are discussed in detail. Different compounds and ionic liquids which are used in this study are composed with their structure. Purification of ionic liquids and the preparations of the solution is explained. The construction of both, a



cell for room temperature measurement and one for temperature studies is described in detail. Different experiments which are designed for this work are explained.

### *Chapter 6:*

Now onward results of different experiments which have been performed are presented in four different parts. This chapter describes the measurements of the iR drop. These measurements are made to get an idea about the quality of the custom made cell. Three different methods will be used for the determination of iR drop. First, concentration dependent measurements second are the uncompensated resistance through Bode plots and finally theoretical calculations.

### *Chapter 7:*

All room temperature measurements are compiled in this chapter. Different equations which are used to investigate the result are expressed here. The results of diffusion coefficients and heterogeneous electron transfer rate constants in ionic liquid are compared with those yielded in organic solvents. The results of binary mixture are also compiled here. These results have been presented:

- Cyclic voltammetric study of heterogeneous electron transfer rate constants of organic compounds in room temperature ionic liquids”  
Noureen Siraj, Günter Grampp, Stephan Landgraf  
2<sup>nd</sup> GOCH-Symposium 2009, Physikalische Chemie in Österreich, 23<sup>rd</sup> to 24<sup>th</sup> February 2009 at Innsbruck, Austria. (Poster presentation)
- “Cyclic voltammetric study of heterogeneous electron transfer rate constants of organic compounds in room temperature ionic liquids”  
Noureen Siraj, Günter Grampp, Stephan Landgraf  
108<sup>th</sup> Bunsen Conference 21<sup>st</sup> to 23<sup>rd</sup> May 2009 at Cologne, Germany (Poster presentation)
- “Cyclic voltammetric study of heterogeneous electron transfer rate constants of organic compounds in room temperature ionic liquids”  
Noureen Siraj, Günter Grampp, Stephan Landgraf  
5<sup>th</sup> ECHEMS Meeting, 7<sup>th</sup> to 10<sup>th</sup> June 2009 at Weingarten, Germany. (Poster presentation)
- "Mass transport and electrode kinetics parameters in room temperature ionic liquids (RTILs) and in its binary mixture with organic solvent"  
Stephan Landgraf, Noureen Siraj, Günter Grampp  
3<sup>rd</sup> EuChems Chemistry Congress, Chemistry-the Creative Force, 29<sup>th</sup> August to 2<sup>nd</sup> September 2010, Nürnberg, Germany. (Poster presentation)

*Chapter 8:*

One can find a detail description of theoretical calculation of inner and outer sphere reorganization energies in this section. The Nelsen-method is used for the calculation of inner sphere reorganization energy. Two different models are used to get the theoretical values for outer sphere reorganization energy in ionic liquids. The publications of this chapter along with some previous results are

- “What is the physical meaning of the outer sphere reorganization energy for electron transfer reactions in ionic liquids?”  
Günter Grampp, Noureen Siraj, Stephan Landgraf  
6<sup>th</sup> ECHEMS Meeting, 20<sup>th</sup> to 23<sup>rd</sup> June 2010, Sandbjerg Estate, (Poster presentation)
- “Is Marcus Theory applicable to Electron Transfer reactions in Ionic Liquids?”  
Günter Grampp, Stephan Landgraf, Noureen Siraj  
5<sup>th</sup> ECHEMS Meeting, 7<sup>th</sup> to 10<sup>th</sup> June 2009 at Weingarten, Germany. (Oral presentation)

*Chapter 9:*

Measurements at different temperature are reported here. The values of activation energies achieved through these measurements for different compounds in ionic liquids are given. Different interionic interaction in ionic liquids is also discussed here. The presentations of this chapter are

- “Temperature dependent heterogeneous electron transfer in room temperature Ionic Liquids”  
Noureen Siraj, Günter Grampp, Stephan Landgraf  
Austrian Chemistry Days, 24<sup>th</sup> to 27<sup>th</sup> August 2009 at Vienna, Austria. (Poster presentation)
- “Kinetics of heterogeneous electron transfer reactions in room temperature ionic liquids”  
Noureen Siraj, Günter Grampp, Stephan Landgraf  
Modern Electroanalytical Methods 2009, 9<sup>th</sup> to 13<sup>th</sup> December 2009 at Prague, The Czech Republic. (Poster presentation)
- “Cyclic voltammetric studies on the kinetics of heterogeneous electron transfer reactions in room temperature ionic liquids”  
Günter Grampp, Noureen Siraj, Stephan Landgraf  
10<sup>th</sup> International Symposium on Kinetics in Analytical Chemistry, 2<sup>nd</sup> to 4<sup>th</sup> December 2009 at Cape Town, South Africa. (Oral presentation)

- "Kinetics of heterogeneous electron transfer reactions in ionic liquids: Effects of temperature and solvent"  
Stephan Landgraf, Noureen Siraj, Günter Grampp  
Chemiedozententagung 2010, Gießen, Germany, 8th to 10th March 2010
- "Heterogeneous electron transfer rates and diffusion coefficients of various organic systems measured in room temperature ionic liquids (RTILs) and in its binary mixture with acetonitrile".  
Noureen Siraj, Günter Grampp, Stephan Landgraf  
EUCHEM 2010, Conference on Molten Salts and Ionic Liquids, 14<sup>th</sup> to 19<sup>th</sup> March 2010, Bamberg, Germany. (Poster presentation)
- "Kinetics of heterogeneous electron transfer reactions in ionic liquids: effects of temperature and solvent"  
Noureen Siraj, Günter Grampp, Stephan Landgraf  
109<sup>th</sup> Bunsen Conference 13<sup>th</sup> to 15<sup>th</sup> May 2010 at Bielefeld, Germany (Poster presentation)
- "Electrochemical kinetics in ionic Liquids"  
Noureen Siraj, Günter Grampp, Stephan Landgraf  
2<sup>nd</sup> International Workshop on Physical Chemistry and Material Physics, 1<sup>st</sup> to 4<sup>th</sup> June 2010 at Casta-Papiernicaka, Slovak Republic (Oral presentation)
- "Effect of solvent and temperature on heterogeneous electron transfer rate constant"  
Noureen Siraj, Günter Grampp, Stephan Landgraf  
6<sup>th</sup> ECHEMS Meeting, 20<sup>th</sup> to 23<sup>rd</sup> June 2010, Sandbjerg Estate, Denmark (Oral presentation)
- "Electrochemical kinetics in room temperature ionic Liquids"  
Noureen Siraj, Günter Grampp, Stephan Landgraf  
218<sup>th</sup> ECS Meeting, Las Vegas, Nevada, USA (Oral presentation)

### *Chapter 10:*

The results obtained through room temperature measurements in pure ionic liquids, in binary mixture and by temperature dependence measurement will be discussed. The drawback of the outer sphere reorganization energies calculated by theoretical calculation is explained.

## CHAPTER 2. INTRODUCTION

### 2.1 Electrochemical Reactions in Organic Solvents

The study of the rate constants of electron transfer reactions at the electrode-electrolyte interface is a fundamental issue in electrochemistry. Information about the kinetics of the reaction at the surface of the electrode is of great importance for the basic understanding of the kinetics of the heterogeneous electron transfer reaction<sup>1-3</sup>. Heterogeneous electron transfer reactions are generally quite fast because the energy barrier of electron transfer is associated with solvent reorientation (outer sphere reorganization energy). The contribution of the inner sphere reorganization energy is considered to be small<sup>4</sup> for such reactions. There are many factors which can affect the magnitude of rate constant for a given reactant such as the nature of solvent<sup>5-7</sup>, the supporting electrolyte and the electrode material<sup>8-9</sup>.

The effect of the solvent on the kinetics of the heterogeneous electron transfer rate constant,  $k_{\text{het}}$ , has got considerable attention for years<sup>10-11</sup>. In the case of electrode reactions it was first studied by Frumkin<sup>12</sup>.

The electro-reduction of simple inorganic ions<sup>13-14</sup>, organic compounds<sup>15, 16</sup> as well as both electrooxidation and electroreduction of transition metal complexes<sup>17</sup> have been studied. Most of the organic redox couples involve simple electron transfer processes; these were used as models to test the predictions of Marcus theory<sup>18-19</sup>.

The importance of solvent dynamical properties in electron transfer reactions have been recognized and elaborated in 1980s<sup>20</sup>. At the same time, solvent effects on the kinetics parameters for simple electron transfer reaction have been studied for both homogeneous<sup>21</sup> and heterogeneous<sup>6-7</sup> process in a wide variety of solvents. Both homogeneous and heterogeneous kinetic data correlates quite well with solvent the relaxation time<sup>22-23</sup>.

Another way to study the solvent effects on the kinetics of simple redox couples is, by analyzing its dependence on the viscosities of the medium<sup>2</sup>.

Physical models have been presented to interpret the effect of specific solvation on the thermodynamics and kinetics of electron transfer<sup>24</sup>. It is now well known that the solvent influences the kinetics of such reactions in two ways i.e. through its dependence

on the magnitude of the activation energy, as it recognized by the Marcus dielectric continuum treatment,<sup>25</sup> and its effect on the pre-exponential factor<sup>11,26</sup>.

Fawcett<sup>27</sup> provided strong evidence that the pre-exponential factor of the electron transfer rate constant is solvent dependent. He<sup>28</sup> found that the Gibbs energy of activation depends on the solvent's dielectric properties. Fawcett et al. also further determined the importance of solvent dynamical effects on the kinetic data and compared results for homogeneous and heterogeneous reactions<sup>29</sup>.

Multiple correlations have been performed for different simple redox couples by plotting the logarithm of standard rate constants versus the logarithm of the longitudinal solvent relaxation times<sup>30,31</sup> and Pekar factor,  $\gamma$ , as the independent variables in order to separate the solvent effect upon the pre-exponential factor and the activation Gibbs energy respectively<sup>10,32</sup>. This type of dependence was also predicted by theoretical investigations of electron transfer reactions<sup>33-34</sup>. The dielectric dynamic properties of the solvent may exert a much stronger influence on the rate of heterogeneous charge transfer than the static properties<sup>35-36</sup>. It has been found that as shorter the dielectric relaxation time of a given solvent,  $\tau_D$ , the faster is the electrode reaction. This conclusion has been confirmed by Weaver and Gennett<sup>6,37</sup> in the case of the electrode reaction of metallocenes.

The changes in the potentials of compounds with the nature of the solvent have been discussed in terms of donor-acceptor interactions<sup>26</sup>. Fernandez et al.<sup>10</sup> studied solvent effects on  $k_{\text{het}}$ , anodic transfer coefficients and formal potentials. They also determined thermodynamic and kinetic parameters<sup>38</sup>.

Solvent effects on the electrode kinetics of simple redox couples have also been studied by using solvent mixtures<sup>39</sup>.

The effect of the nature and concentration of the supporting electrolyte has been the subject of many investigations<sup>24,40-41</sup>. The observed values of  $k_{\text{het}}$  decrease with an increase in cation size of electrolytes<sup>3,42</sup>.

Theoretical treatments<sup>43</sup> imply that the nature of the electrode material should not markedly influence the rates of heterogeneous electron transfer process. Amatore<sup>3</sup> suggested that electron transfer kinetics become much slower on solid metallic electrode than a mercury and very much depend upon pretreatment of the solid electrode<sup>44</sup>. Capon and Parson<sup>45</sup> examined the kinetics at six solid metal electrodes and observed that standard rate constants values were almost constant. Samuelsson et al<sup>40</sup> observed the same behaviour. Rosanske and Evans<sup>9</sup> later reexamined the same quinone system and

observed charge transfer rate constant which differ by several orders of magnitude from those reported by Capon and Parson. Evans concluded that rate constant show small but significant dependence on electrode metal.

Compton et al.<sup>46</sup> demonstrated the dependence of  $k_{\text{het}}$  on the hydrodynamic radius according to the Marcus theory. Many different  $k_{\text{het}}$  values can be found in literature for the same system<sup>47</sup> because different electrochemical methods, different supporting electrolytes with different concentrations and different electrodes were used to study the same system.

## 2.2 Electrochemical Reaction in Ionic Liquids

Recently, ionic liquids have been employed as solvent for heterogeneous electron transfer reactions<sup>48-53</sup>. Room temperature ionic liquids (RTILs) are of growing interest due to their outstanding solvent properties i.e. negligible vapor pressure, high conductivity, large electrochemical window and also they are designable. These unique properties allow us to use these ionic liquids in electrochemistry in the place of both solvent and supporting electrolyte because of their high conductivity, there is no need to add supporting electrolyte. A significant amount of work has focused on measuring diffusion coefficients of simple redox system and comparing the results to those previously reported in more traditional organic solvents<sup>54-57</sup>. It has been observed for ferrocene that the value of diffusion coefficient is concentration dependent, although no definite explanation could be provided<sup>58</sup>.

Evan et al.<sup>59</sup> investigated the diffusion coefficient of  $N,N,N',N'$ -tetraalkyl-para-phenyldiamines (TAPDs) in a series of ionic liquids incorporating the bis(trifluoro methanesulfonylamide)  $[NTF_2^-]$  anions and observed that slowest diffusion in the most viscous ionic liquid, in accordance with Walden's rule. It has also been suggested that variation of diffusion coefficient with temperature follows Arrhenius behaviour<sup>48,57</sup>. They found a linear relationship between diffusion coefficient and solvent viscosity as observed in traditional solvent<sup>57</sup>.

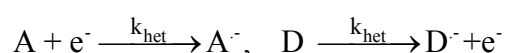
Lagrost et al.<sup>55</sup> suggested that the rate constant of electron transfer is less in ionic liquid than in acetonitrile due to greater amount of reorganization, by analogy with Marcus theory. Hapiot et al.<sup>49</sup> also reported that  $k_{\text{het}}$  values decreased by two orders of magnitude in RTILs than in acetonitrile. The decrease in  $k_{\text{het}}$  values indicates higher solvent reorganization in RTILs during the charge transfer although he could not give

any experimental prove for this. Fietkau et al<sup>60</sup> also observed the decrease in  $k_{\text{het}}$  for a series of ferrocene derivatives and they also found there was no correlation between  $k_{\text{het}}$  and hydrodynamic radius in RTILs. Doherty and coworkers<sup>53,61</sup> also measured heterogeneous rate constants for the reduction of benzaldehyde in two different RTILs. For the first time<sup>62</sup>, cyclic voltammetry for the reduction and oxidation of both  $\text{PCl}_3$  and  $\text{POCl}_3$  has been shown in RTILs because these compounds were not stable in conventional aprotic solvents.

## 2.3 This Work

In the present work,  $k_{\text{het}}$  of organic molecules have been measured by cyclic voltammetry in five different room temperature ionic liquids (RTILs): 1-ethyl-3-methylimidazolium tetrafluoroborate [emim][ $\text{BF}_4$ ], 1-butyl-3-methylimidazolium trifluorosulphane [bmim][OTf] ([bmim][ $\text{CF}_3\text{SO}_3$ ]), 1-butyl-3-methylimidazolium tetrafluoroborate [bmim][ $\text{BF}_4$ ] 1-butyl-3-methylimidazolium hexafluorophosphate [bmim][ $\text{PF}_6$ ] and 1-octyl-3-methylimidazolium tetrafluoroborate [omim][ $\text{BF}_4$ ]. These ionic liquids have been selected to investigate the effect of the anion when the cation is constant in ionic liquids and vice versa. The purity of ionic liquids is a serious issue and hence before starting any measurements it is checked. The amount of moisture impurity is analyzed by NIR and halide ion impurity is checked by cyclic voltammetry.

Various acceptor (A) and donor (D) systems:



like methylbenzoquinone, bromanil, chloranil, 2,5-dimethylbenzoquinone, 2,6-dimethylbenzoquinone, duroquinone, methylviologen, ethylviologen, tetracyanoethylene, ferrocene, p-phenylenediamine, N,N,N',N'-tetraalkyl-para-phenyldiamines, tetrathiafulvalene, 2,2,6,6-tetramethylpiperidinyloxy radical and 4-hydroxy-2,2,6,6-tetramethylpiperidinyloxy radical are used. For all systems, activation energies, diffusion coefficients and half wave potentials versus Ag/AgCl are determined. The results obtained in RTILs are compared with those found in organic solvents<sup>58,60</sup>. Binary mixtures of ionic liquid and acetonitrile is also used to determine the heterogeneous electron transfer rate constant and diffusion coefficients at room temperature. These experiments were designed to examine the effect of viscosity on the

corresponding rate constant and diffusion coefficient because the viscosity of the mixture is changing as the contents of acetonitrile and ionic liquids is changed.

Temperature dependent measurements are carried out for every redox system. Values of diffusion coefficients and heterogeneous electron transfer rate constants are determined at each temperature. The activation energies are determined in the ionic liquids. These activation energies values are used to provide the meaning of reorganization. The outer sphere reorganization energies according to Marcus and Hush are also estimated.

All electrochemical measurements are performed in custom made cyclic voltammetric cell for small amounts. Because of the high cost of ionic liquids, it's not a good idea to use common cyclic voltammetry cell containing 25-50 ml of solution, to do electrochemical measurements. It is a goal of the study to build an electrochemical cell for carrying only small volume of ionic liquids through which trustful results can be obtained. The first concept of this cell was given by Compton<sup>50</sup>, which is improved in our construction by introducing a three electrode assembly. Two different cells is prepared, one for working at room temperature and the second one to work at variable temperature. The  $iR$  drop of the cell is measured by various methods, to check the quality of the cell. Various different concentrations of ferrocene is prepared and cyclic voltammetric experiments are performed at different scan rate for each concentration. First, the response of the width of peak potential is analyzed by changing scan rates at different concentration. Uncompensated resistance is also determined by making Bode-plots for each ionic liquid. Theoretical calculation is done to get the value of uncompensated resistance as well.

For the calculation of the inner sphere reorganization energy, quantum mechanical calculations are carried out by using ORCA programme. Molden software is employed to build the starting geometry of the molecule. This software is also used to check the optimized geometry of the molecule. Inner sphere reorganization energy is determined by a method given by Nelsen<sup>63</sup> which is simply a difference of ionization potential and electron affinity.

It is attempted to understand the role of outer sphere reorganization energies. For this, theoretical calculations are done in order to calculate the value of the outer sphere reorganization energies. These calculations are made by using the published values of dielectric constants. The concept of dielectric constants is discussed. Two different models, Marcus and Hush are employed for these calculations. Two different radius model i.e the ellipsoidal and spherical models are taken into account.



## 2.4 Aim of the Study

The aim of this work is to understand the behaviour of ionic liquids as electrochemical solvents. The viscosity of ionic liquids is very high which give a great advantage to do experiments in a broader range of temperature. The costs of experiment are also taken into account that's why special cell is prepared. The results for heterogeneous electron transfer rate constant and diffusion coefficient are analyzed in the frame-work of existing theories. Marcus theory is applied to get the value of activation energy from the rate constants  $k_{\text{het}}$ . The main problem arising is to understand the role of the solvent reorganization energy  $\lambda_0$ . Commonly used expressions are not applicable to ionic liquids, therefore improvements in the already available theories are necessary.

## 2.5 Scope of the Work

Ionic liquids have very unique properties as a solvent and they are environmentally friendly. These can be used instead of many organic volatile solvent. It provides a great opportunity to do electrochemical measurements with many different compounds which were not possible in conventional organic solvent. There are many question are still open in this field. To understand the interaction of ionic liquids with different compounds, their dielectric response and suitable changes in existing theories are necessary.

1. Kojima, H.; Bard, A. J. Determination of Rate Constants for the Electroreduction of Aromatic Compounds and Their Correlation with Homogeneous Electron Transfer Rates. *J. Am. Chem. Soc.* **1975**, *97*, 6317-6324.
2. Zhang, X.; Leddy, J.; Bard, A. J. Dependence of Rate Constants of Heterogeneous Electron Transfer Reactions on Viscosity. *J. Am. Chem. Soc.* **1985**, *107*, 3719-3721.
3. Amatore, C.; Savéant, J. M.; Tessier, D. Kinetics of Electron Transfer to Organic Molecules at Solid Electrodes in Organic Media. *J. Electroanal. Chem.* **1983**, *146*, 37-45.
4. Frontana, C.; Gonzalez, I. Revisiting the Effects of the Molecular Structure in the Kinetics of Electron Transfer of Quinones: Kinetic Differences in Structural Isomers. *J. Mex. Chem. Soc.* **2008**, *52*, 11-18.
5. Fawcett, W. R.; Jaworski, J. S. Effect of Solvent on the Kinetics of Electroreduction of Organic Molecules in Nonaqueous Media. *J. Phys. Chem.* **1983**, *87*, 2972-2976.

6. Weaver, M. J.; Gennett, T. Influence of Solvent Reorientation Dynamics Upon the Kinetics of Some Electron-Exchange Reactions. *Chemical Physics Letters* **1985**, *113*, 213-218.
7. Rüssel, C.; Jaenicke, W. Heterogeneous Electron Transfer to Quinones in Aprotic Solvents. Part II. The Dependence on Solvent and Supporting Electrolyte. *J. Electroanal. Chem.* **1984**, *180*, 205-217.
8. Fawcett, W. R. The Role of the Metal and the Solvent in Simple Heterogeneous Electron Transfer Reactions. *Electrochim. Acta* **1997**, *42*, 833-839.
9. Rosanske, T. W.; Evans, D. H. Rate Constants for the Electrode Reactions of Some Quinones in Aprotic Media at Platinum, Gold and Mercury Electrodes. *J. Electroanal. Chem.* **1976**, *72*, 277-285.
10. Fernández, H.; Zón, M. A. Solvent Effects on the Kinetics of Heterogeneous Electron Transfer Processes. The Tmpd/Tmpd<sup>+</sup> Redox Couple. *J. Electroanal. Chem.* **1992**, *332*, 237-255.
11. McManis, G. E.; Golovin, M. N.; Weaver, M. J. Role of Solvent Reorganization Dynamics in Electron-Transfer Processes. Anomalous Kinetic Behavior in Alcohol Solvents. *J. Phys. Chem.* **1986**, *90*, 6563-6570.
12. Frumkin, A. N.; Nikolaeva-Fedorovich, N. V.; Berezina, N. P.; Keis, K. E. The Electroreduction of the S<sub>2</sub>O<sub>8</sub><sup>2-</sup> Anion. *J. Electroanal. Chem.* **1975**, *58*, 189-201.
13. Fawcett, W. R.; Opallo, M. Possible Experimental Evidence for Molecular Solvation Effects in Simple Heterogeneous Electron-Transfer Reactions. *J. Phys. Chem.* **1992**, *96*, 2920-2924.
14. Baranski, A.; Fawcett, W. R. Medium Effects in the Electroreduction of Alkali Metal Cations. *J. Electroanal. Chem.* **1978**, *94*, 237-240.
15. Kapturkiewicz, A. Rate Constants of the Electrode Reactions of Some Quinones in Hexamethylphosphoramide Solutions at Mercury Electrodes. *J. Electroanal. Chem. Interfacial Electrochem.* **1986**, *201*, 205-209.
16. Jacob, S. R.; Hong, Q.; Coles, B. A.; Compton, R. G. Variable-Temperature Microelectrode Voltammetry: Application to Diffusion Coefficients and Electrode Reaction Mechanisms. *J. Phys. Chem. B* **1999**, *103*, 2963-2969.
17. Tsierkezos, N. G. Kinetic Investigation of the Electrochemical Oxidation of Bis(Benzene)Chromium(0) in Diethyl Ketone/N,N-Dimethylformamide. *Journal of Solution Chemistry* **2008**, *37*, 1437-1448.
18. Grampp, G.; Jaenicke, W. ESR-Spectroscopic Investigation of the Homogeneous Electron Transfer Reactions between Substituted P-Phenylenediamines and Quinonediimines, and the Validity of Marcus' Theory. I. Measurements at 293 K. *Berichte der Bunsengesellschaft/Physical Chemistry Chemical Physics* **1984**, *88*, 325-334.
19. Grampp, G.; Jaenicke, W. ESR-Spectroscopic Investigation of the Homogeneous Electron Transfer Reactions between Substituted P-Phenylenediamines and Quinonediimines, and the Validity of Marcus' Theory. II. Temperature Dependence and Activation Parameters. *Berichte der Bunsengesellschaft/Physical Chemistry Chemical Physics* **1984**, *88*, 335-340.
20. Marcus, R. A.; Sumi, H. Solvent Dynamics and Vibrational Effects in Electron Transfer Reactions. *J. Electroanal. Chem.* **1986**, *204*, 59-67.
21. Nielson, R. M.; McManis, G. E.; Neal Golovin, M.; Weaver, M. J. Solvent Dynamical Effects in Electron Transfer: Comparisons of Self-Exchange Kinetics for Cobaltocenium-Cobaltocene and Related Redox Couples with Theoretical Predictions. *J. Phys. Chem.* **1988**, *92*, 3441-3450.

22. Opałó, M.; Kapturkiewicz, A. Solvent Effect on the Kinetics of the Electrooxidation of Phenothiazine. *Electrochim. Acta* **1985**, *30*, 1301-1306.
23. Harrer, W.; Grampp, G.; Jaenicke, W. Dependence of the True Rate Constant of Homogeneous Electron Transfer on Solvent Relaxation Time and Viscosity. *J. Electroanal. Chem.* **1986**, *209*, 223-226.
24. Fernández, H.; Zón, M. A. Determination of the Kinetic and Activation Parameters for the Electro-Oxidation of N,N,N', N'-Tetramethyl-P-Phenylenediamine (Tmpd) in Acetonitrile (Acn) by Chronocoulometry and Other Electrochemical Techniques. *J. Electroanal. Chem.* **1990**, *283*, 251-270.
25. Marcus, R. A. On the Theory of Electron-Transfer Reactions. Vi. Unified Treatment for Homogeneous and Electrode Reactions. *The Journal of Chemical Physics* **1965**, *43*, 679-701.
26. Opałó, M. The Solvent Effect on the Electrooxidation of 1,4-Phenylenediamine. The Influence of the Solvent Reorientation Dynamics on the One-Electron Transfer Rate. *J. Chem. Soc., Faraday Trans. 1* **1986**, *82*, 339-347.
27. Fawcett, W. R.; Opałó, M. The Kinetics of Heterogeneous Electron Transfer Reactions in Polar Solvents. *Angewandte Chemie (International Edition in English)* **1994**, *33*, 2131-2143.
28. Fawcett, W. R.; Foss Jr, C. A. The Analysis of Solvent Effects on the Kinetics of Simple Heterogeneous Electron Transfer Reactions. *J. Electroanal. Chem.* **1988**, *252*, 221-229.
29. Fawcett, W. R.; Foss Jr, C. A. Solvent Effects on Simple Electron Transfer Reactions. A Comparison of Results for Homogeneous and Heterogeneous Systems. *J. Electroanal. Chem.* **1989**, *270*, 103-118.
30. Kapturkiewicz, A.; Jaenicke, W. Comparison between Heterogeneous and Homogeneous Electron Transfer in P-Phenylenediamine Systems. *J. Chem. Soc., Faraday Trans. 1* **1987**, *83*, 2727-2734.
31. Clegg, A. D.; Rees, N. V.; Klymenko, O. V.; Coles, B. A.; Compton, R. G. Marcus Theory of Outer-Sphere Heterogeneous Electron Transfer Reactions: Dependence of the Standard Electrochemical Rate Constant on the Hydrodynamic Radius from High Precision Measurements of the Oxidation of Anthracene and Its Derivatives in Nonaqueous Solvents Using the High-Speed Channel Electrode. *J. Am. Chem. Soc.* **2004**, *126*, 6185-6192.
32. Fawcett, W. R.; Foss Jr, C. A. Role of the Solvent in the Kinetics of Heterogeneous Electron and Ion Transfer Reactions. *Electrochim. Acta* **1991**, *36*, 1761-1765.
33. Alexandrov, I. V. Physical Aspects of Charge Transfer Theory. *Chemical Physics* **1980**, *51*, 449-457.
34. Zusman, L. D. The Theory of Transitions between Electronic States. Application to Radiationless Transitions in Polar Solvents. *Chemical Physics* **1983**, *80*, 29-43.
35. Sahami, S.; Weaver, M. J. Solvent Effects on the Kinetics of Simple Electrochemical Reactions. Part I. Comparison of the Behavior of Cobalt(II)/(I) Tris(Ethylenediamine) and Ammine Couples with the Predictions of Dielectric Continuum Theory. *J. Electroanal. Chem. Interfacial Electrochem.* **1981**, *124*, 35-51.
36. Kapturkiewicz, A.; Opałó, M. Medium Effect in the Electroreduction of Nitromesitylene. *J. Electroanal. Chem.* **1985**, *185*, 15-28.
37. Kapturkiewicz, A.; Behr, B. Voltammetric Studies of Co(Salen) and Ni(Salen) in Nonaqueous Solvents at Pt Electrode. *Inorganica Chimica Acta* **1983**, *69*, 247-251.

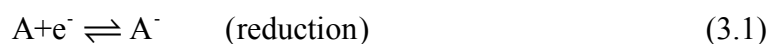
38. Marcela B. Moressi; Zón, M. A.; Fernández, H. The Determination of Thermodynamic and Heterogeneous Kinetic Parameters of the Tmpd/Tmpd<sup>+</sup> Redox Couple in Tetrahydrofuran and N-Butanol Using Ultramicroelectrodes. Quasi Steady-State Voltammetry *JOURNAL OF THE BRAZILIAN CHEMICAL SOCIETY* **1994**, *5*, 167-172.
39. Bhatti, N. K.; Subhani, M. S.; Khan, A. Y.; Qureshi, R.; Rahman, A. Heterogeneous Electron Transfer Rate Constants of Viologen at a Platinum Disk Electrode. *Turk. J. Chem.* **2005**, *29*, 659-668.
40. Samuelsson, R.; Sharp, M. The Effect of Electrode Material on Redox Reactions of Quinones in Acetonitrile. *Electrochim. Acta* **1978**, *23*, 315-317.
41. Baránski, A.; Fawcett, W. R. Medium Effects in the Electroreduction of Cyanobenzenes. *J. Electroanal. Chem.* **1979**, *100*, 185-196.
42. Petersen, R. A.; Evans, D. H. Heterogeneous Electron Transfer Kinetics for a Variety of Organic Electrode Reactions at the Mercury-Acetonitrile Interface Using Either Tetraethylammonium Perchlorate or Tetraheptylammonium Perchlorate Electrolyte. *J. Electroanal. Chem.* **1987**, *222*, 129-150.
43. Parsons, R. The Kinetics of Electrode Reactions and the Electrode Material. *Surface Science* **1964**, *2*, 418-435.
44. Corrigan, D. A.; Evans, D. H. Cyclic Voltammetric Study of Tert-Nitrobutane Reduction in Acetonitrile at Mercury and Platinum Electrodes. Observation of a Potential Dependent Electrochemical Transfer Coefficient and the Influence of the Electrolyte Cation on the Rate Constant. *J. Electroanal. Chem.* **1980**, *106*, 287-304.
45. Capon, A.; Parsons, R. The Rate of a Simple Electron Exchange Reaction as a Function of the Electrode Material\*. *J. Electroanal. Chem.* **1973**, *46*, 215-222.
46. Rees, N. V.; Clegg, A. D.; Klymenko, O. V.; Coles, B. A.; Compton, R. G. Marcus Theory for Outer-Sphere Heterogeneous Electron Transfer: Predicting Electron-Transfer Rates for Quinones. *J. Phys. Chem. B* **2004**, *108*, 13047-13051.
47. Clegg, A. D.; Rees, N. V.; Klymenko, O. V.; Coles, B. A.; Compton, R. G. Marcus Theory of Outer-Sphere Heterogeneous Electron Transfer Reactions: High Precision Steady-State Measurements of the Standard Electrochemical Rate Constant for Ferrocene Derivatives in Alkyl Cyanide Solvents. *J. Electroanal. Chem.* **2005**, *580*, 78-86.
48. Matsumiya, M.; Terazono, M.; Tokuraku, K. Temperature Dependence of Kinetics and Diffusion Coefficients for Ferrocene/Ferricenium in Ammonium-Imide Ionic Liquids. *Electrochim. Acta* **2006**, *51*, 1178-1183.
49. Lagrost, C.; Preda, L.; Volanschi, E.; Hapiot, P. Heterogeneous Electron-Transfer Kinetics of Nitro Compounds in Room-Temperature Ionic Liquids. *J. Electroanal. Chem.* **2005**, *585*, 1-7.
50. Schroder, U.; Wadhawan, J. D.; Compton, R. G.; Marken, F.; Suarez, P. A. Z.; Consorti, C. S.; de Souza, R. F.; Dupont, J. Water-Induced Accelerated Ion Diffusion: Voltammetric Studies in 1-Methyl-3-[2,6-(S)-Dimethylocten-2-Yl]Imidazolium Tetrafluoroborate, 1-Butyl-3-Methylimidazolium Tetrafluoroborate and Hexafluorophosphate Ionic Liquids. *New J. Chem.* **2000**, *24*, 1009-1015.
51. Hapiot, P.; Lagrost, C. Electrochemical Reactivity in Room-Temperature Ionic Liquids. *Chem. Rev. (Washington, DC, U. S.)* **2008**, *108*, 2238-2264.
52. Silvester, D. S.; Compton, R. G. Electrochemistry in Room Temperature Ionic Liquids: A Review and Some Possible Applications. *Z. Phys. Chem. (Muenchen, Ger.)* **2006**, *220*, 1247-1274.

53. Brooks, C. A.; Doherty, A. P. Electrogenerated Radical Anions in Room-Temperature Ionic Liquids. *J. Phys. Chem. B* **2005**, *109*, 6276-6279.
54. Fuller, J.; Carlin, R. T.; Osteryoung, R. A. The Room-Temperature Ionic Liquid 1-Ethyl-3-Methylimidazolium Tetrafluoroborate: Electrochemical Couples and Physical Properties. *J. Electrochem. Soc.* **1997**, *144*, 3881-3886.
55. Lagrost, C.; Carrie, D.; Vaultier, M.; Hapiot, P. Reactivities of Some Electrogenerated Organic Cation Radicals in Room-Temperature Ionic Liquids: Toward an Alternative to Volatile Organic Solvents? *J. Phys. Chem. A* **2003**, *107*, 745-752.
56. Evans, R. G.; Wain, A. J.; Hardacre, C.; Compton, R. G. An Electrochemical and ESR Spectroscopic Study on the Molecular Dynamics of Tempo in Room Temperature Ionic Liquid Solvents. *ChemPhysChem* **2005**, *6*, 1035-1039.
57. Evans, R. G.; Klymenko, O. V.; Price, P. D.; Davies, S. G.; Hardacre, C.; Compton, R. G. A Comparative Electrochemical Study of Diffusion in Room Temperature Ionic Liquid Solvents Versus Acetonitrile. *ChemPhysChem* **2005**, *6*, 526-533.
58. Eisele, S.; Schwarz, M.; Speiser, B.; Tittel, C. Diffusion Coefficient of Ferrocene in 1-Butyl-3-Methylimidazolium Tetrafluoroborate - Concentration Dependence and Solvent Purity. *Electrochim. Acta* **2006**, *51*, 5304-5306.
59. Evans, R. G.; Klymenko, O. V.; Hardacre, C.; Seddon, K. R.; Compton, R. G. Oxidation of N,N,N',N'-Tetraalkyl-Para-Phenylenediamines in a Series of Room Temperature Ionic Liquids Incorporating the Bis(Trifluoromethylsulfonyl)Imide Anion. *J. Electroanal. Chem.* **2003**, *556*, 179-188.
60. Fietkau, N.; Clegg, A. D.; Evans, R. G.; Villagrán, C.; Hardacre, C.; Compton, R. G. Electrochemical Rate Constants in Room Temperature Ionic Liquids: The Oxidation of a Series of Ferrocene Derivatives. *ChemPhysChem* **2006**, *7*, 1041-1045.
61. Doherty, A. P.; Brooks, C. A. Electrosynthesis in Room-Temperature Ionic Liquids: Benzaldehyde Reduction. *Electrochim. Acta* **2004**, *49*, 3821-3826.
62. Silvester, D. S.; Aldous, L.; Lagunas, M. C.; Hardacre, C.; Compton, R. G. An Electrochemical Study of  $\text{Pcl}_3$  and  $\text{PoCl}_3$  in the Room Temperature Ionic Liquid  $[\text{C}_4\text{Mpyrr}][\text{N}(\text{Tf})_2]$ . *J. Phys. Chem. B* **2006**, *110*, 22035-22042.
63. Nelsen, S. F.; Blackstock, S. C.; Kim, Y. Estimation of Inner Shell Marcus Terms for Amino Nitrogen Compounds by Molecular Orbital Calculations. *J. Am. Chem. Soc.* **1987**, *109*, 677-682.

## CHAPTER 3. THEORY OF ELECTROCHEMICAL ELECTRON TRANSFER

The theory of electrochemical electron transfer has been elaborated in detail by Marcus and others<sup>1-5</sup>. Various aspects, relating to the rate of electrochemical transfer, such as role of solvent, solvent dynamics, effects of electrode material and that of size of supporting electrolyte have been reported in these studies of Marcus and others.

The electron transfer process between any species A (or D) in a solution and a solid electrode, acting as a source or sink for electron, can be either as,



Or

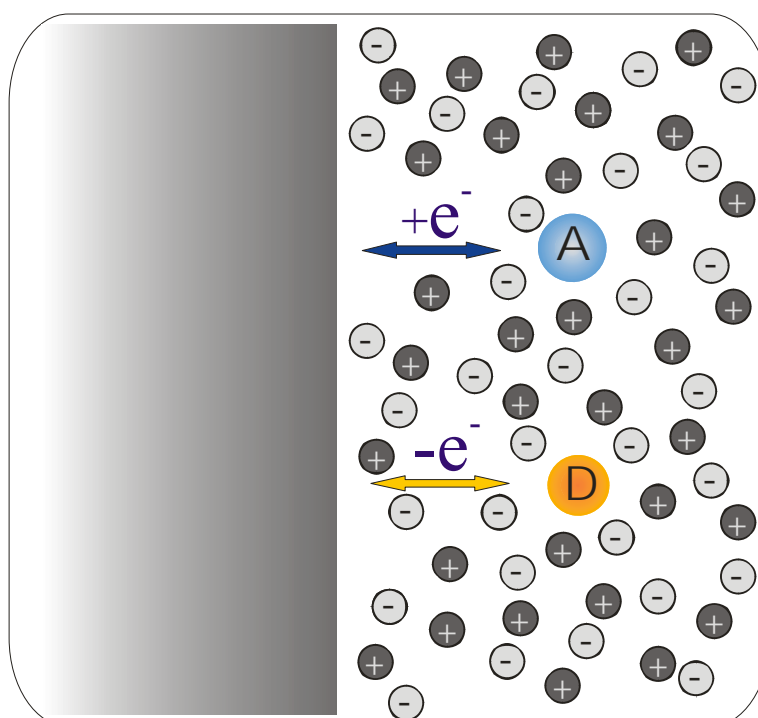
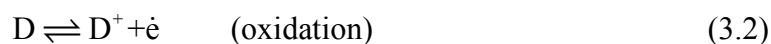


Figure 3.1 The heterogeneous electron transfer paradigm in Ionic Liquids.

### 3.1 Types of Electron Transfer Reaction

There are two types of electron transfer reactions

- 1- Inner sphere mechanism
- 2- Outer sphere mechanism

#### 3.1.1 Inner Sphere Mechanism

In the inner sphere mechanism, which is also known as the bonded mechanism, the redox species penetrate into the inner Helmholtz plane so that direct contact is formed with the electrode surface. This is known as strong interactions between the donor or acceptor and the electrode surface.

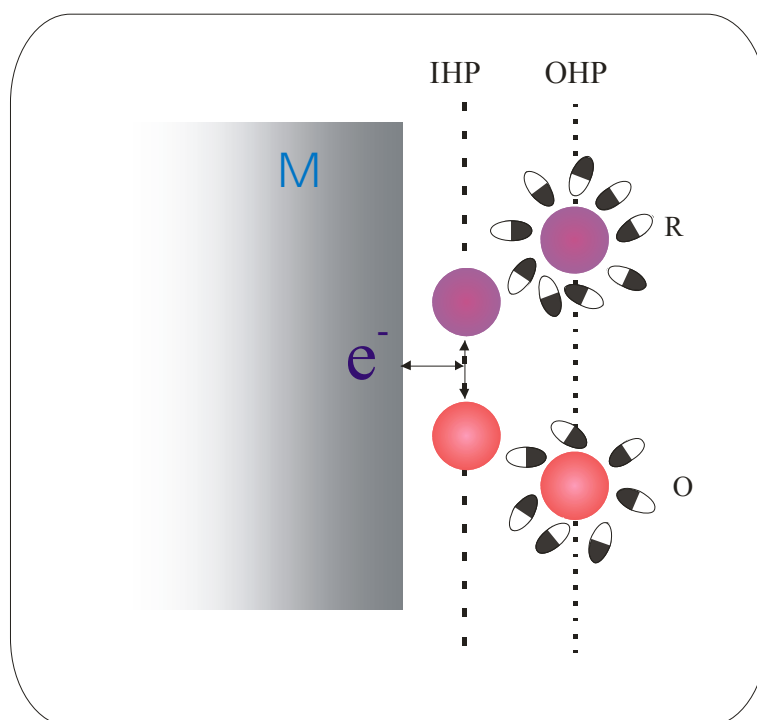


Figure 3.2 Inner sphere mechanism

### 3.1.2 Outer Sphere Mechanism

In the outer sphere mechanism, which is also called non-bonded mechanism, both the oxidized and reduced forms remain in solution, only the electron is transferred and no chemical bonds are broken and formed. There occur only weak interactions.

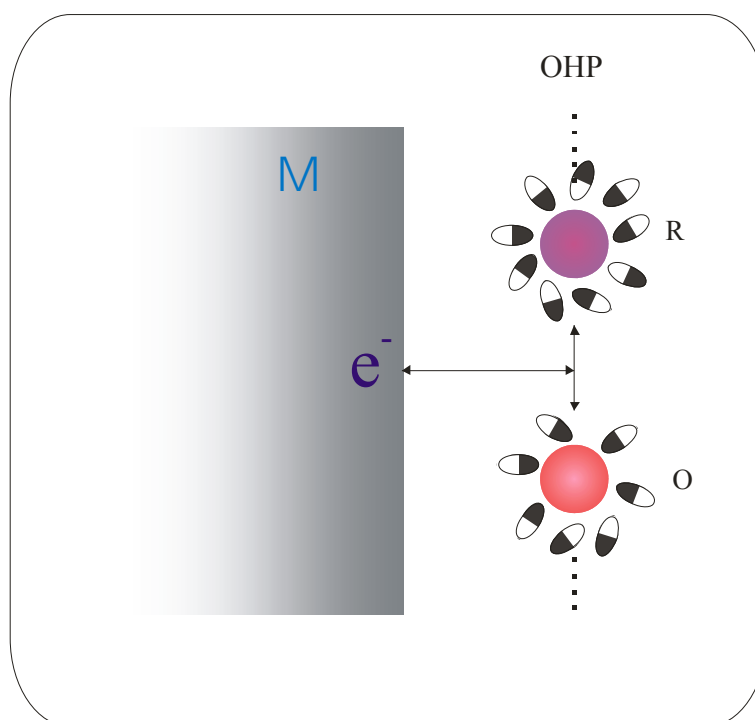


Figure 3.3 Outer sphere mechanism

## 3.2 Electrochemical Rate Constant

Electron exchange reactions proceed via activated processes. The rate constant is related to the overall Gibbs free energy barrier,  $\Delta G^*$  and the pre-exponential factor. The observed rate constant for electron transfer may be written as,

$$k_{\text{ob}} = \kappa_{\text{el}} A_n \exp\left(\frac{-\Delta G^*}{RT}\right) \quad (3.3)$$

Where  $\kappa_{\text{el}}$  is the electronic transmission coefficient and  $A_n$  is the nuclear frequency factor.



$\kappa_{el}$  describes the probability that electron transfer will occur once the system has reached the transition state (intersection region). Its value is unity for an adiabatic process (no heat flow), electronic interaction of the reactant is sufficiently strong and the electron transfer will occur with near unit probability in the intersection region.  $\kappa_{el} \ll 1$  for a diabatic process (heat flow).

$A_n$  is the effective frequency at which the transition state is approached from the reacting species via rearrangement of the appropriate nuclear coordinates.

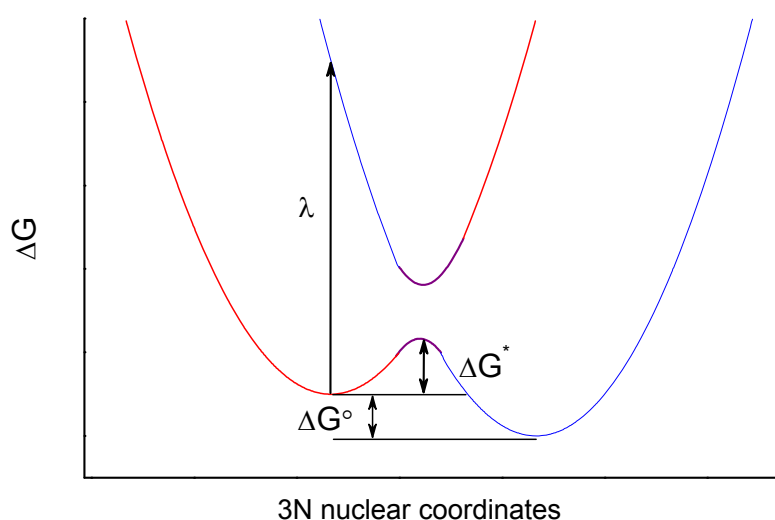


Figure 3.4 Energy diagram for an electron transfer reaction

### 3.2.1 Pre Exponential Factor

The pre-exponential terms are sensitive to the system. Different models exist in the literature for the pre-exponential terms.

#### a) The Collision Model

According to the collision model for electron transfer reactions,

$$A_n = Z_{het} \quad (3.4)$$

$Z_{het}$  is the collision frequency of the reactant molecules upon the electrode surface, is often estimated by kinetic molecular theory by the following equation

$$Z_{\text{het}} = \left( \frac{k_B T}{2\pi m} \right)^{1/2} \quad (3.5)$$

Here  $k_B$  is the Boltzmann constant and  $m$  the reduced mass of the reactant.

## b) The Encounter Pre-Equilibrium Model

According to the encounter pre-equilibrium model,

$$A_n = K_p \Gamma_n v_n \quad (3.6)$$

where  $K_p$  is the equilibrium constant for forming the activated complex (precursor complex), pertaining to the reactant-electrode system prior to the electron transfer,  $\Gamma_n$  is the nuclear tunnelling factor and  $v_n$  is the nuclear frequency factor.

$K_p$  can be expressed as

$$K_p^{\text{het}} = \delta r \exp(-w_e/RT) \quad (3.7)$$

$\delta r$  is the thickness of a reaction zone, beyond the plane of closest approach within which the reactant molecule reside in order to contribute significantly to the over all reaction rate. Sutin<sup>6</sup> gave a value of  $0.8\text{\AA}$  for  $\delta r$ , whereas Weaver et al<sup>7</sup>. suggested that  $\delta r$  should be set equal to the reactant radius, since reactants within this distance of the plane of closest approach might be expected to have roughly equal chance of undergoing electron transfer.

$w_e$  is the free energy required to transport the reactant from the bulk solution to the reaction zone. It can be expressed by the potential drop across the diffused part of the double layer and this term is always non-zero within the context of the Frumkin model for double layer effects<sup>8</sup>.

$v_n$  is the nuclear frequency factor given the effective frequency with which the system crosses the Gibbs energy barrier. This quantity can be determined both by bond vibrations and solvent reorientation associated with the characteristic frequencies  $\nu_i$  and  $\nu_o$ , respectively.

A simple formula, which has been employed, is

$$v_n = \left( \frac{v_i^2 \lambda_i + v_o^2 \lambda_o}{\lambda} \right)^{1/2} \quad (3.8)$$

This is valid only for rapid dielectric relaxation in the solvent. For organic compounds

$v_n$  is normally assumed to be  $5 \cdot 10^{13} \text{ s}^{-1}$ .

In the limit that  $\lambda_o$  is much greater than  $\lambda_i$ , this reduces to  $v_n = v_o$

### c) The Solvent Dynamical Model

In solvent dynamic model,  $v_n$  has explained in a different manner as in encounter pre-equilibrium model. It has been shown for adiabatic reactions<sup>9</sup> that can be expressed as

$$v_n = \frac{1}{\tau_L} \left( \frac{\lambda_o}{4\pi RT} \right)^{1/2} \quad (3.9)$$

This expression indicates that the solvent dielectric relaxation can have marked effect on the reaction rate.  $\tau_L$  is longitudinal solvent relaxation time and it is related to Debye relaxation time  $\tau_D$ , through the expression

$$\tau_L = \tau_D \frac{\epsilon_\infty}{\epsilon_s} \quad (3.10)$$

where  $\epsilon_\infty$  is the high frequency dielectric constant for  $\omega \rightarrow \infty$ , sometimes approximated by the square of the solvent refractive index  $n$ .  $\tau_D$  can be obtained from the Debye relation:

$$\tau_D = \frac{3V_M \eta}{RT} \quad (3.11)$$

where  $V_M$  is the molar volume of the reactant and  $\eta$  denotes the solvent viscosity.

Experimental  $\tau_D$  values of ILs are reported in the literature. Buchner et al.<sup>10-11</sup> have reported detailed measurements for different ionic liquids over a large frequency range.

### 3.3 Activation Energy

$\Delta G^*$  represents the activation energy required for charge transfer. It is the difference between the free energies of the reactants (products) at their transition state configuration and that of the reactants' equilibrium configuration.

The free energy of activation is related to the reorganization parameter neglecting the resonance energy gap

$$\Delta G^* = \frac{\lambda}{4} \quad (3.12)$$

$\lambda$  denotes the reorganization energy.

### 3.4 The Reorganization Energy

The reorganization energy ( $\lambda$ ) represents the energy needed to transform the nuclear configuration in the reactant and the solvent to the product state.

The reorganization parameter is the sum of inner shell (bond) and outer shell (solvent) components.

$$\lambda = \lambda_i + \lambda_o \quad (3.13)$$

The first one corresponds to the changes in bond length and bond angles of the reactant (inner reorganization energy) and second is the energy of the solvent reorganization (outer reorganization energy)

#### 3.4.1 Inner-shell Reorganization Energy

Inner-shell reorganization energy depends upon the changes of bond lengths and angles in going from the reactants to products.

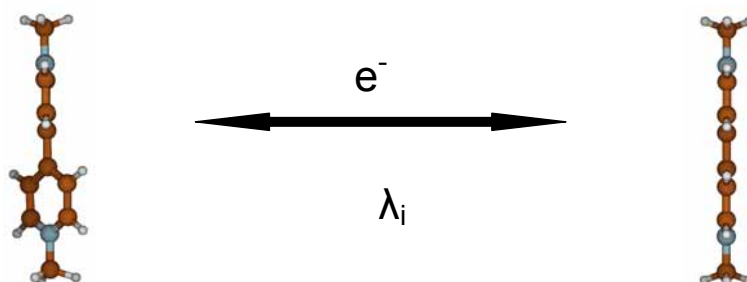


Figure 3.5 Geometrical changes in methylviologen upon electron transfer

It is usually determined from measured crystal structures of the reactants and products and from their vibrational spectra.

$$\lambda_i = \sum_i \frac{f_i \cdot f_i^*}{f_i + f_i^*} (\Delta q_i)^2 \quad (3.15)$$

Here  $f_i$  and  $f_i^*$  are the force constants of the  $i$ -th normal vibration of the oxidized and reduced molecule,  $\Delta q_i$  is the change of the coordinate, which accompanies the electron transfer reaction.

Another approach for the estimation of  $\lambda_i$  has been given by Nelson<sup>12</sup>.  $\lambda_i$  can be determined by quantum chemical calculations. According to this,  $\lambda_i$  can be ascertained using the relative energies for the conformations of oxidized and reduced specie with or without relaxation. This method deals with the electron affinity and the vertical ionization potential together with the corresponding relaxations.

In the case of aromatic molecules it is often be assumed that  $\lambda_i$  is small in comparison with  $\lambda_o$  and therefore neglected.

### 3.4.2 Outer-shell Reorganization Energy

The outer-shell reorganization energy depends upon the properties of the solvent. When the continuum model for the solvent is used,  $\lambda_o$  is a function of the dielectric properties

of the medium, the distance between the reactant and the electrode surface, and the shape of the reactant. Various models for the solvent reorganization are available.

The value of  $\lambda_o$  may be estimated on the basis of a simple extension of the Born model.

For one electron electrode process  $\lambda_o$  is given as follows

$$\lambda_o = \frac{e_o^2 \cdot N_L}{8 \cdot \pi \cdot \epsilon_o} \left( \frac{1}{r} - \frac{1}{d_{het}} \right) \cdot \gamma \quad (3.16)$$

Where  $e$  is the electronic charge,  $N_L$  is Avogadro's constant,  $\epsilon_o$  is the permittivity of vacuum  $r$  is the radius of the molecule,  $d_{het}$  is the distance from the reactant to the metal surface,  $\gamma$  is the Pekar factor

The radius,  $r$ , can be estimated by considering molecules to be spherical with the help of following equation,

$$r = \sqrt[3]{\frac{3M}{4\rho N_L \pi}} \quad (3.17)$$

Here,  $M$  is the molecular weight and  $\rho$  is the density of the reactant.

Another method for estimating  $r$  has also been explained by considering organic molecules as ellipsoids with semi axes  $a > b > c$  obtained from crystallography<sup>13</sup>, then

$$\frac{1}{r} = \frac{F(\varphi, \alpha)}{(a^2 - c^2)^{1/2}} \quad (3.18)$$

With  $F(\varphi, \alpha)$  being elliptic integrals of the first kind

$$\varphi = \arcsin \left( (a^2 - c^2)^{1/2} / c \right) \quad (3.19)$$

$$\alpha = \arcsin \left[ (a^2 - b^2) / (a^2 - c^2) \right]^{1/2} \quad (3.20)$$

$d_{het}$ , the reaction distance to the electrode surface, is assumed by Marcus to be  $2r$ , based on the classical electrodynamic picture of a reactant-electrode image interaction. In contrast to this Hush<sup>14</sup> argues that  $d_{het}$  is larger than  $2r$  since the molecules react in the outer Helmholtz plane. This idea is expressed by  $d_{het} \approx \infty$ .

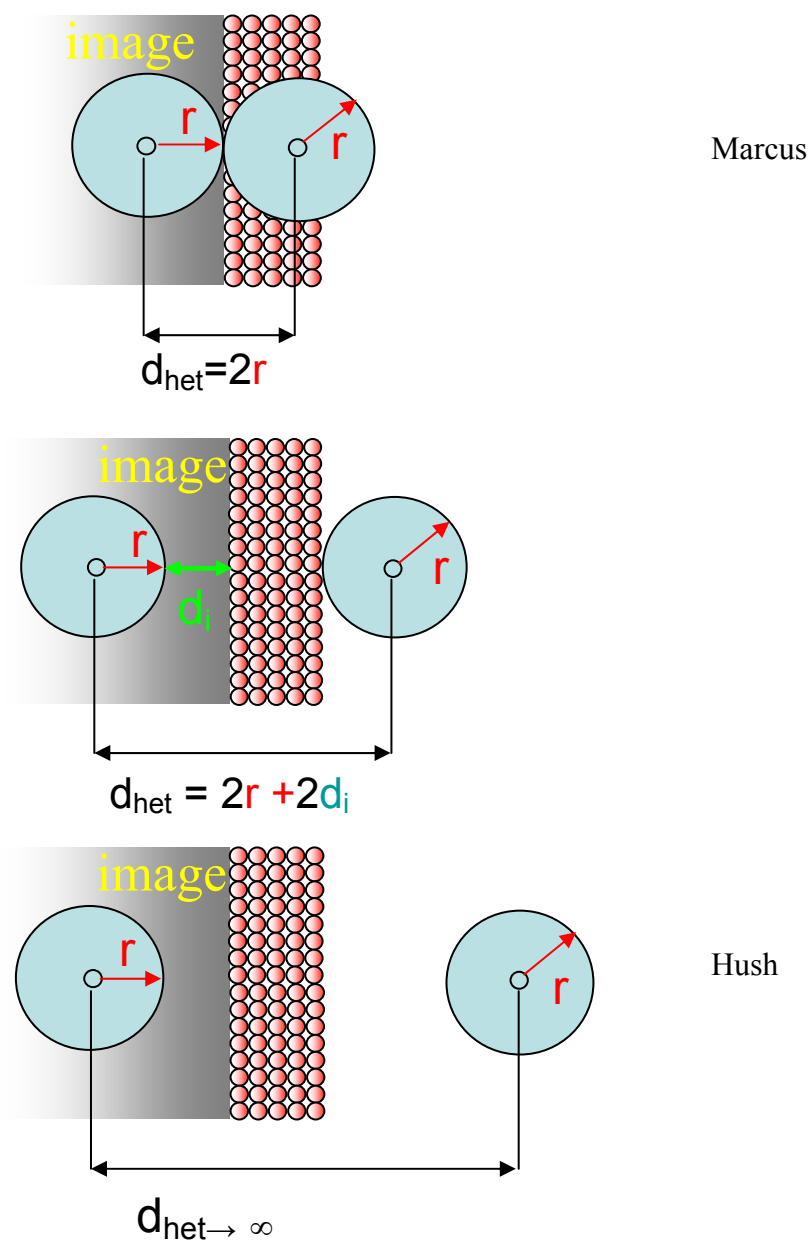


**Figure 3.6** Different concepts of reaction distance to the electrode surface

The Pekar factor  $\gamma$  includes the solvent properties and is given by

$$\gamma = \frac{1}{\epsilon_{\text{op}}} - \frac{1}{\epsilon_s} \quad (3.21)$$

$\epsilon_{\text{op}}$  is the solvent permittivity at optical frequencies which is equal to square of the refractive index,  $n$  and  $\epsilon_s$  is the static dielectric constant so that the solvent dependence of  $\lambda_0$  comes only from Pekar factor.

$$\lambda_o^{\text{het}} = \frac{e_o^2 \cdot N_L}{8 \cdot \pi \cdot \epsilon_o} \left( \frac{1}{r} - \frac{1}{d_{\text{het}}} \right) \cdot \left( \frac{1}{n^2} - \frac{1}{\epsilon_s} \right) \quad (3.22)$$

Solvation effects may play a dominant role in determining the corresponding activation energies.

In the case of RTILs acting as solvents, the main problem is to understand the role of the solvent reorganization energy  $\lambda_o$ , since Marcus theory uses a dielectric polarization model based on the dielectric constant and the refractive index of the solvent. Such a polarization concept based on solvent dipoles is not applicable to the charged ions of the RTILs acting as solvents. Additionally, the static dielectric constants of RTILs are not measurable by conventional methods because the samples are largely short-circuited by their intrinsic electrical conductance<sup>15</sup>. Microwave dielectric relaxation spectroscopy has been used to deduce  $\epsilon_s$ -values for RTILs. Reported  $\epsilon_s$ -values are between 10.0 and 13.2 for various RTILs. Similar results questioning the Marcusian concept of  $\lambda_o$  are found from ESR-spectroscopic measurements of the homogeneous electron-self exchange rate constants of the  $MV^{++}/MV^+$ -redox couple in RTILs<sup>16</sup>. To understand the solvent contribution arising from RTILs, temperature dependent measurements are necessary to get values for the different activation energies  $\Delta G^*$ . In this work, temperature dependent measurements have been carried out to obtain the corresponding activation energies.

### 3.4.3 The Mean Spherical Approximation

According to this model, solvent has been considered as hard sphere which is in contrast the solvent take as a dielectric continuum. The outer-shell reorganization energy can be expressed by the mean sphere approximation (MSA) as,



$$\lambda_o^{\text{msa}} = \frac{N_o e_o^2}{8\pi\epsilon_o} \left[ \left( 1 - \frac{1}{\epsilon_s} \right) \frac{1}{(r_A + r_s/\lambda_{ri})} - \left( 1 - \frac{1}{\epsilon_{op}} \right) \frac{1}{r_A} \right] \quad (3.23)$$

Where  $r_A$  is the radius of the reactants A represented by sphere,  $r_s$  is the radius of the solvent represented as a sphere and  $\lambda_{ri}$  is the MSA polarization parameter.

MSA model is applicable only to approximately spherical reactants. MSA polarization parameter depends on whether the reactant is a cation or an anion. It has been described in detail by Fawcett et al<sup>17,18</sup>.

MSA gives lower value for outer sphere reorganization energy as compared to the continuum model because MSA contains more solvent parameters than the continuum model.

1. Marcus, R. A. On the Theory of Electron-Transfer Reactions. Vi. Unified Treatment for Homogeneous and Electrode Reactions. *The Journal of Chemical Physics* **1965**, *43*, 679-701.
2. Marcus, R. A. The Theory of Oxidation-Reduction Reactions Involving Electron Transfer. V. Comparison and Properties of Electrochemical and Chemical Rate Constants. *J. Phys. Chem.* **1963**, *67*, 853-857.
3. Hush, N. S. Homogeneous and Heterogeneous Optical and Thermal Electron Transfer. *Electrochim. Acta* **1968**, *13*, 1005-1023.
4. Dogonadze, R. R.; Kuznetsov, A. M.; Marsagishvili, T. A. The Present State of the Theory of Charge Transfer Processes in Condensed Phase. *Electrochim. Acta* **1980**, *25*, 1-28.
5. Levich, V. G.; Dogonadze, R. R. Theory of Non-Radiative Electronic Transitions between Ions in Solution. *Dokl. Akad. Nauk SSSR, Ser. Fiz. Khim* **1959**, *124*, 123.
6. Sutin, N. Theory of Electron Transfer Reactions: Insights and Hints. *Prog. Inorg. Chem.* **1983**, *30*, 441-498.
7. Hupp, J. T.; Weaver, M. J. The Frequency Factor for Outer-Sphere Electrochemical Reactions. *J. Electroanal. Chem. Interfacial Electrochem.* **1983**, *152*, 1-14.
8. Fawcett, W. R. The Location of the Reaction Site and Discreteness-of-Charge Effects in Electrode Kinetics. *Can. J. Chem.* **1981**, *59*, 1844-1853.
9. Calef, D. F.; Wolynes, P. G. Classical Solvent Dynamics and Electron Transfer. 1. Continuum Theory. *J. Phys. Chem.* **1983**, *87*, 3387-3400.
10. Hunger, J.; Stoppa, A.; Schroedle, S.; Hefter, G.; Buchner, R. Temperature Dependence of the Dielectric Properties and Dynamics of Ionic Liquids. *ChemPhysChem* **2009**, *10*, 723-733.
11. Stoppa, A.; Hunger, J.; Buchner, R.; Hefter, G.; Thoman, A.; Helm, H. Interactions and Dynamics in Ionic Liquids. *J. Phys. Chem. B* **2008**, *112*, 4854-4858.
12. Nelsen, S. F.; Blackstock, S. C.; Kim, Y. Estimation of Inner Shell Marcus Terms for Amino Nitrogen Compounds by Molecular Orbital Calculations. *J. Am. Chem. Soc.* **1987**, *109*, 677-682.
13. German, E. D.; Kuznetsov, A. M. Outer Sphere Energy of Reorganization in Charge-Transfer Processes. *Electrochim. Acta* **1981**, *26*, 1595-1608.

14. Hush, N. S. Homogeneous and Heterogeneous Optical and Thermal Electron Transfer. *Electrochim. Acta* **1968**, *13*, 1005-1023.
15. Weingaertner, H. The Static Dielectric Constant of Ionic Liquids. *Z. Phys. Chem. (Muenchen, Ger.)* **2006**, *220*, 1395-1405.
16. Grampp, G.; Kattnig, D.; Mladenova, B. ESR-Spectroscopy in Ionic Liquids: Dynamic Linebroadening Effects Caused by Electron-Self Exchange Reactions within the Methylviologene Redox Couple. *Spectrochim Acta A Mol Biomol Spectrosc* **2006**, *63*, 821-825.
17. Fawcett, W. R.; Opallo, M. Possible Experimental Evidence for Molecular Solvation Effects in Simple Heterogeneous Electron-Transfer Reactions. *J. Phys. Chem.* **1992**, *96*, 2920-2924.
18. Fawcett, W. R. The Role of the Metal and the Solvent in Simple Heterogeneous Electron Transfer Reactions. *Electrochim. Acta* **1996**, *42*, 833-839.

## CHAPTER 4. ROOM TEMPERATURE IONIC LIQUIDS (RTILS)

Room temperature ionic liquids (RTILs) are liquid at room temperature and comprised only of ions. They remain liquid over a wide range of temperature i.e. 473-573 K. They have no vapour pressure and are being highly used in place of volatile solvent, so they are also known as Green solvents<sup>1</sup>. They are being considered as environmentally friendly. However, a few issues have been reported about their toxicity<sup>2</sup>. Rogers also challenged the stability of RTILs and suggested that RTILs are not always green.

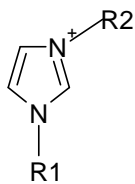
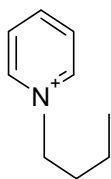
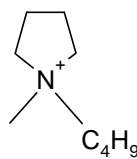
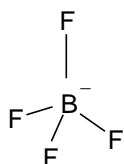
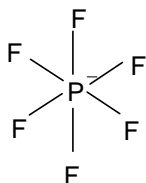
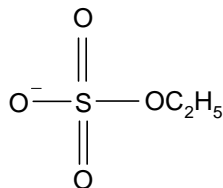
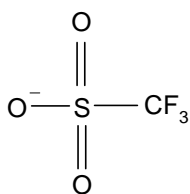
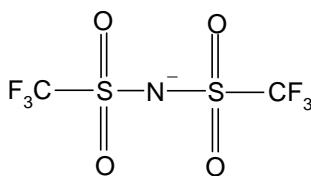
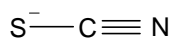
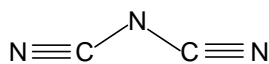
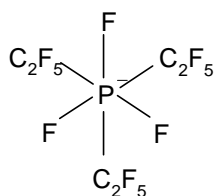
RTILs consist of two opposite ions and unlimited combinations of cations and anions are possible. Because of this option of varying cations and anions, ionic liquids (RTILs) can be designed to obtain desired properties. Functional groups can also be added to the ions to have further control on its properties.  $10^{12}$ - $10^{18}$  different RTILs with versatile properties have been predicted. There are numerous reviews, papers and books that have been devoted to RTILs<sup>3-7</sup>. The subject of a number of studies is the utility as 'green' alternative solvent to conventional organic solvent.

### 4.1 History of Ionic liquids

RTILs have been known for many years. For instance ethyl ammonium nitrate, which has a melting point of 12 °C, was first introduced in 1914 by Walden<sup>8</sup>, but ILs were not in common use for a long time. A dramatic increase of activity in this area was started since the discovery of binary RTILs made from mixture of aluminium (III) chloride and N- alkyl pyridinium<sup>9</sup>, or 1,3 dialkylimidazolium chloride<sup>10</sup>.

In the early 1980s, Seddon and co-workers started to use RTILs as non aqueous polar solvent for electrochemical and spectroscopic studies of transition metal complexes<sup>7,11</sup>. After this work, RTILs become more familiar to the broad public.

A brief history of the development of RTILs up to 1994 has been excellently described by John S. Wilkes<sup>12</sup>

Imidazolium,  $[C_n\text{mim}]^+$ Pyridinium,  $[C_4\text{py}]^+$ Pyrrolidinium,  $[C_4\text{mpyrr}]^+$ Tetrafluoroborate,  $[\text{BF}_4]^-$ Hexafluorophosphate,  $[\text{PF}_6]^-$ Ethyl sulphate  $[\text{EtSO}_4]^-$ Trifluoromethanesulfonate,  $[\text{Otf}]^-$ Bis(trifluoromethylsulfonyl)imide,  $[\text{N}(\text{tf})_2]^-$ Thiocyanate,  $[\text{SCN}]^-$ Dicyanamide,  $[\text{N}(\text{CN})_2]^-$ Trifluorotrakis(pentafluoroethyl)phosphate,  $[\text{FAP}]^-$ **Scheme 1: Structures of various cations and anions of RTILs.**

## 4.2 Classification of RTILs

Different groups of people categorise RTILs differently by taking into account various fundamental features of RTILs. Generally these can be classified into two main categories, namely simple salts (made up of single anion and cation) and binary RTILs (salts where equilibrium is involved)<sup>13</sup>.

Compton<sup>14</sup> classified RTILs on the basis of somewhat different features. He classified RTILs into three generations.

### 4.2.1 First Generation

They contain haloaluminate anions e.g.  $[\text{AlCl}_4]^-$ <sup>10</sup>. They are very sensitive towards moisture and are used under anhydrous conditions

### 4.2.2 Second Generation

They are based on anions which are less reactive with water, but still absorb moisture and change their physical and chemical properties. e.g.  $[\text{BF}_4]^-$  and  $[\text{PF}_6]^-$  anions<sup>15</sup>. For a variety of redox species, electrochemical investigations of the mass and charge transfer kinetics has been studied using second generation RTILs<sup>16-17</sup>.

Some more RTILs containing hydrophobic anions, like  $[\text{NTf}_2]^-$  or  $[\text{FAP}]^-$ , which are less moisture sensitive can be classified between 2<sup>nd</sup> and 3<sup>rd</sup> generation. RTILs, containing  $[\text{NTf}_2]^-$  anion showed the best stability as they do not form HF when in contact with water<sup>18</sup>.

### 4.2.3 Third Generation

In this class, the anions and cations contain functional groups within their structure. These are called task-specific ionic liquids  $[\text{TSRTILs}]$ <sup>19</sup>.

Finally there are other RTILs which are difficult to categorize e.g.  $[\text{N}(\text{CN})_2]^-$ ,  $[\text{SCN}]^-$  and  $[\text{EtSO}_4]^-$  containing anions and some are halide free, possess lower viscosity and high conductivity.

Common cations include imidazolium  $[\text{C}_n\text{mim}]$ , pyrrolidinium  $[\text{C}_4\text{mpyr}]$ , pyridinium  $[\text{C}_4\text{Py}]$ , tetraalkylammonium  $[\text{N}_{6,2,2,2}]$  and tetraalkylphosphonium  $[\text{P}_{6,6,6,14}]$ .

### 4.3 Impurities in RTILs<sup>4</sup>

In general, the synthesis of RTILs is relatively simple organic chemistry, but the major problems faced during preparation are impurities. Presence of impurities, matter a lot for any measurement with RTILs. The purity of RTILs is very important because of the fact that the presence of even small amounts of impurities can significantly influence the RTILs properties<sup>20</sup>.

#### 4.3.1 Color

RTILs are all nearly colorless. The appearance of some coloured impurities is common during synthesis. They are only present in trace amounts, so that the chemical nature of the coloured impurities is still not known. But they probably originate from the starting material during synthesis. RTILs containing pyridinium as a cation form colored impurities more easily than those RTILs which contain imidazolium as a cation. One can get rid of them by taking care of some important points (distilled starting material, low temperature processing, and drying step) during synthesis.

#### 4.3.2 Organic and Inorganic Impurity

Some unreacted compound or solvent remaining left in the final product during synthesis may play an unfavourable role in application of RTILs. It also affects the physical properties e.g. electrochemical window of RTILs.

Out of these, volatile impurities can easily be removed by simple evaporation under high vacuum at constant temperature. Unreacted reactants which have high boiling points are difficult to remove by evaporation. So it is necessary to use appropriate controlled condition for synthesis that no unreacted reactants are left at the end.

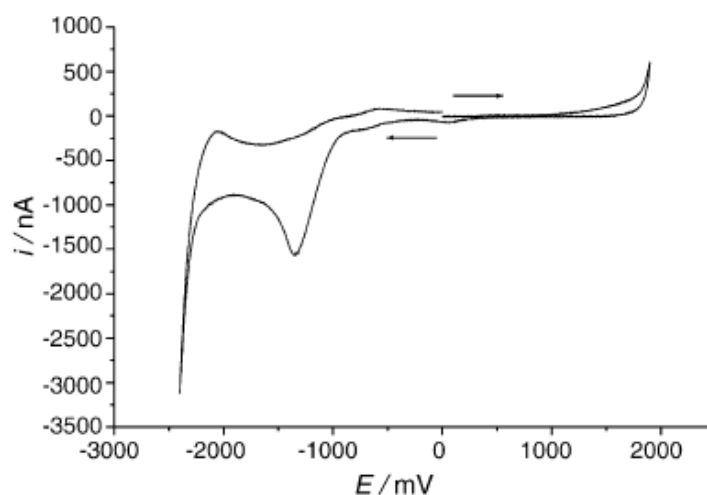


**Figure 4.1** Cyclic voltammetry of [bmim][BF<sub>4</sub>] prepared by anion exchange with AgBF<sub>4</sub> from [bmim]Cl containing Ag<sup>+</sup> impurity [Adapted from 21]

### 4.3.3 Halide Impurities

In the synthesis of RTILs, during the alkylation step, alkyl halides are frequently used as alkylating agents. It may cause halide impurities in the final product. These halide contents seriously influence the application and also on physicochemical properties i.e. electrochemical window, viscosity etc. These can easily be removed from those RTILs which are immiscible with water by solvent separation methods. For the RTILs that are miscible with aqueous solvent, some other special procedures need to be applied in synthesis such as ion-exchange resins or alkylation by appropriate alkylating agents.

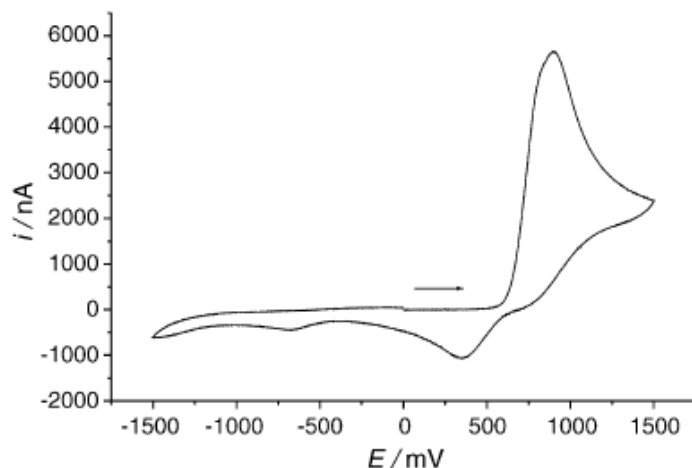


Figure 4.2 Cyclic voltammety of [bmim][BF<sub>4</sub>] prepared by anion exchange with AgBF<sub>4</sub> from [bmim]Cl containing Cl impurity. [Adapted from 21]

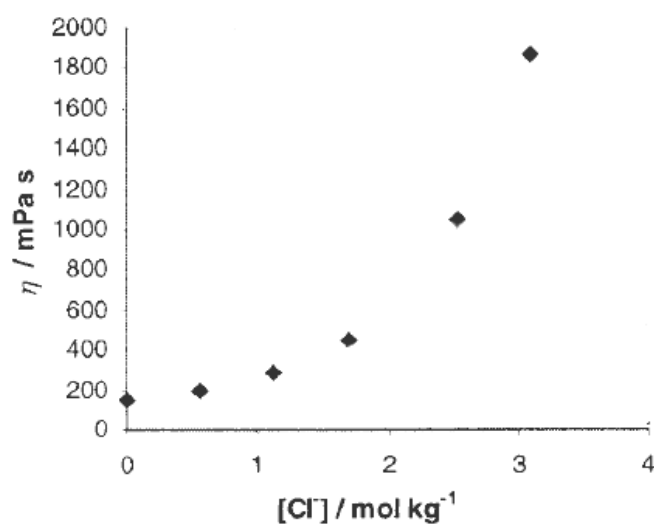


Figure 4.3 Viscosity of [bmim][BF<sub>4</sub>] at 20 °C vs. molal concentration of chloride, added as [bmim]Cl. [Adapted from 20]

#### 4.3.4 Water

Water is usually present in RTILs. Imadazolium halide salts are famous due to their extremely hygroscopic nature. Hydrophilic RTILs usually take up water from the air, however, hydrophobic RTILs may also have water content as impurity. The water impurity is not completely inert in RTILs. It may be a problem for some applications but it influences up to a considerable extent the physicochemical properties and also its stability. For example, Viscosity can be decreased by 50% by the presence of 2% of



water in  $[\text{bmim}][\text{BF}_4]^4$  and also 3% water (by weight) in the same RTILs reduces the electrochemical window from 4.10 V to 1.95 V<sup>16</sup>. So intensive care is needed to work with such RTILs.

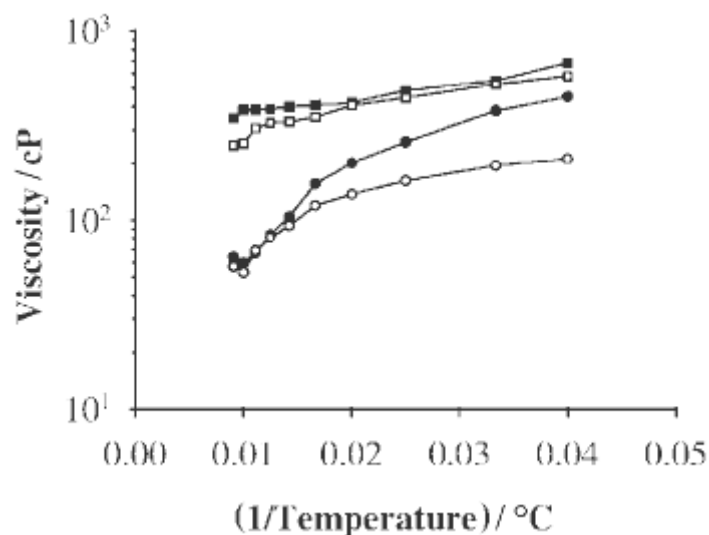


Figure 4.4 Viscosity as a function of temperature (●) dried  $[\text{bmim}][\text{PF}_6]$ , (○) water equilibrated  $[\text{bmim}][\text{PF}_6]$ , (■) dried  $[\text{omim}][\text{PF}_6]$ , (□) water equilibrated  $[\text{omim}][\text{PF}_6]$ . [Adapted from 22]

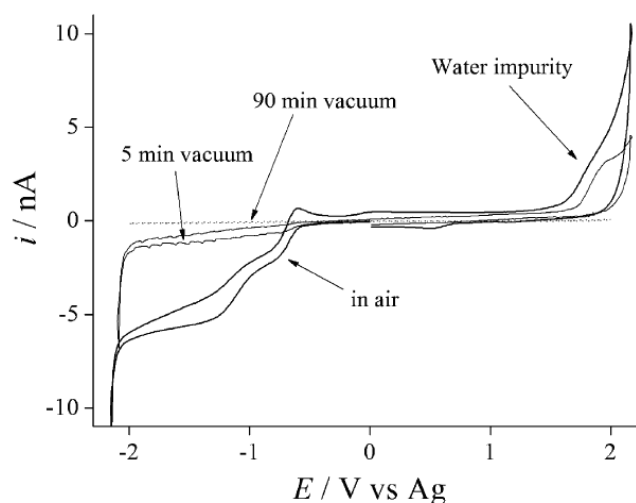


Figure 4.5 Cyclic voltammograms of  $[\text{bmim}][\text{OTf}]$  showing moisture impurity, and the use of vacuum techniques to remove these impurities. [Adapted from 14]

Imidazolium based RTILs, containing various anion such as  $[\text{BF}_4]$ ,  $[\text{OTf}]$  and  $[\text{NTf}_2]$  and  $[(\text{CF}_3\text{SO}_2)_3\text{C}]$  trifluoromethanesulfone methides have received much attention because of their low moisture sensitivity.

## 4.4 Physicochemical Properties of RTILs

The knowledge of physicochemical properties of the RTILs is necessary for their successful application.

In the first international congress on RTILs (COIL) at Salzburg (Austria-2005), many experimental and theoretical physical studies suggested that the unique properties of RTILs arise from their composition and interionic interactions. In the 2<sup>nd</sup> congress at Yokohama (Japan-2007) and 3<sup>rd</sup> congress at Cairns (Australia-2009), a lot of research works have documented their vast application and their properties.

Data on physicochemical properties shows that it is difficult to relate the properties of a RTILs to its chemical structure. But on the other hand, the nature and size of both cation and anion significantly affect the physicochemical properties of RTILs. Drastic changes in the properties of RTILs have been observed by the presence of even small amount of impurities<sup>20</sup>.

The physicochemical properties of the imidazolium based RTILs have been discussed and reported in this chapter, because these are relevant to the experimental work presented later.

### 4.4.1 Melting Point and Glass Transition

The melting point is the key criterion for the evaluation of RTILs. The charge, size and distribution of charge on the respective ions are the main factor that influences the melting point of RTILs.

The effect of anion and cation cannot be discussed separately, but nevertheless the melting point increases as the interaction between ions increases by hydrogen bonding. Generally with an increase in anion size, there is a decrease in melting point<sup>23</sup>. Large cations and increases in asymmetric substitution decrease the melting point<sup>4</sup>. Branches on the alkyl chain also have a strong influence on the melting point. Generally, increase in the branching on the alkyl chain cause, rise in melting point.

Many imidazolium RTILs shows glass formation characteristic<sup>24-26</sup> and they become highly viscous and turn finally into glasses without the observation of a melting point.

Table 4.1 Melting points and glass transition temperature of various RTILs

RTILs	M. P. / °C (water equilibrated)	M. P. / °C (dried)	T <sub>g</sub> / °C (water equilibrated)	T <sub>g</sub> / °C (dried)	Ref.
[mmim][NTf <sub>2</sub> ]		22			18
			26		27
[mmim][CF <sub>3</sub> CO <sub>2</sub> ]		52			18
[emim][BF <sub>4</sub> ]		11			25
			13	-92	28
			15		15
[emim][OTf]		-9			18
[emim][NTf <sub>2</sub> ]				-98	25
			-3		18
			-18	-87	27
[emim][PF <sub>6</sub> ]		58-60			15
			62		25
			58		29
[pmim][PF <sub>6</sub> ]		40			25
[emim][CF <sub>3</sub> CO <sub>2</sub> ]		-14			18
[bmim][BF <sub>4</sub> ]				-97	22
			-81		30
				-83	27
				-85	28
[bmim][CF <sub>3</sub> CO <sub>2</sub> ]				-78	27
				-50	18
				-30	18
[bmim][C <sub>3</sub> F <sub>7</sub> CO <sub>2</sub> ]				-40	31
[bmim][OTf]		16			18
			17	-82	27
[bmim][NTf <sub>2</sub> ]	-25		-102	-104	22
			-3	-87	27
			-4		18
[bmim][(C <sub>2</sub> F <sub>5</sub> SO <sub>2</sub> ) <sub>2</sub> N]			-84		27

RTILs	M. P. / °C (water equilibrated)	M. P. / °C (dried)	T <sub>g</sub> / °C (water equilibrated)	T <sub>g</sub> / °C (dried)	Ref.
[bmim][PF <sub>6</sub> ]	4	10	-83	-80	22
		-61			32
		10		-77	27
				-61	30
			-8		31
[hmim][PF <sub>6</sub> ]		-61			30
			-75	-78	22
		-6		-81	27
[omim][PF <sub>6</sub> ]			-75	-82	22
			-80		27

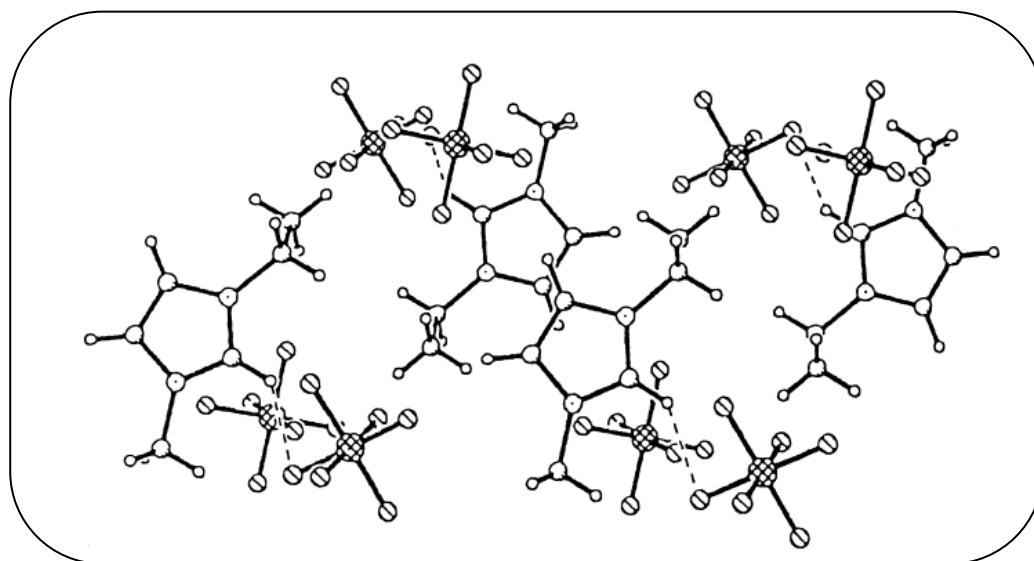


Figure 4.6 Crystal structure of [emim][PF<sub>6</sub>]. [Adapted from 29]

#### 4.4.2 Electrochemical Windows

Electrochemical window is the potential range over which the electrolyte is neither reduced nor oxidized. This value shows the stability of the solvent. RTILs exhibit a much larger potential window in relation to the organic solvent. This high range of electrochemical window is the most considerable point which allows

electrochemist to use RTILs as an electrochemical solvent. Typically 4-6 V has been reported as potential windows in literature for non haloaluminate ionic liquids<sup>33-34</sup> while for common electrochemical solvents, the range of electrochemical window is low. These high electrochemical windows allow us to perform experiments of various compounds in RTILs which are not possible in other solvents.

Different values of electrochemical windows have been reported in literature for the same ionic liquids (Table 4.2). The reason for the variation of the reported values are as follows:

- the presence of impurity can have a profound impact on the potential limits and the corresponding potential window<sup>16</sup>.
- electrochemical windows have been determined by using different quasi reference electrode and the values can not be compared to high degree of accuracy.
- different materials<sup>14</sup> which can change the decomposition potential of the electrolyte have been used as working electrode.

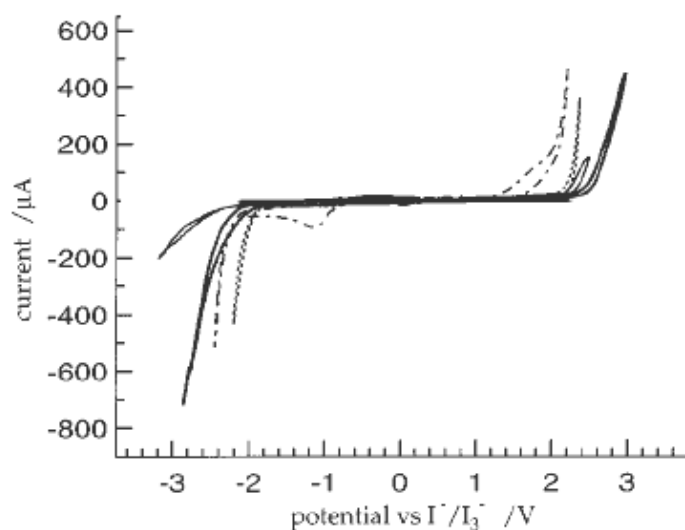


**Figure 4.7** Potential window of various RTILs at Pt electrode in (—) [emim][NTf<sub>2</sub>], (—) [emmim][NTf<sub>2</sub>], (.....) [emim][OTf], (- - -) [emim][CF<sub>3</sub>COO]. [Adapted from 18]

Table 4.2 Electrochemical window of various RTILs at different electrode.

RTILs	WE	RE	Electrochemical window/V	References
[emim][BF <sub>4</sub> ]	Pt	Al in AlCl <sub>3</sub> <sup>+</sup> EMIC(1.5:1.0)	5	24
	Pt	Al in AlCl <sub>3</sub> <sup>+</sup> EMIC(1.5:1.0)	4.3	35
[emim][OTf]	Pt	I-/I <sub>3</sub> <sup>-</sup> vs Fc/Fc <sup>+</sup>	4.1	18
	Pt	I-/I <sub>3</sub> <sup>-</sup> vs Fc/Fc <sup>+</sup>	4.3	24
[emim][CF <sub>3</sub> CO <sub>2</sub> ]	Pt		3.8	18
[emim][NTf <sub>2</sub> ]	GC		4.1	26
	Pt		4.5	18
	GC		4.5	24
	Pt	I-/I <sub>3</sub> <sup>-</sup> vs Fc/Fc <sup>+</sup>	4.3	18
[bmim][BF <sub>4</sub> ]	W(RDE)	Pt(QRE)	6.10	36
	GC(RDE)	Pt(QRE)	5.45	36
	Au(RDE)	Pt(QRE)	4.20	36
	Pt		4.1	16
	Pt(RDE)	Pt(QRE)	4.60	36
	Pt(UME)	Pt(QRE)	4.00	36
[bmim][PF <sub>6</sub> ]	GC(RDE)	Pt(QRE)	6.35	36
	Au(RDE)	Pt(QRE)	5.95	36
	Pt(RDE)	Pt(QRE)	5.70	36
	Pt(UME)	Pt(QRE)	5.00	36
	Pt		4.2	16

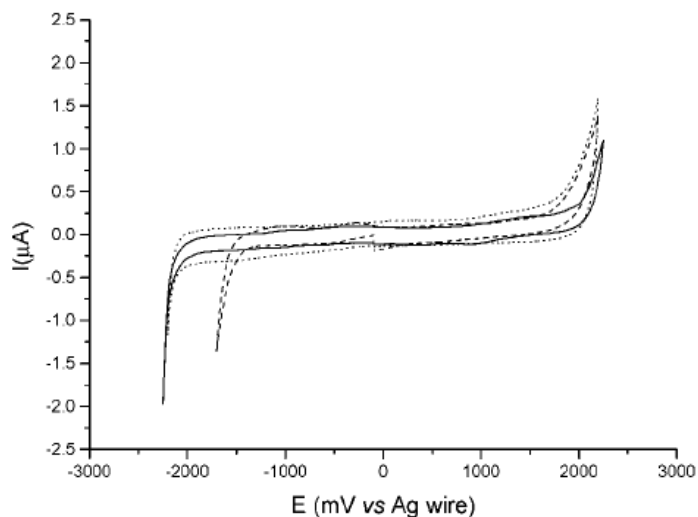


Figure 4.8 Potential window of [bmim][PF<sub>6</sub>] at (.....) Pt, (.....) GC, (—) Au. [Adapted from 37]

#### 4.4.3 Vapor Pressure and Thermal Stability

The vapor pressure is one of the most important properties of any solvent. For RTILs, the vapor pressure is extremely low, which is an advantage. As it has already been discussed earlier that presence of even small amount of water content caused serious problem for measurement in RTILS. So removal of water contents can easily be done by applying high vacuum with slow heating due to the low value of vapor pressure.

Mostly RTILs exhibit high thermal stability which provides the opportunity to work in the wide range of temperature. They start to decompose at around 673 K. This high thermal stability of RTILs is also very helpful to remove volatile impurity at constant temperature. The decomposition temperature of some RTILs has been listed in Table 4.3. The thermal decomposition temperature decreases as the hydrophilicity of the anion increases for the same cation<sup>22</sup>. RTILs containing halide anions reduce the thermal stability as compared to the RTILs with non halides anions<sup>25</sup>. The order of thermal stability with anions can be written as [PF<sub>6</sub>] > [NTf<sub>2</sub>] ≥ [BF<sub>4</sub>] > halides.

Table 4.3 Thermal decomposition of several RTILs

RTILs	Decomposition temperature/ $^{\circ}\text{C}$		Reference
	(water equilibrated)	(dried)	
[emim][Cl]		285	25
[emim][I]		303	25
[emim][BF <sub>4</sub> ]		412	25
		447	28
[emim][PF <sub>6</sub> ]		375	25
[emim][NTf <sub>2</sub> ]		440	18
		455	25
[emim][OTf]		440	18,30
[bmim][Cl]		254	22
[bmim][I]		265	22
[bmim][BF <sub>4</sub> ]		403	22
		435	30
[bmim][PF <sub>6</sub> ]	360	349	22
[bmim][NTf <sub>2</sub> ]	394	439	22
[hmim][Cl]		253	22
[hmim][PF <sub>6</sub> ]	390	417	22
[omim][PF <sub>6</sub> ]	374	376	22

#### 4.4.4 Viscosity

Viscosity is another key physical property. RTILs are famous by virtue of their high viscosities compared to typical organic solvent's viscosities. Unfortunately, many different values of viscosity for the same RTILs have been reported in literature because it dramatically changes by the presence of small amounts of water<sup>38</sup> and halide ion impurities<sup>20</sup>. These values are given in



Table 4.5.

It can easily be seen that viscosity is greatly affected by the nature of the anion. The perfluorinated ion causes greater viscosity as compared to other anions because of its strong ability to form hydrogen bonds<sup>30</sup> and their basicity. As the cation size increases, viscosity also increases because of the increase in van der Waals interactions<sup>18</sup>.

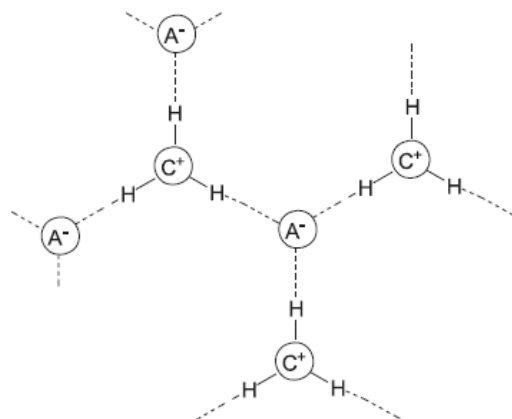


**Figure 4.9** Two dimensional simplified solid-state model of the polymeric supramolecular structure of 1,3-dialkyl imidazolium RTILs showing the hydrogen bonds between the imidazolium cation (C) and the anions (A). [Adapted from 39]

The viscosity of RTILs is a strong function of temperature. Small changes in temperature may effect large changes in viscosity values. For example 20 % change in viscosity over 5 K near room temperature is very common<sup>26</sup>. Although deviation from classical Arrhenius behaviour is observed because of glass transition<sup>40</sup>. Temperature dependence of the viscosity of RTILs is well represented by Vogel-Fulcher-Tamman [VFT]-equation

$$\eta = \eta_0 \exp\left(\frac{B}{T-T_0}\right)$$

Here,  $\eta_0$ , B and  $T_0$  are constants

**Table 4.4** VFT-equation parameters for viscosity data<sup>3</sup>

RTILs	$\eta_0 / 10^{-1}$ mPas	B/ $10^2$ K	$T_0 / 10^2$ K
[emim][BF <sub>4</sub> ]	2.0	7.5	1.5

[emim][NTf <sub>2</sub> ]	1.5	8.4	1.4
[BP][BF <sub>4</sub> ]	2.3	7.2	1.8
[BP][NTf <sub>2</sub> ]	1.2	8.5	1.6

The viscosity of RTILs can be lowered by the addition of small amounts of organic co-solvents because all other organic solvent have smaller viscosities than RTILs.

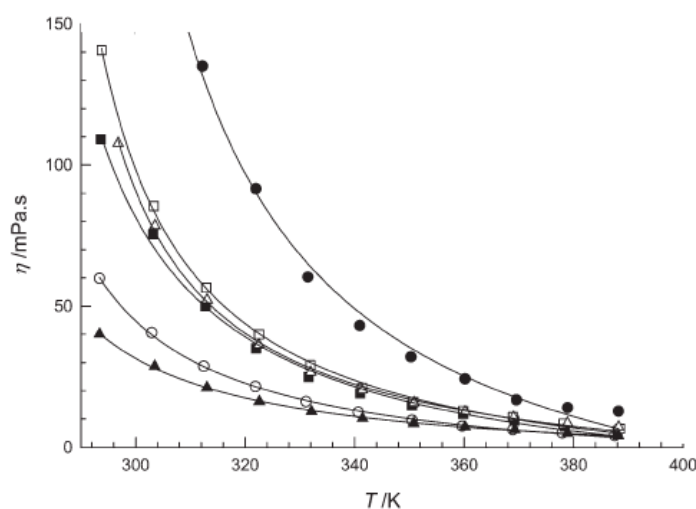


Figure 4.10 Experimental viscosities of the dried RTILs as a function of temperature in (●) [bmim][PF<sub>6</sub>], (○) [bmim][NTf<sub>2</sub>], (■) [bmim][BF<sub>4</sub>], (□) N4111[NTf<sub>2</sub>], (▲) [emim][NTf<sub>2</sub>], (△) [emim][EtSO<sub>4</sub>]. The lines correspond to the fit of the data by VFT-equation. [Adapted from 41]

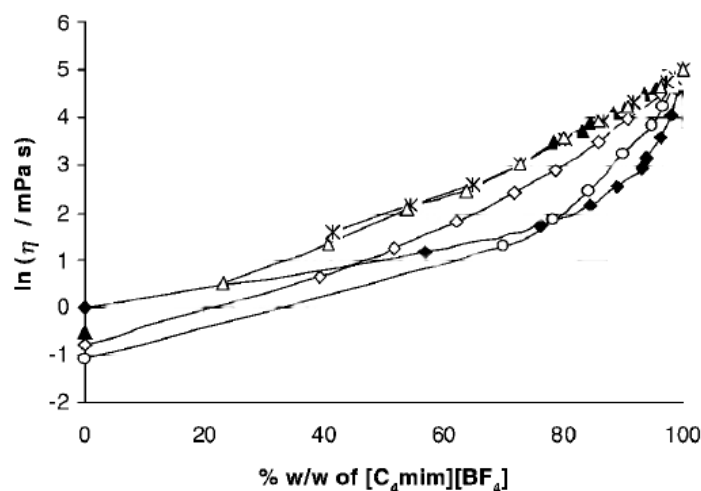


Figure 4.11 Viscosity at 20 °C of cosolvents-[bmim][BF<sub>4</sub>] mixtures vs. % w/w of [bmim][BF<sub>4</sub>] (○) acetonitrile, (◆) water, (×) 1 methylimidazole, (▲) toluene, (◇) 1,2-dimethoxyethane, (△) trimethylacetonitrile. [Adapted from 20]



Table 4.5 Viscosity of several RTILs.

RTILs	T (°C)	Viscosity (cP)	Reference
[mmim][NTf <sub>2</sub> ]	30	31	27
	20	44	31
[emim][BF <sub>4</sub> ]	25	37-66.5	42
		25.7	43
		32	44
		37	28
		34	35
	22	43	26
	22	37.7	35
	25	43	26
	20	66.5	20
	30	43	20
[emim][PF <sub>6</sub> ]	26		42
[emim][NTf <sub>2</sub> ]	25	31	44
	20	34	18
	25	28	22
	30	27	27
[emim]OTf]	20	45	18
[emim][CF <sub>3</sub> CO <sub>2</sub> ]	20	35	18
[bmim][BF <sub>4</sub> ]	25	180	28
	25	219	22
	30	233	30
	20	233	31
	20	154	45
	20	112	18
	30	91.4	20
	30	75	27
		52	22
		69	22
[bmim][NTf <sub>2</sub> ]	20	83	18
	25	44	18
	30	40	27

RTILs	T (°C)	Viscosity (cP)	Reference
[bmim][PF <sub>6</sub> ]	25	308	42
	20	312	31
	20	371	20
	25	207	46
	30	312	30
	25	275	18
	25	450	22
	25	219	30
	25	312	30
	30	182	27
	30	204	20
	[bmim][OTf]	25	90
20		90	45
30		64	27
[bmim][(C <sub>2</sub> F <sub>5</sub> SO <sub>2</sub> ) <sub>2</sub> N]	30	87	27
[bmim][C <sub>4</sub> F <sub>9</sub> SO <sub>3</sub> ]	25	373	18
[bmim][CF <sub>3</sub> CO <sub>2</sub> ]	25	73	18
	30	58	27
[hmim][NTf <sub>2</sub> ]	30	56	27
[omim][NTf <sub>2</sub> ]	30	71	27
	25	74	47
[dmim][NTf <sub>2</sub> ]	25	128	47

#### 4.4.5 Surface Tension

Surface tension values for RTILs are higher than for conventional solvents [e.g., acetonitrile: 27.64 dyn cm<sup>-1</sup>) but lower than water (73 dyn cm<sup>-1</sup>). It is dependent upon temperature and alkyl chain length. It decreases as the length of alkyl chain increases. For a particular cation, the surface tension value is higher for large anions<sup>48</sup>.

Table 4.6 Surface tension of several ionic liquids<sup>22</sup>

RTILs	Surface tension /dyn cm <sup>-1</sup> (water equilibrated)	Surface tension /dyn cm <sup>-1</sup> (dried)
[bmim]BF <sub>4</sub>		46.6
[bmim][PF <sub>6</sub> ]	49.8	48.8
[bmim][NTf <sub>2</sub> ]	36.8	37.5
[hmim][PF <sub>6</sub> ]	36.8	43.4
[omim][PF <sub>6</sub> ]	34.2	36.5

#### 4.4.6 Density

In general, RTILs are denser than water with values ranging from 1 to 1.6 g cm<sup>-3</sup>. Such high densities have advantages in the phase separation with immiscible liquid mixtures, but drawback with this high density is faced when mixing is required. Their densities decrease with increase in the length of the alkyl chain in the cation. The molar mass of the anion significantly affects the overall density of the RTILs. The density increases as the molar mass increases<sup>49</sup>. Addition of CH<sub>2</sub>-groups to the alkyl chain of [C<sub>n</sub>mim]<sup>+</sup> cation decreases the density due to the fact that CH<sub>2</sub> is less dense than imidazolium ring<sup>22</sup>. The density of RTILs having [bmim]<sup>+</sup> cation decrease with increase in anion volume<sup>50</sup>. An increase in the water content decreases the density.

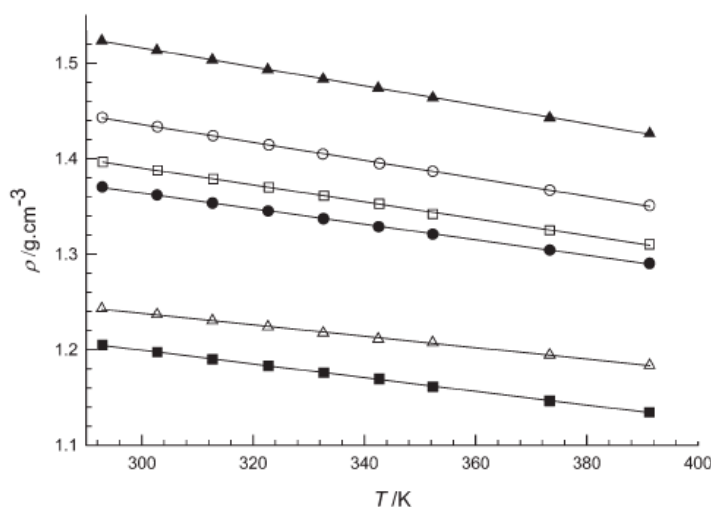


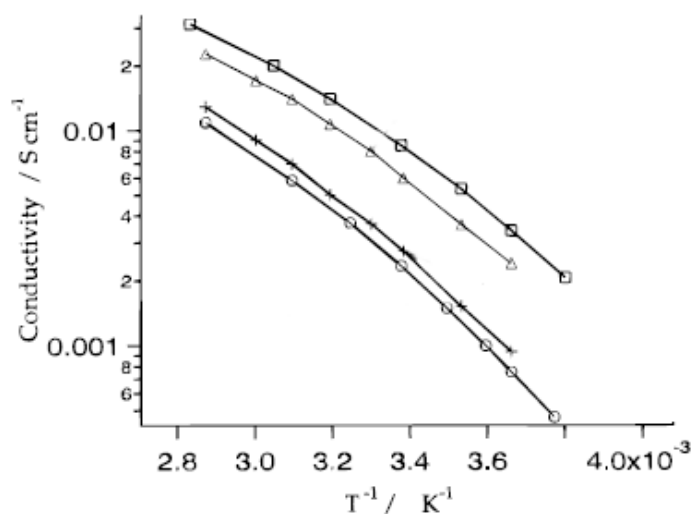
Figure 4.12 Experimental densities of the dried RTILs as a function of temperature: (●) [bmim][PF<sub>6</sub>], (○) [bmim][NTf<sub>2</sub>], (■) [bmim][BF<sub>4</sub>], (□) N<sub>4111</sub>[NTf<sub>2</sub>], (▲) [emim][NTf<sub>2</sub>], (Δ) [emim][EtSO<sub>4</sub>]. [Adapted from 41]

Table 4.7 Densities of several RTILs

RTILs	T (°C)	Density (gcm <sup>-3</sup> )	Reference
[mmim][NTf <sub>2</sub> ]	30	1.57	27
[emim][BF <sub>4</sub> ]	25	1.28	42
		1.24	43
		1.279	44
		1.28	28
[emim][PF <sub>6</sub> ]	26	1.52	42
[emim][NTf <sub>2</sub> ]	25	1.518	44
	22	1.52	18
	30	1.51	27
[emim][NMs <sub>2</sub> ]	25	1.34	49
[bmim]BF <sub>4</sub> ]	25	1.26	42
	25	1.21	28
	25	1.12	22
	20	1.17	31
	30	1.17	30
	30	1.2	27
[bmim][NTf <sub>2</sub> ]	25	1.43	42
	20	1.43	18
	30	1.43	27
[bmim][PF <sub>6</sub> ]	25	1.35	42
	20	1.36	31
	30	1.37	27
	25	1.37	30
[bmim][OTf]	25	1.29	42
	25	1.22	18
	30	1.29	27
[bmim][CF <sub>3</sub> CO <sub>2</sub> ]	30	1.21	27
	25	0.32	18
[bmim][C <sub>2</sub> F <sub>5</sub> SO <sub>2</sub> ] <sub>2</sub> N]	30	1.51	27
[hmim][NTf <sub>2</sub> ]	30	1.37	27
[omim][NTf <sub>2</sub> ]	30	1.31	27

#### 4.4.7 Conductivity

Conductivity is one of the very important electrochemical properties. RTILs are concentrated electrolyte solutions and due to this it would be expected that they should have high conductivities but it is not the case. The highest reported conductivity of RTILs is much lower in comparison to conventional aqueous electrolyte solutions. The conductivity depend not only the numbers of ions, but also on their mobility. The bulky size ions<sup>18,26</sup> reduces its mobility which in turns reduces its conductivity. It can also be understood, that conductivity decreases by increasing the alkyl chain. Furthermore, anionic charge delocalization<sup>18</sup>, density<sup>26</sup> ion pair formation and ion aggregation<sup>44</sup> lead the conductivity. Conductivity and viscosity has an inverse relationship<sup>26</sup>. The less viscous [NTf<sub>2</sub>] salts usually exhibit among the highest conductivities. By increasing temperature, conductivity increases and viscosity decreases.



**Figure 4.13** Specific conductivity of some RTILs as a function of the reciprocal temperature: (□) [emim][OTf], (Δ) [emim][NTf<sub>2</sub>], (+) [bmim][NTf<sub>2</sub>], (○) [bmim][OTf]. [Adapted from 18]

Not only viscosity can account for these behaviour of the conductivity, but there are some other properties of the RTILs which influence the conductivity of RTILs. For example, [emim][OTf] and [bmim][NTf<sub>2</sub>] have similar viscosities and densities but the conductivity of [emim][OTf] is double.



Table 4.8 Conductivities of several RTILs

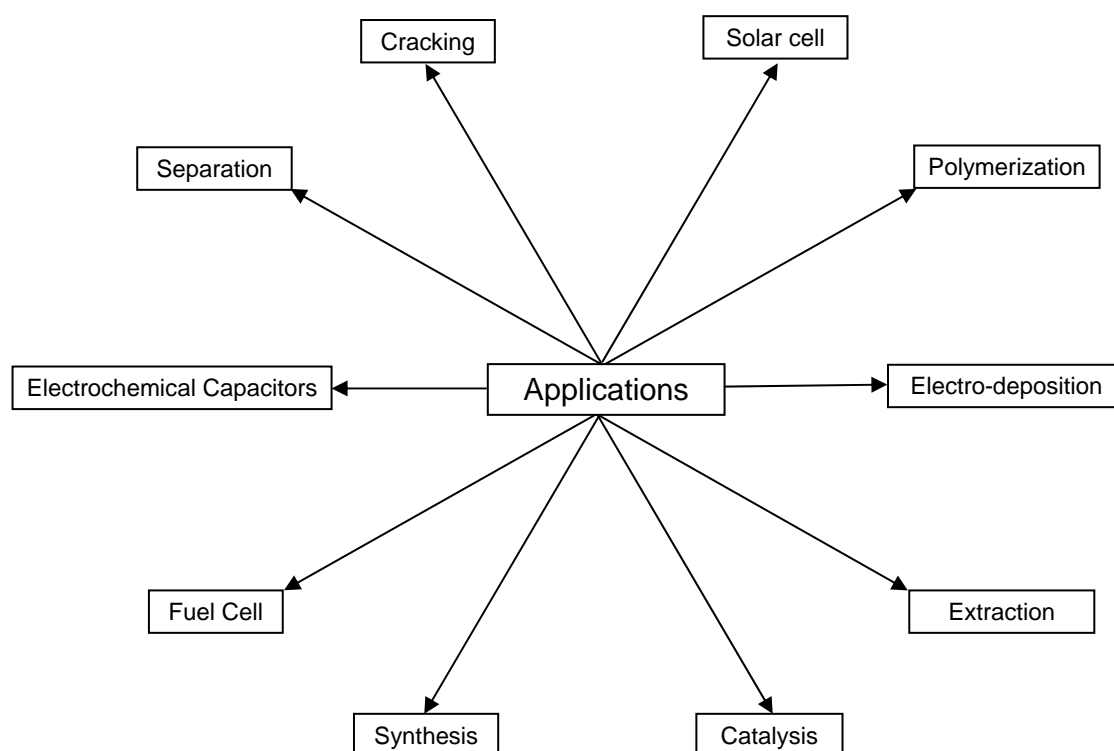
RTILs	T (°C)	Conductivity (Sm <sup>-1</sup> )	Reference
[mmim][NTf <sub>2</sub> ]	30	1.1	27
[emim][BF <sub>4</sub> ]	25	1.58-1.38	42
			30,43
		1.4	28
		1.3	26
[emim][PF <sub>6</sub> ]	26	0.52	42
[emim][NTf <sub>2</sub> ]	25	0.57	44
	22	0.88	31
	30	1.1	27
[emim][NMs <sub>2</sub> ]	25	0.17	49
[bmim]BF <sub>4</sub> ]	25	0.35	42
	25	0.35	28
	20	0.17	31
	30	0.45	27
[bmim][NTf <sub>2</sub> ]	25	0.4	42
	20	0.26	18
	30	0.46	27
[bmim][PF <sub>6</sub> ]	25	0.146-0.1	42
	20	0.14	31
	30	0.19	27
	25	0.15	30
	25	0.16	30
[bmim][OTf]	25	0.29	42
	25	0.37	18
	30	0.36	27
[bmim][CF <sub>3</sub> CO <sub>2</sub> ]	25	0.32	18
	30	0.38	27
[bmim][C <sub>2</sub> F <sub>5</sub> SO <sub>2</sub> ) <sub>2</sub> N]	30	0.19	27
[c <sub>6</sub> mim][NTf <sub>2</sub> ]	30	0.27	27
[c <sub>8</sub> mim][NTf <sub>2</sub> ]	30	0.16	27

## 4.5 Application

Excellent reviews to the expanding applications of RTILs<sup>1,7,24</sup> in organic synthesis, organometallic catalysis<sup>1,23</sup>, enzymatic catalysis, separation processes, nanochemistry, electrochemistry and new material are available.

Their high thermal stability and lack of measurable vapour pressure characterize them as green solvent. They can replace volatile organic solvents in several chemical reactions. Physical chemists, engineers, electrochemists, and scientists are interested to use different techniques for exciting applications by use of RTILs. They are commercially available and remain popular in applications development.

It is being used as a solvent in many different applications.



**Scheme 2: Application of RTILs as solvent**

## Reference:

1. Welton, T. Room-Temperature Ionic Liquids. Solvents for Synthesis and Catalysis. *Chem. Rev. (Washington, D. C.)* **1999**, *99*, 2071-2083.
2. Swatloski, R. P.; Holbrey, J. D.; Rogers, R. D. Ionic Liquids Are Not Always Green: Hydrolysis of 1-Butyl-3-Methylimidazolium Hexafluorophosphate. *Green Chem.* **2003**, *5*, 361-363.
3. Ohno, K. *Electrochemical Aspects of Ionic Liquids*, 2004.
4. Wasserscheid, P.; Welton, T.; Editors *Ionic Liquids in Synthesis*, 2003.
5. Seddon, K. R. Ionic Liquids for Clean Technology. *Journal of Chemical Technology & Biotechnology* **1997**, *68*, 351-356.
6. Dupont, J.; De Souza, R. F.; Suarez, P. A. Z. Ionic Liquid (Molten Salt) Phase Organometallic Catalysis. *Chemical Reviews* **2002**, *102*, 3667-3692.
7. Earle, M. J.; Seddon, K. R. Ionic Liquids. Green Solvents for the Future. *Pure and Applied Chemistry* **2000**, *72*, 1391-1398.
8. Walden, P. *Bull. Acad. Imper. Sci. St. Pétersbourg.* **1914**, *6* 405-422.
9. Chum, H. L.; Koch, V. R.; Miller, L. L.; Osteryoung, R. A. An Electrochemical Scrutiny of Organometallic Iron Complexes and Hexamethylbenzene in a Room Temperature Molten Salt [32]. *J. Am. Chem. Soc.* **1975**, *97*, 3264-3265.
10. Wilkes, J. S.; Levisky, J. A.; Wilson, R. A.; Hussey, C. L. Dialkylimidazolium Chloroaluminate Melts: A New Class of Room-Temperature Ionic Liquids for Electrochemistry, Spectroscopy, and Synthesis. *Inorganic Chemistry* **1982**, *21*, 1263-1264.
11. Hitchcock, P. B.; Mohammed, T. J.; Seddon, K. R.; Zora, J. A.; Hussey, C. L.; Haynes Ward, E. 1-Methyl-3-Ethylimidazolium Hexachlorouranate(IV) and 1-Methyl-3-Ethylimidazolium Tetrachlorodioxo-Uranate(VI): Synthesis, Structure, and Electrochemistry in a Room Temperature Ionic Liquid. *Inorganica Chimica Acta* **1986**, *113*.
12. Wilkes, J. S. A Short History of Ionic Liquids - from Molten Salts to Neoteric Solvents. *Green Chem.* **2002**, *4*, 73-80.
13. Hussey, C. L.; Scheffler, T. B.; Wilkes, J. S.; Fannin Jr, A. A. Chloroaluminate Equilibria in the Aluminum Chloride-1-Methyl-3-Ethylimidazolium Chloride Ionic Liquid. *J. Electrochem. Soc.* **1986**, *133*, 1389-1391.
14. Silvester, D. S.; Compton, R. G. Electrochemistry in Room Temperature Ionic Liquids: A Review and Some Possible Applications. *Z. Phys. Chem. (Muenchen, Ger.)* **2006**, *220*, 1247-1274.

15. Wilkes, J. S.; Zaworotko, M. J. Air and Water Stable 1-Ethyl-3-Methylimidazolium Based Ionic Liquids. *Journal of the Chemical Society, Chemical Communications* **1992**, 965-967.
16. Schroder, U.; Wadhawan, J. D.; Compton, R. G.; Marken, F.; Suarez, P. A. Z.; Consorti, C. S.; de Souza, R. F.; Dupont, J. Water-Induced Accelerated Ion Diffusion: Voltammetric Studies in 1-Methyl-3-[2,6-(S)-Dimethylocten-2-Yl]imidazolium Tetrafluoroborate, 1-Butyl-3-Methylimidazolium Tetrafluoroborate and Hexafluorophosphate Ionic Liquids. *New J. Chem.* **2000**, *24*, 1009-1015.
17. Matsumiya, M.; Terazono, M.; Tokuraku, K. Temperature Dependence of Kinetics and Diffusion Coefficients for Ferrocene/Ferricenium in Ammonium-Imide Ionic Liquids. *Electrochim. Acta* **2006**, *51*, 1178-1183.
18. Bonhote, P.; Dias, A.-P.; Papageorgiou, N.; Kalyanasundaram, K.; Gratzel, M. Hydrophobic, Highly Conductive Ambient-Temperature Molten Salts†. *Inorganic Chemistry* **1996**, *35*, 1168-1178.
19. Davis Jr, J. H. Task-Specific Ionic Liquids. *Chemistry Letters* **2004**, *33*, 1072-1077.
20. Seddon, K. R.; Stark, A.; Torres, M. J. Influence of Chloride, Water, and Organic Solvents on the Physical Properties of Ionic Liquids. *Pure and Applied Chemistry* **2000**, *72*, 2275-2287.
21. Eisele, S.; Schwarz, M.; Speiser, B.; Tittel, C. Diffusion Coefficient of Ferrocene in 1-Butyl-3-Methylimidazolium Tetrafluoroborate - Concentration Dependence and Solvent Purity. *Electrochim. Acta* **2006**, *51*, 5304-5306.
22. Huddleston, J. G.; Visser, A. E.; Reichert, W. M.; Willauer, H. D.; Broker, G. A.; Rogers, R. D. Characterization and Comparison of Hydrophilic and Hydrophobic Room Temperature Ionic Liquids Incorporating the Imidazolium Cation. *Green Chem.* **2001**, *3*, 156-164.
23. Wasserscheid, P.; Keim, W. Ionic Liquids - New 'Solutions' for Transition Metal Catalysis. *Angewandte Chemie - International Edition* **2000**, *39*, 3773-3789.
24. Hagiwara, R.; Ito, Y. Room Temperature Ionic Liquids of Alkylimidazolium Cations and Fluoroanions. *Journal of Fluorine Chemistry* **2000**, *105*, 221-227.
25. Ngo, H. L.; LeCompte, K.; Hargens, L.; McEwen, A. B. Thermal Properties of Imidazolium Ionic Liquids. *Thermochimica Acta* **2000**, *357-358*, 97-102.
26. McEwen, A. B.; Ngo, H. L.; LeCompte, K.; Goldman, J. L. Electrochemical Properties of Imidazolium Salt Electrolytes for Electrochemical Capacitor Applications. *J. Electrochem. Soc.* **1999**, *146*, 1687-1695.
27. Tokuda, H.; Tsuzuki, S.; Susan, M. A. B. H.; Hayamizu, K.; Watanabe, M. How Ionic Are Room-Temperature Ionic Liquids? An Indicator of the Physicochemical Properties. *J. Phys. Chem. B* **2006**, *110*, 19593-19600.
28. Nishida, T.; Tashiro, Y.; Yamamoto, M. Physical and Electrochemical Properties of 1-Alkyl-3-Methylimidazolium Tetrafluoroborate for Electrolyte. *Journal of Fluorine Chemistry* **2003**, *120*, 135-141.
29. Fuller, J.; Carlin, R. T.; De Long, H. C.; Haworth, D. Structure of 1-Ethyl-3-Methylimidazolium Hexafluorophosphate: Model for Room Temperature Molten Salts. *Journal of the Chemical Society, Chemical Communications* **1994**, 299-300.
30. Suarez, P., A.Z.; Einloft, S.; Dullius, J., E.L.; de Souza, R., F.; Dupont, J. Synthesis and Physical-Chemical Properties of Ionic Liquids Based on 1-Butyl-3-Methylimidazolium Cation. *J. Chim. Phys.* **1998**, *95*, 1626-1639.

31. Carda-Broch, S.; Berthod, A.; Armstrong, D. W. Solvent Properties of the 1-Butyl-3-Methylimidazolium Hexafluorophosphate Ionic Liquid. *Analytical and Bioanalytical Chemistry* **2003**, *375*, 191-199.
32. Suarez, P. A. Z.; Dullius, J. E. L.; Einloft, S.; De Souza, R. F.; Dupont, J. The Use of New Ionic Liquids in Two-Phase Catalytic Hydrogenation Reaction by Rhodium Complexes. *Polyhedron* **1996**, *15*, 1217-1219.
33. Buzzeo, M. C.; Hardacre, C.; Compton, R. G. Extended Electrochemical Windows Made Accessible by Room Temperature Ionic Liquid/Organic Solvent Electrolyte Systems. *ChemPhysChem* **2006**, *7*, 176-180.
34. Zein El Abedin, S.; Endres, F. Electrodeposition of Metals and Semiconductors in Air- and Water-Stable Ionic Liquids. *ChemPhysChem* **2006**, *7*, 58-61.
35. Fuller, J.; Carlin, R. T.; Osteryoung, R. A. The Room-Temperature Ionic Liquid 1-Ethyl-3-Methylimidazolium Tetrafluoroborate: Electrochemical Couples and Physical Properties. *J. Electrochem. Soc.* **1997**, *144*, 3881-3886.
36. Suarez, P. A. Z.; Selbach, V. M.; Dullius, J. E. L.; Einloft, S.; Piatnicki, C. M. S.; Azambuja, D. S.; De Souza, R. F.; Dupont, J. Enlarged Electrochemical Window in Dialkyl-Imidazolium Cation Based Room-Temperature Air and Water-Stable Molten Salts. *Electrochim. Acta* **1997**, *42*, 2533-2535.
37. Hultgren, V. M.; Mariotti, A. W. A.; Bond, A. M.; Wedd, A. G. Reference Potential Calibration and Voltammetry at Macrodisk Electrodes of Metallocene Derivatives in the Ionic Liquid [Bmim][Pf<sub>6</sub>]. *Analytical Chemistry* **2002**, *74*, 3151-3156.
38. Widegren Jason, A.; Laesecke, A.; Magee Joseph, W. The Effect of Dissolved Water on the Viscosities of Hydrophobic Room-Temperature Ionic Liquids. *Chem Commun (Camb)* **2005**, 1610-1612.
39. Dupont, J. On the Solid, Liquid and Solution Structural Organization of Imidazolium Ionic Liquids. *JOURNAL OF THE BRAZILIAN CHEMICAL SOCIETY* **2004**, *15*, 341-350.
40. Xu, W.; Cooper, E. I.; Angell, C. A. Ionic Liquids: Ion Mobilities, Glass Temperatures, and Fragilities. *J. Phys. Chem. B* **2003**, *107*, 6170-6178.
41. Jacquemin, J.; Husson, P.; Padua, A. A. H.; Majer, V. Density and Viscosity of Several Pure and Water-Saturated Ionic Liquids. *Green Chem.* **2006**, *8*, 172-180.
42. Hapiot, P.; Lagrost, C. Electrochemical Reactivity in Room-Temperature Ionic Liquids. *Chem. Rev. (Washington, DC, U. S.)* **2008**, *108*, 2238-2264.
43. Earle, M. J.; Esperança, J. M. S. S.; Gilea, M. A.; Lopes, J. N. C.; Rebelo, L. P. N.; Magee, J. W.; Seddon, K. R.; Widegren, J. A. The Distillation and Volatility of Ionic Liquids. *Nature* **2006**, *439*, 831-834.
44. Noda, A.; Hayamizu, K.; Watanabe, M. Pulsed-Gradient Spin-Echo <sup>1</sup>H and <sup>19</sup>F Nmr Ionic Diffusion Coefficient, Viscosity, and Ionic Conductivity of Non-Chloroaluminate Room-Temperature Ionic Liquids. *J. Phys. Chem. B* **2001**, *105*, 4603-4610.
45. Okoturo, O. O.; VanderNoot, T. J. Temperature Dependence of Viscosity for Room Temperature Ionic Liquids. *J. Electroanal. Chem.* **2004**, *568*, 167-181.
46. Baker, S. N.; Baker, G. A.; Kane, M. A.; Bright, F. V. The Cybotactic Region Surrounding Fluorescent Probes Dissolved in 1-Butyl-3-Methylimidazolium Hexafluorophosphate: Effects of Temperature and Added Carbon Dioxide. *J. Phys. Chem. B* **2001**, *105*, 9663-9668.

- 
47. Buzzeo, M. C.; Evans, R. G.; Compton, R. G. Non-Haloaluminate Room-Temperature Ionic Liquids in Electrochemistry - a Review. *ChemPhysChem* **2004**, *5*, 1106-1120.
48. Chiappe, C.; Pieraccini, D. Ionic Liquids: Solvent Properties and Organic Reactivity. *Journal of Physical Organic Chemistry* **2005**, *18*, 275-297.
49. Pringle, J. M.; Golding, J.; Baranyai, K.; Forsyth, C. M.; Deacon, G. B.; Scott, J. L.; MacFarlane, D. R. The Effect of Anion Fluorination in Ionic Liquids - Physical Properties of a Range of Bis(Methanesulfonyl)Amide Salts. *New J. Chem.* **2003**, *27*, 1504-1510.
50. Xu, W.; Wang, L. M.; Nieman, R. A.; Angell, C. A. Ionic Liquids of Chelated Orthoborates as Model Ionic Glassformers. *J. Phys. Chem. B* **2003**, *107*, 11749-11756.

## CHAPTER 5. EXPERIMENTAL WORK

### 5.1 Ionic Liquids

Five different RTILs have been used to investigate the effect of cations and anions on the heterogeneous electron transfer rate constant. 1-ethyl-3-methylimidazolium tetrafluoroborate ([emim][BF<sub>4</sub>], 98%), 1-butyl-3-methylimidazolium trifluorosulfane ([bmim][CF<sub>3</sub>SO<sub>3</sub>]) ([bmim][OTf], 99%), 1-butyl-3-methylimidazolium tetrafluoroborate ([bmim][BF<sub>4</sub>], 99%), 1-butyl-3-methylimidazolium hexafluorophosphate ([bmim][PF<sub>6</sub>], 99%) and 1-octyl-3-methylimidazolium tetrafluoroborate ([omim][BF<sub>4</sub>], 99%) were purchased from Io-li-tec (Germany) except [bmim][OTf] which has been purchased from Solvent Innovation, Cologne (Germany). These have been selected to observe the change in physicochemical influence of RTILs on electron transfer rates following an anion replacement, while keeping cations constant and vice versa. Not only the viscosity of these ionic liquids gets enhanced as a function of enlarged cation chain (due to increase in van der Waals interaction) but other physical properties are also affected by this change. On the other hand when different anions get incorporated along same cation i.e. [bmim], the viscosity gets increased as the ability to form hydrogen bond increases between the ions.

The physical properties of RTILs are greatly affected by the presence of even small amount of moisture<sup>1,2</sup>. Special care was taken into account to carry out different measurements in undried (as received) and dried ionic liquids. The measurements in undried (as received) RTILs have been undertaken for different compounds. For the measurements in dried RTILs, their water content was removed from the RTILs before use, by placing them under high vacuum ( $5 \times 10^{-5}$  Torr) for one day at a constant temperature of 60 °C and thereafter kept in a desiccator containing P<sub>4</sub>O<sub>10</sub>. The water content in the RTILs has been assessed by Near infrared (NIR) (spectrometry). In literature, it has been described that water strongly absorbs in the region of 1428nm and 1920nm<sup>3</sup>. The recorded spectra for the undried and dried ionic liquids are shown in figure 1. By comparing it can be observed that after applying high vacuum for one day, moisture has been almost eliminated from the RTILs. The absence of other impurity has also been confirmed by recording cyclic voltammograms of the RTILs.

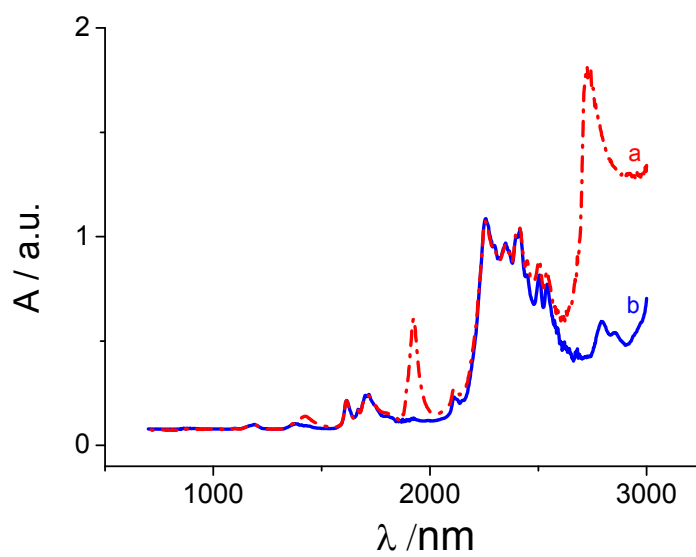


Figure 5.1 NIR spectra for [bmim][OTf] (a) undried (b) dried.

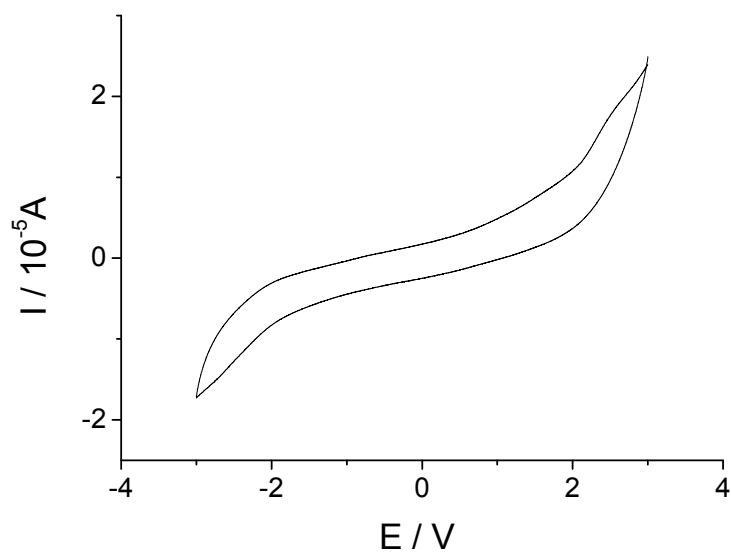


Figure 5.2 CV of [emim][BF<sub>4</sub>] at scan rate 100 mV s<sup>-1</sup>



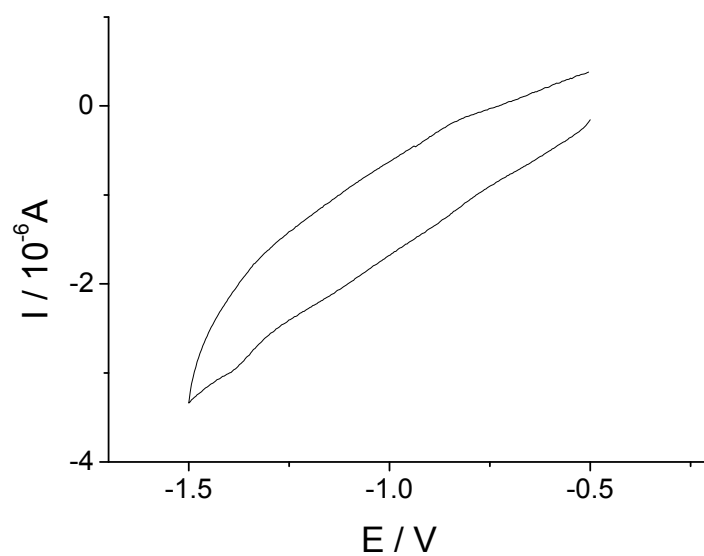


Figure 5.3 CV of [bmim][OTf] at scan rate  $20 \text{ mV s}^{-1}$

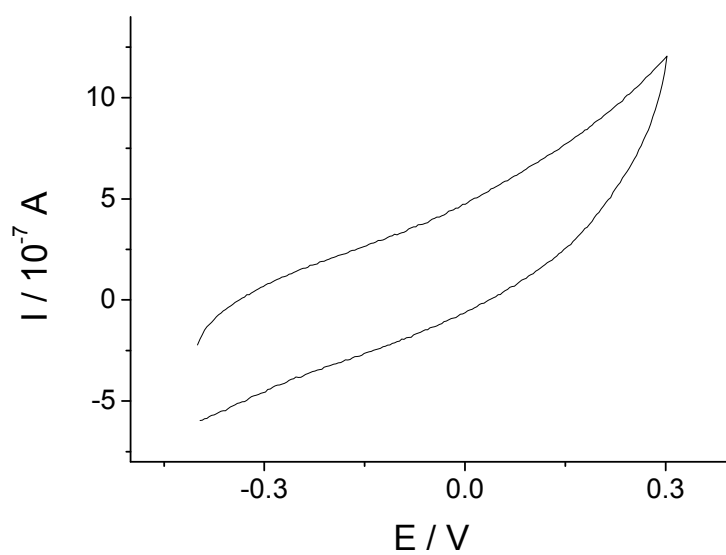


Figure 5.4 CV of [bmim][OTf] at scan rate  $20 \text{ mV s}^{-1}$

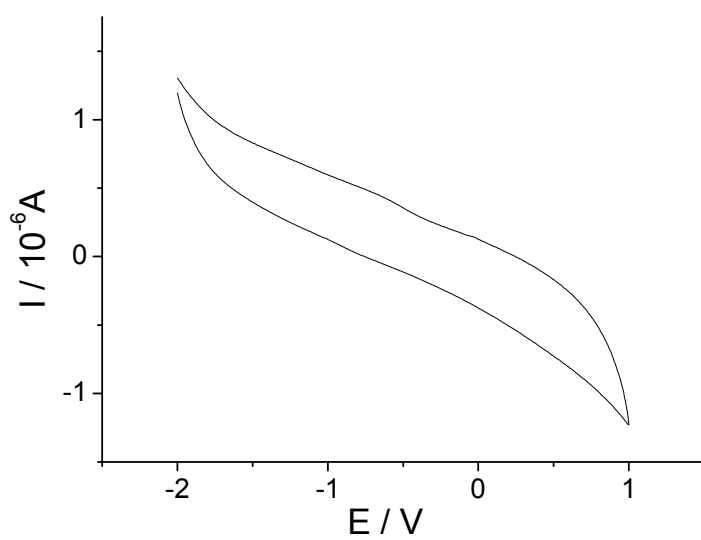
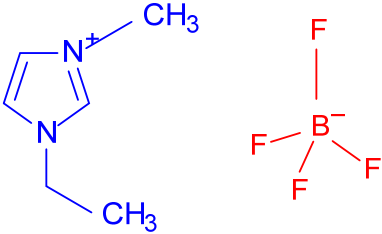
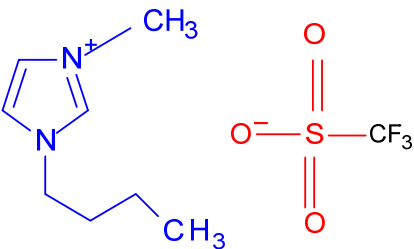
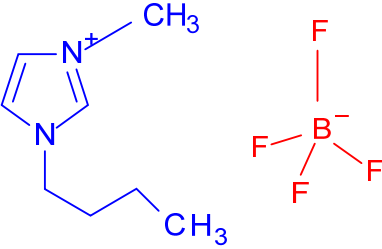
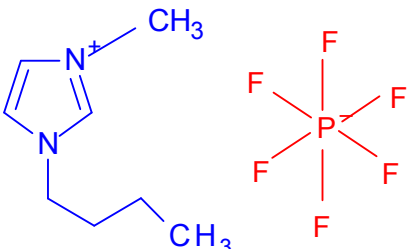
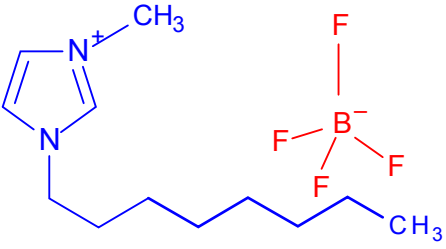


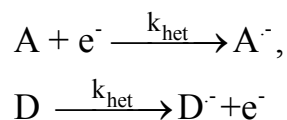
Figure 5.5 CV of [bmim][PF<sub>6</sub>] at scan rate 100 mV s<sup>-1</sup>

Table 5.1 Physical properties of RTILs

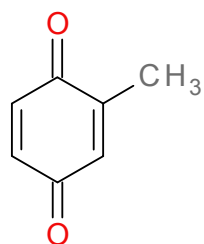
RTIL	Structure	Properties
1 [emim][BF <sub>4</sub> ]		1-ethyl-3-methylimidazolium tetrafluoroborate $\eta = 43 \text{ cP}^4$ $r^+ = 3.03 \text{ \AA}^5$ $r^- = 2.29 \text{ \AA}^6$
2 [bmim][OTf]		1-butyl-3-methylimidazolium trifluorosulfate $\eta = 90 \text{ cP}^7$ $r^+ = 3.36 \text{ \AA}^6$
3 [bmim][BF <sub>4</sub> ]		1-butyl-3-methylimidazolium tetrafluoroborate $\eta = 219 \text{ cP}^1$ $r^+ = 3.36 \text{ \AA}^6$ $r^- = 2.29 \text{ \AA}^6$
4 [bmim][PF <sub>6</sub> ]		1-butyl-3-methylimidazolium hexafluoro- phosphate $\eta = 312 \text{ cP}^8$ $r^+ = 3.36 \text{ \AA}^6$ $r^- = 2.72 \text{ \AA}^6$
5 [omim][BF <sub>4</sub> ]		1-octyl-3-methylimidazolium tetrafluoroborate $\eta = 341 \text{ cP}^9$ $r^+ = 3.73 \text{ \AA}^5$ $r^- = 2.72 \text{ \AA}^6$

## 5.2 Reagents

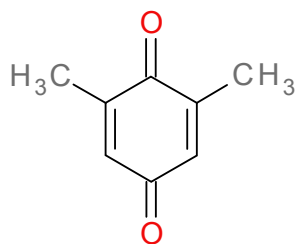
Various acceptor (A) and donor (D) systems have been used to study the heterogeneous electron transfer in RTILs.



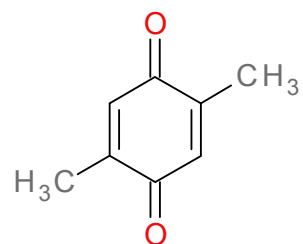
Different quinone derivatives and also some other redox couples have been used, like methylbenzoquinones (MBQ) (Aldrich, 98%), 2,5-dimethylbenzoquinone (2,5-DMBQ) (Eastman, 98%), 2,6-dimethylbenzoquinone (2,6-DMBQ) (Aldrich, 98%), duroquinone (DQ) (Merck, 99%), tetrabromobenzoquinone (bromanil) (TBBQ) (Alfa Aesar, 95%), tetrachlorobenzoquinone (chloranil) (TCBQ) (Aldrich, 99%), methylviologen ( $MV^{2+}$ ) (Fluka, 98%) and ethylviologen ( $EV^{2+}$ ) (Fluka, 98%), tetracyanoethylene (TCNE) (Fluka, 97%). Electrochemical oxidation has been studied by using numerous donor systems in RTILs. Ferrocene (Fc) (Fluka, 98%), p-phenylenediamine (PPD) (Roth, 99%), N,N,N',N'-tetramethyl-p-phenylenediamine (TMPPD) (Fluka, 98%), 2,3,5,6-tetramethyl-p-phenylenediamine (Duro-PPD) (97%), 2,2,6,6-tetramethylpiperidinyloxy radical (TEMPO) (Aldrich, 99%), 4-hydroxy-2,2,6,6-tetramethylpiperidinyloxy radical (TEMPOL) (Aldrich, 99.9%), tetrathiofulvalene (TTF) (Fluka, 97%).



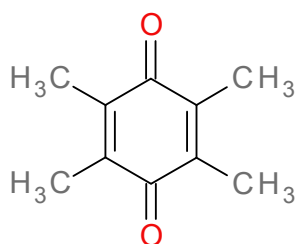
MBQ



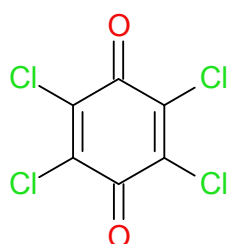
2,6-DMBQ



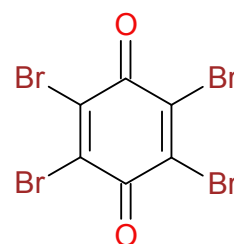
2,5-DMBQ



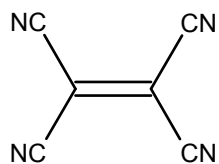
DQ



TCBQ



TBBQ



TCNE

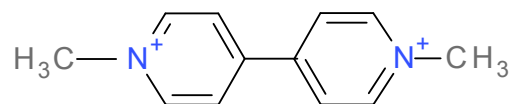
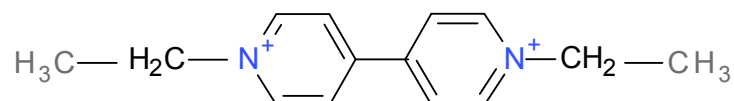
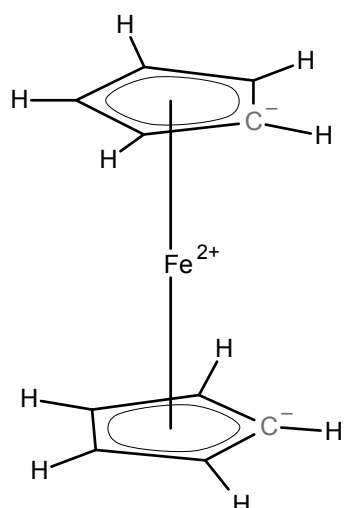
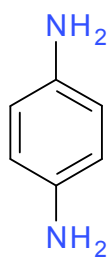
MV<sup>2+</sup>EV<sup>2+</sup>

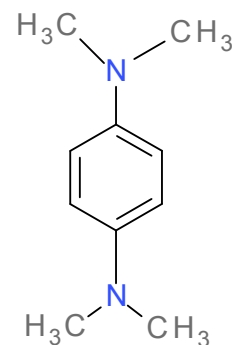
Figure 5.6 Acceptor Systems



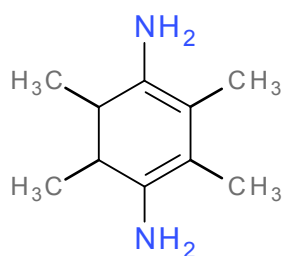
Fc



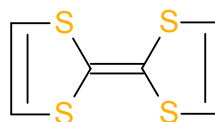
PPD



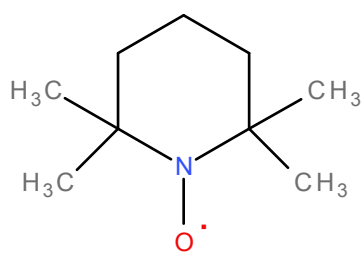
TMPPD



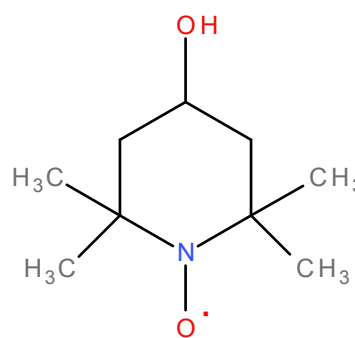
Duro-PPD



TTF



TEMPO



TEMPOL

Figure 5.7 Donor systems

### 5.3 Sample Handling

Compounds were purified by different standard methods. Sublimation has been employed to purify Fc, MBQ, 2,5-DMBQ, 2,6-DMBQ, DQ, 2,6-DTBBQ, TBBQ, TCBQ, TCNE, TEMPO, TEMPOL, PPD and TMPPD compounds. Purification of  $MV^{2+}$  and  $EV^{2+}$  has been done by recrystallization from ethanol. Duro-PPD was also recrystallized from ethanol. Acetonitrile has been purified by distillation after drying over molecular sieve (3 Å).

Because of the sensitivity of the RTILs towards moisture, samples have been prepared under dry argon in dried RTILs using the Sehlenck-technique to avoid moisture impurity.

### 5.4 Apparatus

#### 5.4.1 NIR Spectrometer

NIR spectra have been recorded for the RTILs by using a Shimadzu UV-VIS-NIR scanning spectrophotometer type UV-3101PC. A special quartz cell has been used which is specially made for NIR measurements. The optical path length of this cell is 1 mm. Only one millilitre of the RTILs has been used to do NIR measurements.

#### 5.4.2 iR Drop Measurements

Determination of the iR drop has been done by using a frequency generator, Feedback sine square Oscillator SSO603. Voltage has been measured by a Voltcraft plus, Digital multimeter VC 940. A DMM 3020 Digital multimeter has been used for current measurements.

#### 5.4.3 Room Temperature Electrochemical Cell

At room temperature all cyclic voltammetric experiments were carried out using a custom made electrochemical cell, designed for investigation of micro-volume samples of ionic liquids under argon (Fig 2). This cell is similar to that first described by Compton et al<sup>10</sup>. All experiments were performed with a three electrode arrangement in a drop of ionic liquid solution. Ag/AgCl or a tungsten wire was used as a reference electrode. A glassy carbon rod of 2mm diameter functioned as working electrode. A Pt-wire served as a counter electrode. A drop of ionic liquid solution is placed in the cell at the surface of the working electrode which is surrounded by the Pt-wire counter

electrode. The reference electrode is in contact with the solution from the upper side of the cell.

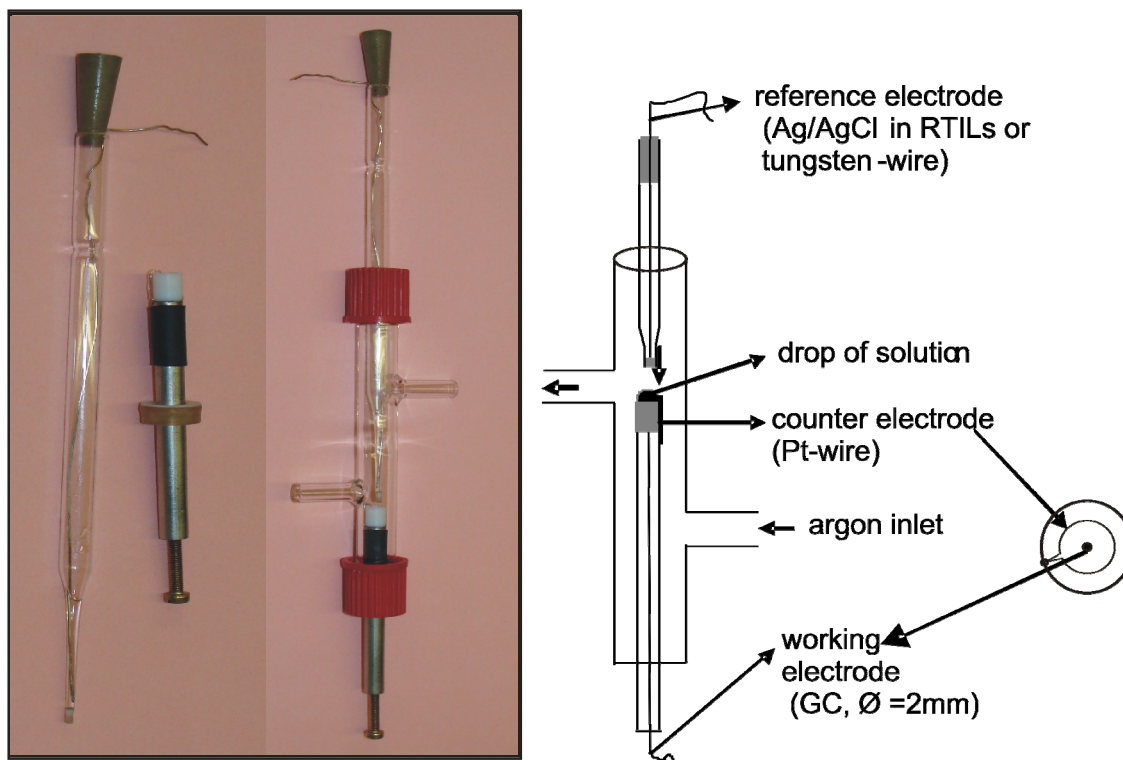


Figure 5.8 Cell design for electrochemical measurement in RTILs at room temperature

#### 5.4.4 Temperature Controlled Electrochemical Cell

Measurements at various temperatures have been performed by using a specifically designed temperature controlled cell. There are different groups in the world, who are working with electrochemistry in RTILs but no one is using this type of temperature controlled cell. It has been employed for the first time in our lab. The size of the working electrode is similar to that described in the room temperature electrochemical cell. Only Ag/AgCl dipped in RTILs has been used as reference in temperature cell because tungsten is unable to provide a stable potential window as the temperature is varied. The design is also similar to the room temperature cell but there are two additional lines for water. These water lines are connected with a thermostat to work at a particular temperature. 0.2 ml solution of RTILs has been used in this cell to work at different temperature. A thermocouple is attached close to the solution side of the cell to measure the exact temperature of the cell. Figure 5.9



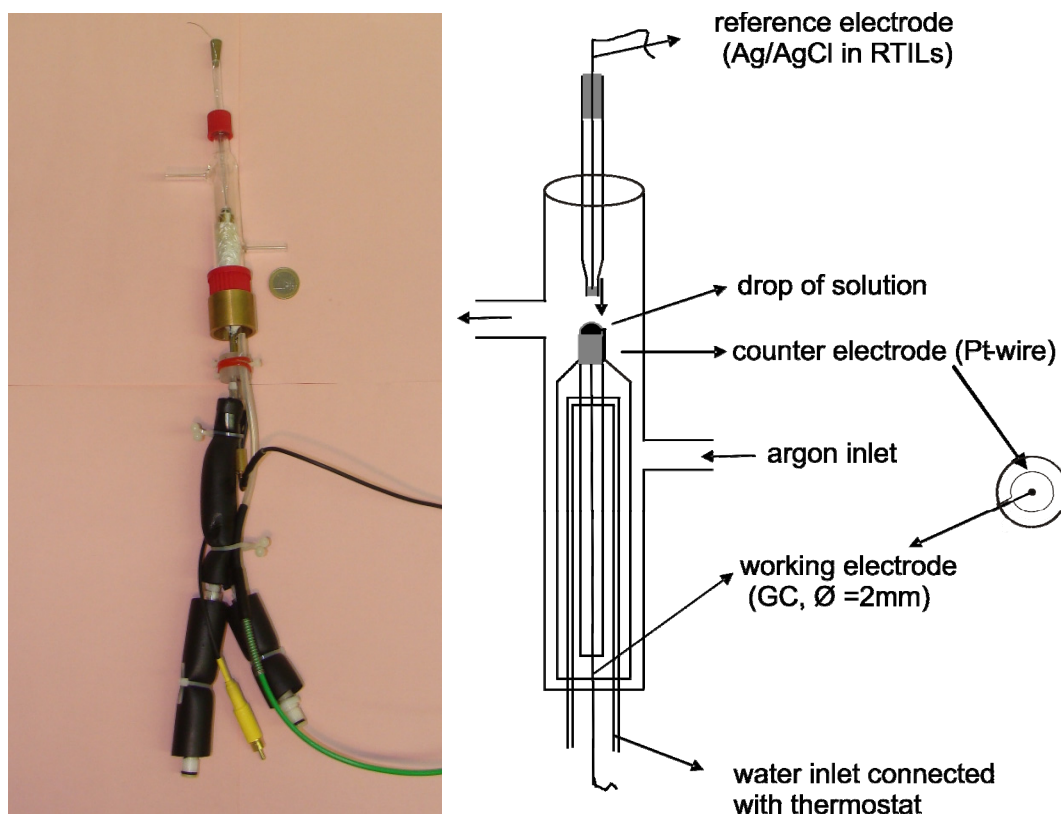


Figure 5.9 Temperature controlled cell constructed for RTILs

#### 5.4.5 Potentiostat and Software

The measurements were performed using an Autolab/EAs 2 computer-controlled electrochemical system equipped with a potentiostat (model PGSTAT 302N). The software GPES (version 4.9.007) was used for the electrochemical measurements.

#### 5.4.6 Computational Work

The Molden software has been used for the visualization of the structure of the reactant specie. The program Orca has been employed for all computation.

Mopac has also been used for AM-1 computation calculation.

### 5.5 Procedure

#### 5.5.1 NIR Spectrum

NIR spectra of dried and undried RTILs have been recorded. RTILs were carefully transferred into the quartz cell under argon to avoid moisture as impurity. Very slow scanning has been applied from 700 to 3000 nm to observe the small peaks in NIR spectra.

### 5.5.2 iR drop Measurements

iR drop has been determined by Bode plot. Concentration dependent measurements have been done as well for this regard. Cyclic voltammograms have also been recorded for ferrocene with different concentration in ionic liquids. These measurements have been carried out at room temperature at various scan rates in five different concentrations of an analyte in ionic liquids. The change in width of the peak potential has been observed by changing scan rate and concentration. The effect of concentration has been observed by comparing the values of diffusion coefficients as well.

### 5.5.3 Room Temperature Measurements

All compounds listed above have been subjected to studying the heterogeneous electron transfer rate constant at room temperature. Both dried and undried ILs have been utilized for this purpose. Only Duro-PPD has been studied in undried ILs. All experiments have been conducted at room temperature  $T = 298 \pm 2$  K by utilizing the specially designed room temperature cell for RTILs. Cyclic voltammograms have been recorded at different scan rates from 20 to 500  $\text{mV sec}^{-1}$ . (20, 50, 75, 100, 125, 150, 175, 200, 300, 400 and 500  $\text{mV sec}^{-1}$ ).

### 5.5.4 Temperature Dependent Measurements

Temperature dependent measurements have been carried out by using the different compounds, which have been listed above in both dried and undried RTILs. All experiments have been done at various temperatures from 288 K to 353 K with a 5 K interval. At each temperature, cyclic voltammograms have been recorded at different scan rates from 20 to 500  $\text{mV sec}^{-1}$ .

### 5.5.5 Measurements in Binary Mixtures

A few measurements have also been done in binary mixture of RTILs and acetonitrile. Different percentage mixtures have been prepared by taking these two solvents. 20%, 40%, 60%, 80% and 100% (v/v) solution has been prepared by volume from RTILs and acetonitrile. Only room temperature measurements have been studied with binary mixtures. Cyclic voltammograms have been recorded at various scan rates as in the room temperature measurements.

1. Huddleston, J. G.; Visser, A. E.; Reichert, W. M.; Willauer, H. D.; Broker, G. A.; Rogers, R. D. Characterization and Comparison of Hydrophilic and Hydrophobic Room Temperature Ionic Liquids Incorporating the Imidazolium Cation. *Green Chem.* **2001**, *3*, 156-164.
2. Wasserscheid, P.; Welton, T.; Editors *Ionic Liquids in Synthesis*, 2003.
3. Tran, C. D.; De Paoli Lacerda, S. H.; Oliveira, D. Absorption of Water by Room-Temperature Ionic Liquids: Effect of Anions on Concentration and State of Water. *Appl. Spectrosc.* **2003**, *57*, 152-157.
4. McEwen, A. B.; Ngo, H. L.; LeCompte, K.; Goldman, J. L. Electrochemical Properties of Imidazolium Salt Electrolytes for Electrochemical Capacitor Applications. *J. Electrochem. Soc.* **1999**, *146*, 1687-1695.
5. Tokuda, H.; Hayamizu, K.; Ishii, K.; Susan, M. A. B. H.; Watanabe, M. Physicochemical Properties and Structures of Room Temperature Ionic Liquids. 2. Variation of Alkyl Chain Length in Imidazolium Cation. *J. Phys. Chem. B* **2005**, *109*, 6103-6110.
6. Arzhantsev, S.; Jin, H.; Baker, G. A.; Maroncelli, M. Measurements of the Complete Solvation Response in Ionic Liquids. *J. Phys. Chem. B* **2007**, *111*, 4978-4989.
7. Bonhote, P.; Dias, A.-P.; Papageorgiou, N.; Kalyanasundaram, K.; Gratzel, M. Hydrophobic, Highly Conductive Ambient-Temperature Molten Salts†. *Inorganic Chemistry* **1996**, *35*, 1168-1178.
8. Suarez, P., A.Z.; Einloft, S.; Dullius, J., E.L.; de Souza, R., F.; Dupont, J. Synthesis and Physical-Chemical Properties of Ionic Liquids Based on 1-Butyl-3-Methylimidazolium Cation. *J. Chim. Phys.* **1998**, *95*, 1626-1639.
9. Harris, K. R.; Kanakubo, M.; Woolf, L. A. Temperature and Pressure Dependence of the Viscosity of the Ionic Liquids 1-Methyl-3-Octylimidazolium Hexafluorophosphate and 1-Methyl-3-Octylimidazolium Tetrafluoroborate. *Journal of Chemical & Engineering Data* **2006**, *51*, 1161-1167.
10. Schroder, U.; Wadhawan, J. D.; Compton, R. G.; Marken, F.; Suarez, P. A. Z.; Consorti, C. S.; de Souza, R. F.; Dupont, J. Water-Induced Accelerated Ion Diffusion: Voltammetric Studies in 1-Methyl-3-[2,6-(S)-Dimethylocten-2-Yl]Imidazolium Tetrafluoroborate, 1-Butyl-3-Methylimidazolium Tetrafluoroborate and Hexafluorophosphate Ionic Liquids. *New J. Chem.* **2000**, *24*, 1009-1015.

## CHAPTER 6. THE iR DROP

A drop in potential caused by solution resistance is called an iR drop. When a faradic current flows through a working electrode it changes its potential. Accordingly, the iR drop can have a significant effect on electrochemical measurements and therefore during interpretation of electrochemical results iR drop effects must be given due importance.

The problems, in interpretation of electrochemical data, associated with iR drop are well documented<sup>1-2</sup>. Efforts that have been directed towards overcoming the problem resulted in the availability of potentiostats which provide an automatic iR compensation<sup>3</sup>. One should be very careful about iR drop phenomenon while measuring with high current densities or working in a media of low conductivity.

If uncompensated resistance is significant it can affect the shape of voltammograms. The likely outcome of this lacuna is that the peak potential separation,  $\Delta E_p$  (width of peak potential) increases; the peak width gets enlarged and the peak current drops due to such uncompensated resistance. This effect gets more pronounced with increasing scan rate. However such behaviour is also a characteristic of quasi reversible reactions, where with an increase in scan rate,  $\Delta E_p$  gets enhanced<sup>4</sup>.

One can distinguish between the quasi reversible reaction and the iR drop effect by changing scan rate for two different experiments performed at two different concentrations. If the reason of peak separation is a kinetic based phenomenon, the same behaviour is likely to be observed at two different concentrations. If it is due to iR drop, then only at the higher concentration, the increase in peak separation is large.

### 6.1 Factors Affecting the iR Drop

Uncompensated resistance mainly depends on the following factors:

- Specific conductivity of the solution
- Design of the cell
- Arrangements of the electrode in the cell

Uncompensated resistance can be minimized by increasing the concentration of supporting electrolyte (in electrochemical experiments performed in conventional

solvents). An increase in the concentration of the supporting electrolyte helps raise the conductivity which reduces the resistance of the solution.

The distance between the working and reference electrode also affects the iR drop. The reference electrode should be placed in closed proximity to the working electrode surface to reduce the iR drop. Alternatively, by using a three electrode assembly, the iR drop can be minimized because in this type of arrangement the current is flowing through the counter electrode. It can also be minimized by using a microelectrode<sup>5</sup> and in such an arrangement iR drop decreases approximately in proportion to the electrode diameter<sup>6</sup>. Less current is flowing through the small surface of working electrode. A special microelectrode has been prepared by B.D. Cahan<sup>7-8</sup> showing undisturbed linear electric field.

## 6.2 The iR Drop in Ionic Liquids

All electrochemical measurements have been done in ionic liquids without adding any supporting electrolyte. Ionic liquids are composed of ions, having good conductivity values. These ions may serve a dual purpose. They act as solvent as well as electrolyte for electrochemical measurements. Each ionic liquid has a particular conductivity value so it is not possible for these particular experiments, to change its conductivity by adding electrolyte solution as it has been explained in Chapter 4. However, the electrochemical cell has been designed in a way that the reference and the working electrodes are kept roughly 0.5 mm apart. Ionic liquids may also have some resistance value. It is interesting to know these values for making the results more meaningful.

## 6.3 Calculation of the iR Drop

iR drop in ionic liquids has been measured by performing various experiments such as

- Concentration dependent Measurements
- Determination of uncompensated resistance by Bode plot
- Theoretical calculations for the iR drop

### 6.3.1 Concentration Dependent Measurements

The concentration dependent measurements have been performed to see the effect of concentration on the shape of the cyclic voltammogram. In order to evaluate the iR drop, such type of investigations have been performed in literature<sup>6,9-11</sup>.

Five different concentrations of ferrocene have been used to study the IR drop in ionic liquids. All solutions have been prepared in [emim][BF<sub>4</sub>] by solvent evaporation method. The concentration difference is not very high because of the low solubility of ferrocene in ionic liquids.

Cyclic voltammograms have been recorded between 10 mV s<sup>-1</sup> and 1 V s<sup>-1</sup> scan rate for each concentration at room temperature. Change in current can be seen with increase in scan rate. At high concentration, the highest peak current has been observed.

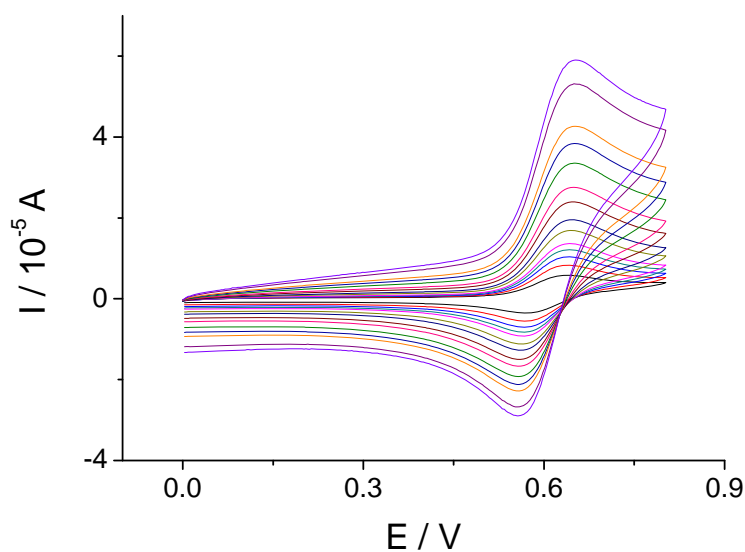


Figure 6.1 Cyclic voltammograms of  $5.51 \times 10^{-3}$  M ferrocene at a different scan rates

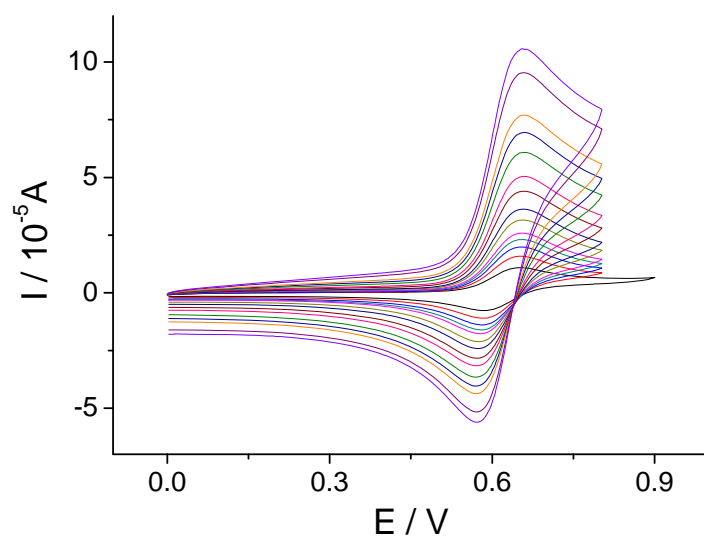


Figure 6.2 Cyclic voltammogram of  $1.10 \times 10^{-2} \text{ M}$  ferrocene at a different scan rates

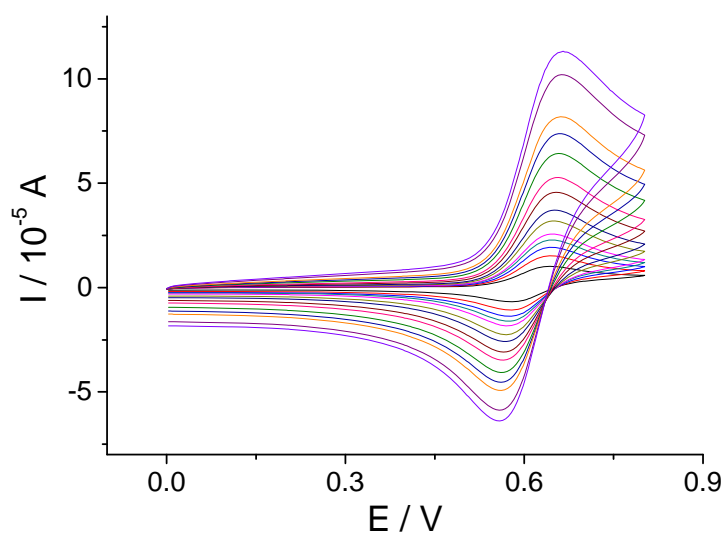


Figure 6.3 Cyclic voltammogram of  $1.65 \times 10^{-2} \text{ M}$  ferrocene at a different scan rates

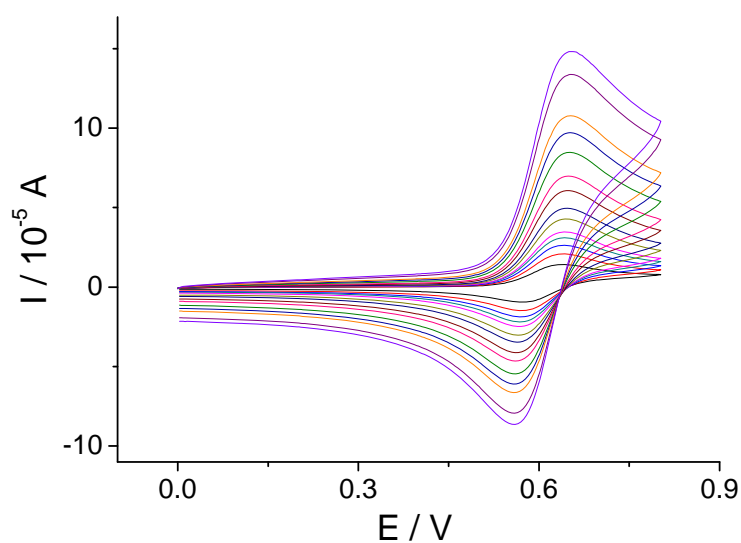


Figure 6.4 Cyclic voltammogram of  $2.20 \times 10^{-2}$  M ferrocene at a different scan rates

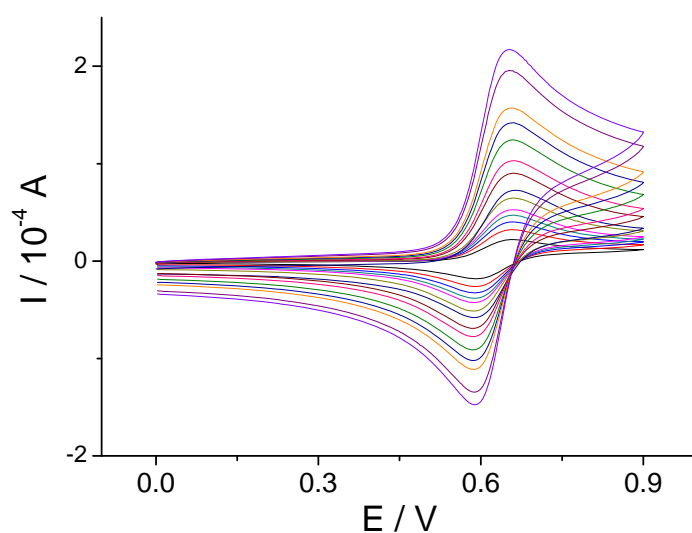


Figure 6.5 Cyclic voltammogram of  $5.09 \times 10^{-2}$  M ferrocene at a different scan rates

The value of peak separation ( $\Delta E_p$ ) has been measured at each scan rate for every concentration and it has been tabulated in

Table 6.1.

There is not a big difference in peak separation with change in concentration. It is in the range of 66 mV to 68 mV at  $20 \text{ mV s}^{-1}$ .

It can be seen from table that  $\Delta E_p$  is not changing very much at different scan rates as the concentration is varied.





Table 6.1 Value of  $\Delta E_p$  at different concentrations and at different scan rates for ferrocene

scan rate/ $\text{mVs}^{-1}$	$5.51 \times 10^{-3}$ (M)	$1.10 \times 10^{-2}$ (M)	$1.65 \times 10^{-2}$ (M)	$2.20 \times 10^{-2}$ (M)	$5.09 \times 10^{-2}$ (M)	Average
10	61.04	67.13	64.03	64.09	67.14	64.69
20	68.05	68.33	66.39	68.04	67.83	67.73
30	70.19	73.25	70.19	70.19	70.19	70.80
40	73.24	73.25	70.19	70.19	70.19	71.41
50	73.24	79.35	73.24	73.24	70.19	73.85
75	79.35	82.4	76.29	76.29	73.24	77.51
100	82.4	82.4	79.34	73.24	73.24	78.12
150	85.45	82.4	85.45	85.45	73.24	82.40
200	85.45	82.4	91.55	85.45	73.24	83.62
300	88.5	85.45	94.61	85.45	73.24	85.45
400	88.5	85.45	94.61	88.5	67.14	84.84
500	91.55	85.15	97.66	89.44	64.09	85.58
800	88.5	82.4	97.66	85.45	64.09	83.62
1000	88.5	85.45	100.71	88.5	67.14	86.06
Average	80.28	79.63	82.99	78.82	69.59	

### 6.3.2 Determination of Uncompensated Resistance by Bode Plots

The uncompensated resistance can easily be determined from Bode plots. The logarithm of the resistance has been plotted against the logarithm of the frequency in order to determine the value of the uncompensated resistance. Such a plot is known as Bode plot. Sine-Wave generator SSO603 has been used as frequency source. Voltage has been measured between the reference and working electrodes using a Voltcraft plus, Digital multimeter VC 940 while the current has been measured through counter and working electrode using a Kontron electronic, DMM 3020 Digital multimeter. The resistance has been calculated from voltage and current data which has been recorded at different frequencies for each ionic liquid.

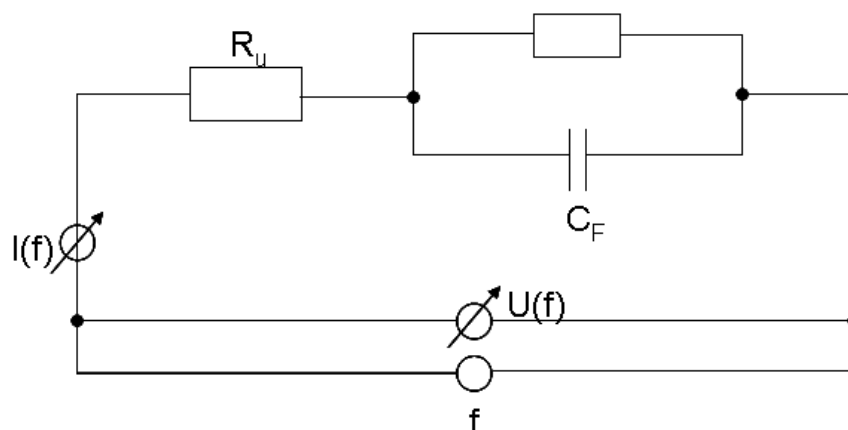


Figure 6.6 Circuit diagram for measuring the uncompensated resistance by Bode plot

The value of the resistance which has been obtained for all used ionic liquids is in the range of few hundred ohms, and usually the current which has been recorded during measurement is in micro ampere range. It suggests that the IR drop is few millivolt which is negligible.

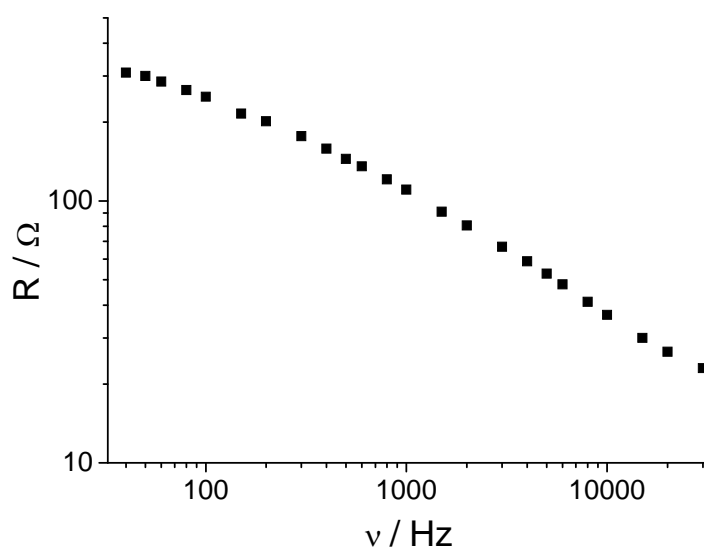


Figure 6.7 Bode plot for [emim][BF<sub>4</sub>]

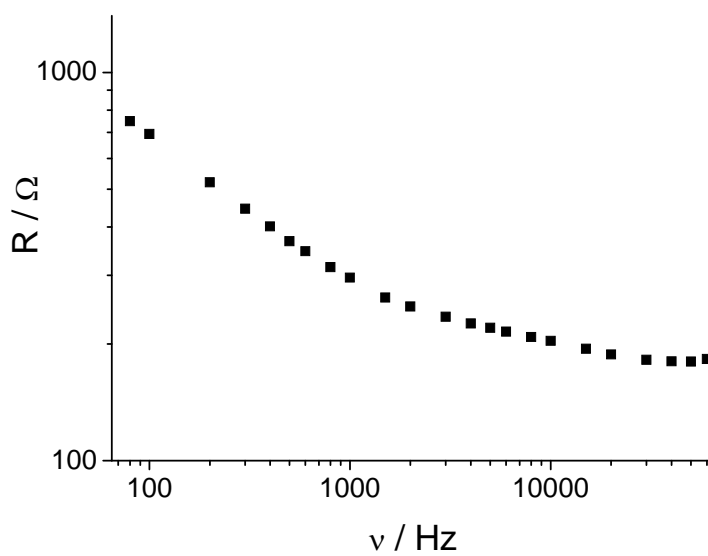


Figure 6.8 Bode plot for [bmim][OTf]

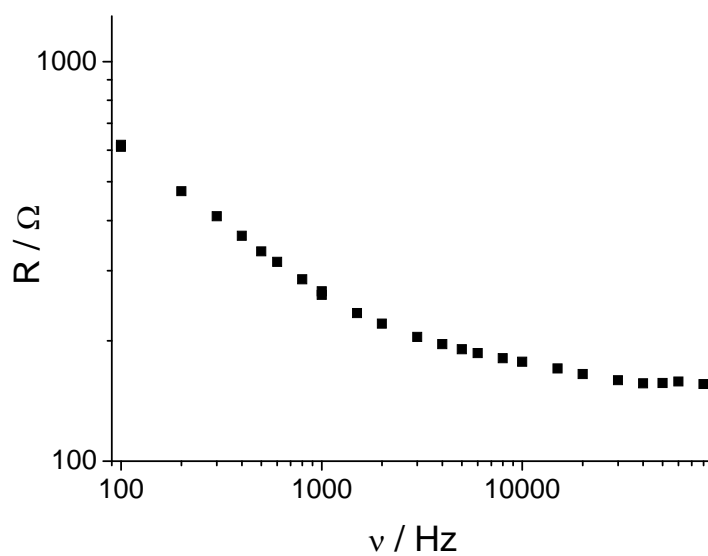


Figure 6.9 Bode plot for [bmim][BF<sub>4</sub>]

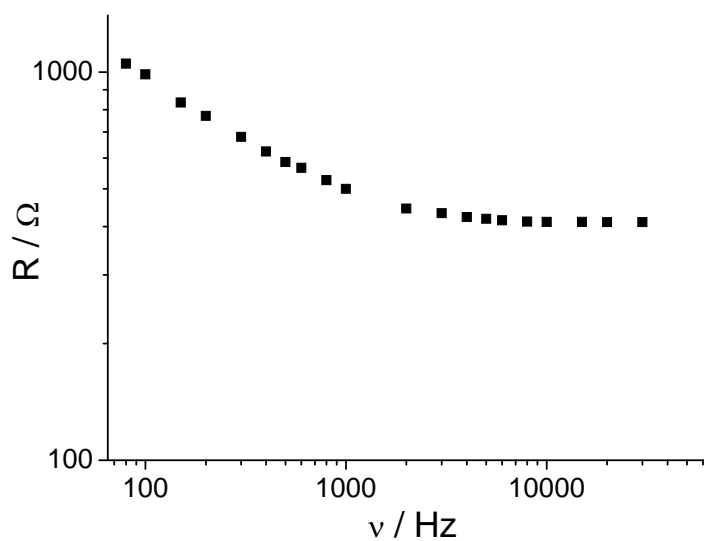


Figure 6.10 Bode plot for [bmim][PF<sub>6</sub>]

The uncompensated resistance has been measured by Bode plots. 156 Ω has been obtained for [bmim][BF<sub>4</sub>] and for [emim][BF<sub>4</sub>] it is very small in the range of 20 Ω.

### 6.3.3 Theoretical Calculation

It has been explained by Oelssner that the iR drop can be estimated at a circular working electrode by the following formula <sup>3</sup>,

$$R_u = \frac{\arctan(z/r)}{2\pi\kappa r} \quad (5.1)$$

Where  $r$  is radius of the circular working electrode,  $z$  is the distance between the working electrode and the luggin capillary and  $\kappa$  is the specific conductivity of the electrolyte solution.

Different conductivities for one ionic liquid have been reported which has also been described in chapter 4. The uncompensated resistance has been calculated with all published conductivities. Different distances between working and reference electrode have also been considered to calculate uncompensated resistance.

Table 6.2  $R_u$  in  $\Omega$ 

Conductance / $10^{-3} \text{ s cm}^{-1}$	$z = 0.1 \text{ cm}$	$z = 0.2 \text{ cm}$	$z = 0.3 \text{ cm}$
	[emim][BF <sub>4</sub> ]		
15.8	79	112	126
13.8	91	128	144
14	89	126	142
13	96	136	153
12	104	147	166
	[bmim][PF <sub>6</sub> ]		
1.46	857	1208	1362
1	1251	1763	1989
1.4	893	1259	1421
1.9	658	928	1047
1.8	695	979	1105
1.5	834	1175	1326
1.6	782	1102	1243
	[bmim][BF <sub>4</sub> ]		
3.5	357	504	568
1.7	736	1037	1170
4.5	278	392	442
	[bmim][OTf]		
2.9	431	608	686
3.7	338	476	538
3.6	347	490	552

Theoretical results are showing larger values of uncompensated resistance but the values are not very big when the distance between working and reference electrode is 0.5 mm. The total depth of the cell which has been used for electrochemical measurements in ionic liquids is 1 cm so the distance between the reference and working electrode can not be more than 1 mm. These results are not comparable with the experimental results obtained by Bode plots and concentration dependent measurements.

These investigations lead us to conclude that iR drop which has been obtained from three different measurements suggested that iR drop in the specifically designed cell of ours is not very large and that it can be neglected.

1. Imbeaux, J. C.; Savéant, J. M. Linear Sweep Voltammetry. Ohmic Drop and Chemical Polarization. *J. Electroanal. Chem.* **1971**, *31*, 183-192.
2. Imbeaux, J. C.; Savéant, J. M. Linear Sweep Voltammetry. Effect of Uncompensated Cell Resistance and Double Layer Charging on Polarization Curves. *J. Electroanal. Chem.* **1970**, *28*, 325-338.
3. Oelssner, W.; Berthold, F.; Guth, U. The Ir Drop - Well-Known but Often Underestimated in Electrochemical Polarization Measurements and Corrosion Testing. *Mater. Corros.* **2006**, *57*, 455-466.
4. Nicholson, R. S. Theory and Application of Cyclic Voltammetry for Measurement of Electrode Reaction Kinetics. *Analytical Chemistry* **1965**, *37*, 1351-1355.
5. Åberg, S.; Sharp, M. A Theoretical Expression for the Effect of Ir Drop on the Current Response in a Potential Step Experiment. *J. Electroanal. Chem.* **1996**, *403*, 31-38.
6. Eichhorn, E.; Rieker, A.; Speiser, B. Numerical Method to Correct Ir Drop Errors in Cyclic Voltammetric Potential Data for (Quasi) Reversible Electrode Processes. *Analytica Chimica Acta* **1992**, *256*, 243-249.
7. Cahan, B. D.; Nagy, Z.; Genshaw, M. A. Cell Design for Potentiostatic Measuring System. *J. Electrochem. Soc.* **1972**, *119*, 64-69.
8. Cahan, B. D.; Ockerman, J. B.; Amlie, R. F.; Ruetschi, P. The Silver-Silver Oxide Electrode. *J. Electrochem. Soc.* **1960**, *107*, 725-731.
9. Ahlberg, E.; Parker, V. D. Quantitative Cyclic Voltammetry: Part I. Acquisition of Precise Electrode Potential Data During Measurements in Resistive Media. *J. Electroanal. Chem.* **1981**, *121*, 57-71.
10. Ahlberg, E.; Parker, V. D. The Effect of Heterogeneous Charge Transfer Kinetics on Electrode Measurements. *Acta Chem. Scand., Ser. B* **1980**, *B34*, 109-112.
11. Kadish, K. M.; Ding, J. Q.; Malinski, T. Resistance of Nonaqueous Solvent Systems Containing Tetraalkylammonium Salts. Evaluation of Heterogeneous Electron Transfer Rate Constants for the Ferrocene/Ferrocenium Couple. *Analytical Chemistry* **1984**, *56*, 1741-1744.

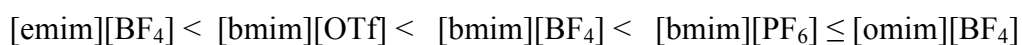


## CHAPTER 7. ELECTROCHEMICAL KINETICS AT ROOM TEMPERATURE

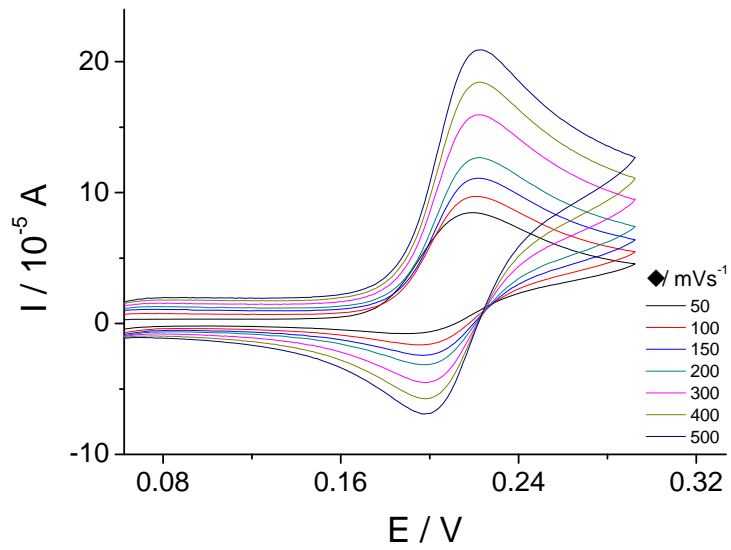
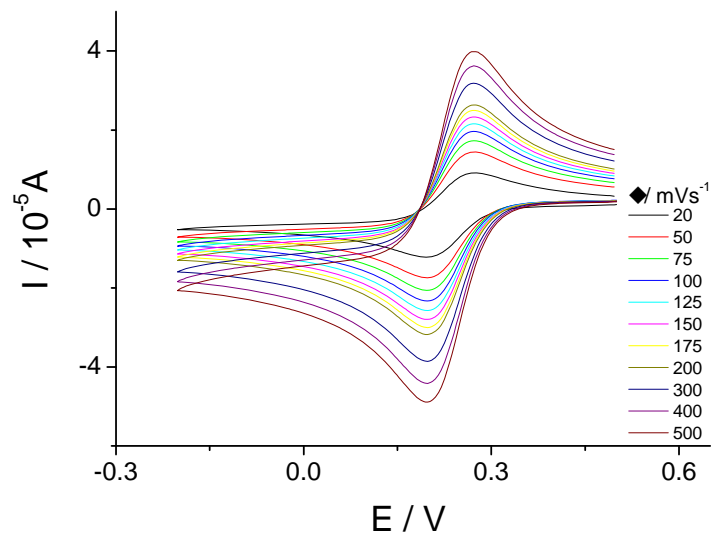
Nine acceptor and six donor systems have been studied pertaining to their electrochemical kinetic behaviour in five different RTILs. These compounds have been chosen due to their easy handling, good cyclic voltammetric response and already published available data for conventional organic solvents. Cyclic voltammetric experiments have been performed at various scan rates from 0.02 to 0.5 V sec<sup>-1</sup> at room temperature. All the measurements were done at room temperature by using the specially designed cell for RTILs, as has been discussed in 5.4.3. In this work only the first electrochemical electron transfer step of the redox couples were taken into account.

All acceptor and donor systems showed reversible or quasideversible behaviour in the all five different RTILs which suggested that the nature of electrochemical reaction did not change in RTILs, cf. Figure 1-10 which depicts one oxidation and reduction compound in each RTILs. An increase in peak current has been observed by the increase in scan rate.

The values of diffusion coefficients have been calculated at room temperature using the Randles-Sevick equation. The corresponding heterogeneous electron transfer rate constants have been evaluated by the Nicholson method. The values obtained for diffusion coefficients and heterogeneous electron transfer rate constants in all RTILs were compared with the data in literature for organic solvents e.g. acetonitrile and DMF etc. The values of diffusion coefficients which have been calculated in RTILs were also analyzed in terms of viscosity. The orders of viscosity in the five ILs are as follows:



It was really difficult to obtain reliable values of viscosity for RTILs from literature because of various different viscosity values are reported for the same ionic liquids<sup>1-4</sup>. Cf. chapter 4. The RTILs which have been used in these experiments were dried by applying high vacuum for one day. Hence the moisture contents are very small what is checked by NIR spectroscopy. We used such viscosity values where detailed experimental conditioned are reported about the purity of the corresponding ionic liquid. Viscosities ( $\eta$ ) were taken as 43 cP<sup>5</sup>, 90 cP<sup>6</sup>, 219 cP<sup>2</sup>, 312 cP<sup>7</sup> and 341 cP<sup>8</sup> for [emim][BF<sub>4</sub>], [bmim][OTf], [bmim][BF<sub>4</sub>], [bmim][PF<sub>6</sub>] and [omim][BF<sub>4</sub>] respectively.

Cyclic voltammograms in [emim][BF<sub>4</sub>]Figure 7.1 PPD in [emim][BF<sub>4</sub>]Figure 7.2 TCNE in [emim][BF<sub>4</sub>]

## Cyclic voltammograms in [bmim][OTf]

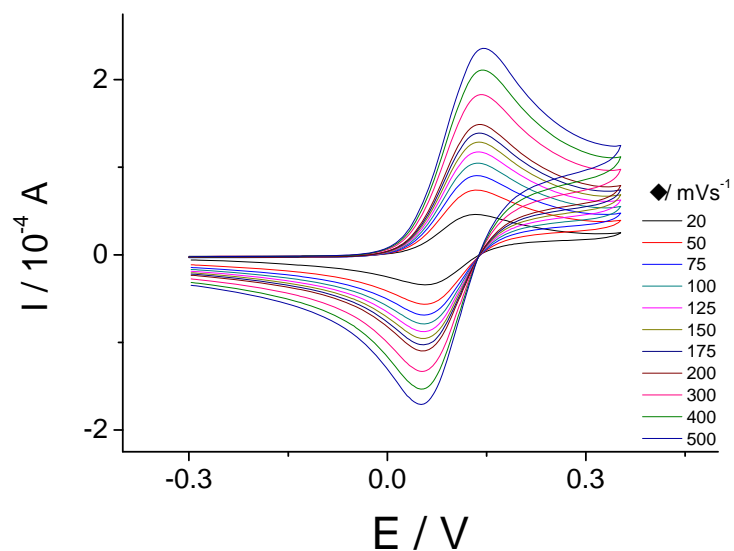
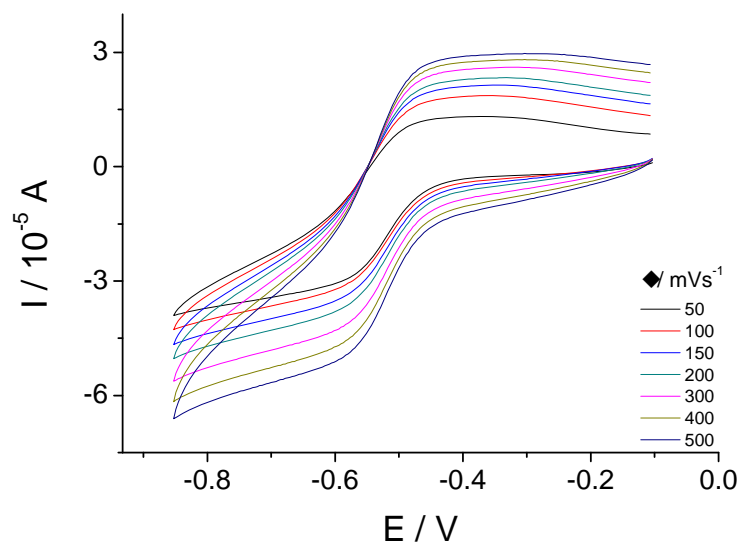
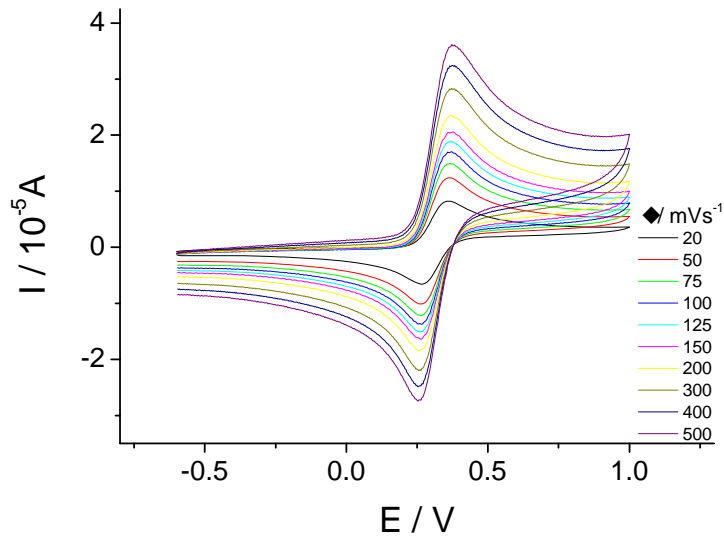
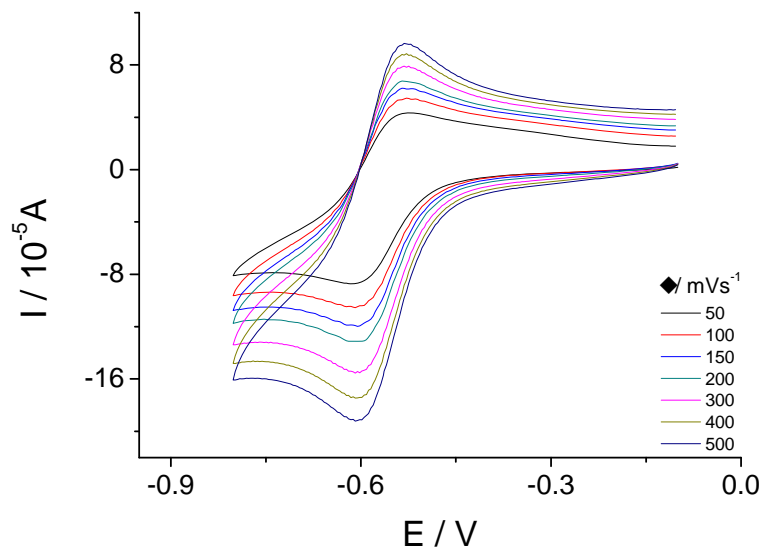
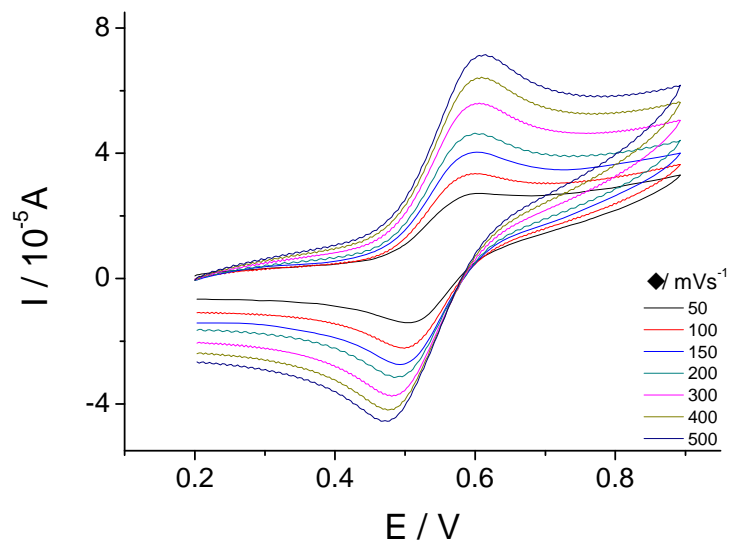
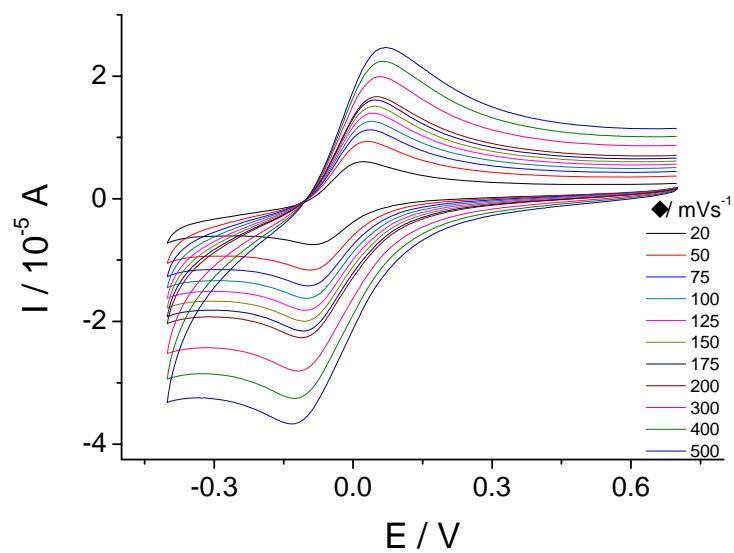
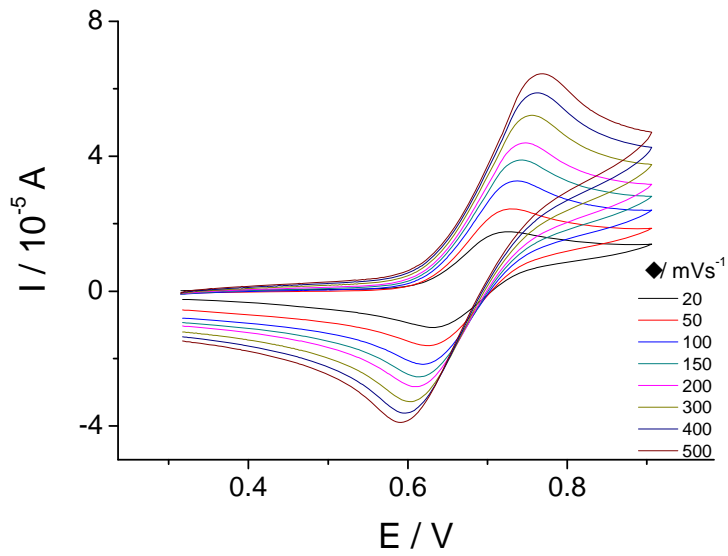
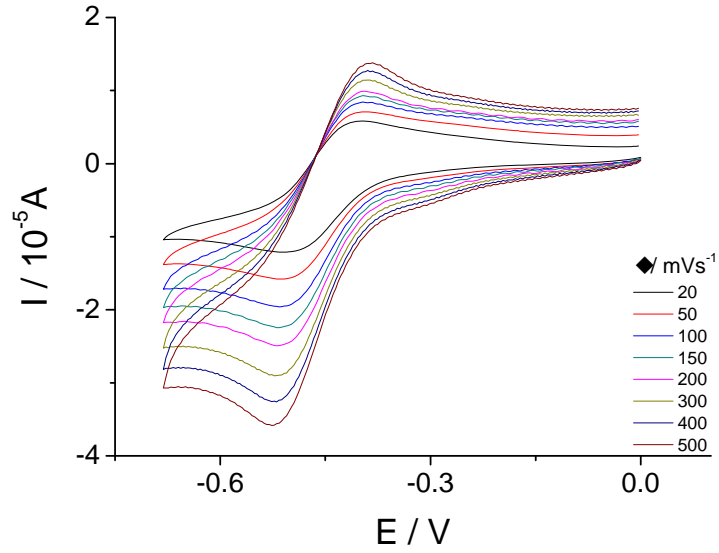


Figure 7.3 TMPPD in [bmim][OTf]

Figure 7.4  $\text{EV}^{2+}$  in [bmim][OTf]

Cyclic voltammograms in [bmim][BF<sub>4</sub>]Figure 7.5 Fc in [bmim][BF<sub>4</sub>]Figure 7.6 2,6-DMBQ in [bmim][BF<sub>4</sub>]

Cyclic voltammograms in [bmim][PF<sub>6</sub>]Figure 7.7 TEMPO in [bmim][PF<sub>6</sub>]Figure 7.8 TBBQ in [bmim][PF<sub>6</sub>]

Cyclic voltammograms in [omim][BF<sub>4</sub>]Figure 7.9 TEMPOL in [omim][BF<sub>4</sub>]Figure 7.10 DQ in [omim][BF<sub>4</sub>]

## 7.1 Diffusion Coefficients

Diffusion coefficients have been calculated using the Randles-Sevick equation

$$I_p = 0.4463nF \left( \frac{nF}{RT} \right)^{1/2} A D^{1/2} C \nu^{1/2} \quad (7.1)$$

Here  $I_p$  is the peak current (A),  $A$  the area of electrode ( $\text{cm}^2$ ),  $C$  the concentration of analyte ( $\text{mol}/\text{cm}^3$ ),  $\nu$  the scan rate ( $\text{V}/\text{s}$ ) and  $D$  is the diffusion coefficient of analyte ( $\text{cm}^2/\text{s}$ ).

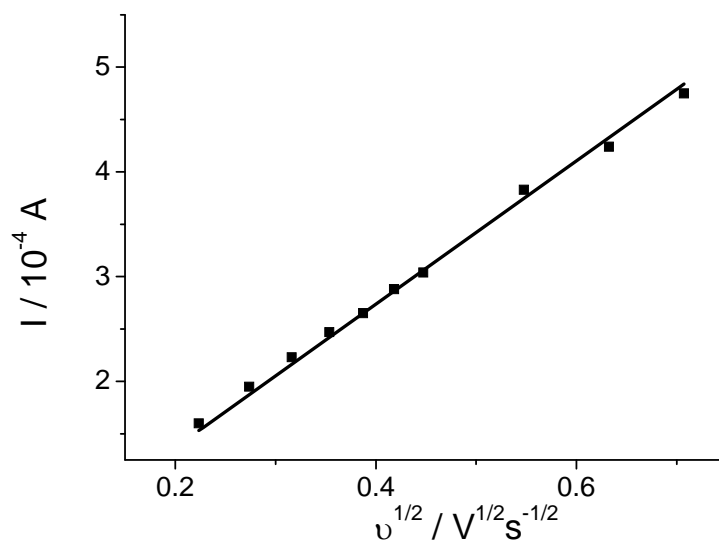


Figure 7.11 2,5-DMBQ in [emim][BF<sub>4</sub>]

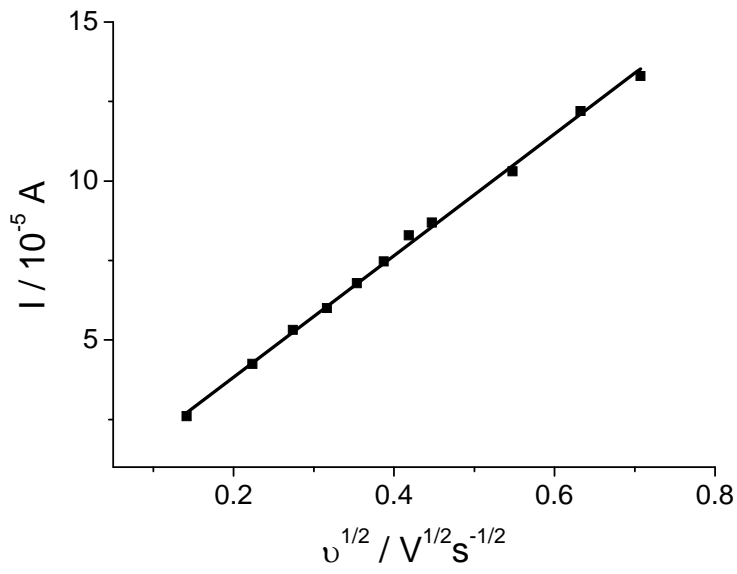


Figure 7.12 TMPPD in [bmim][OTf]

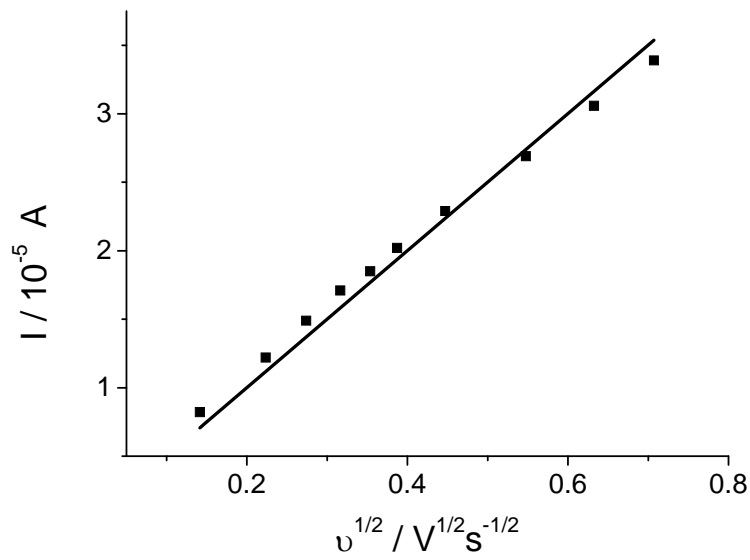
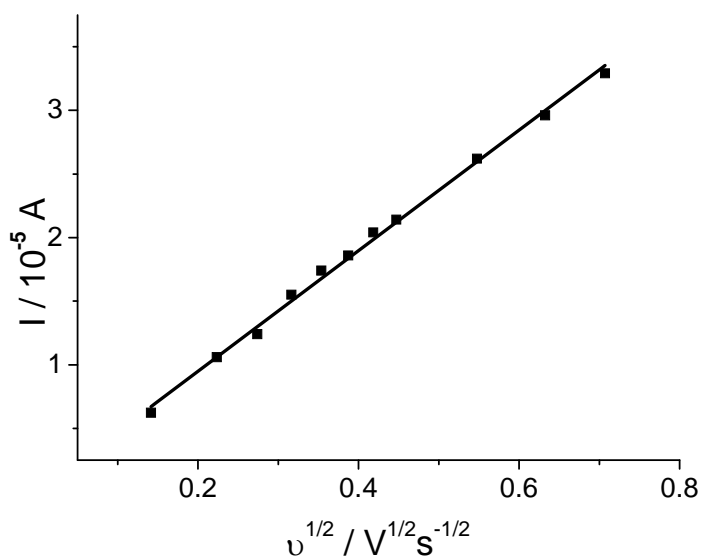
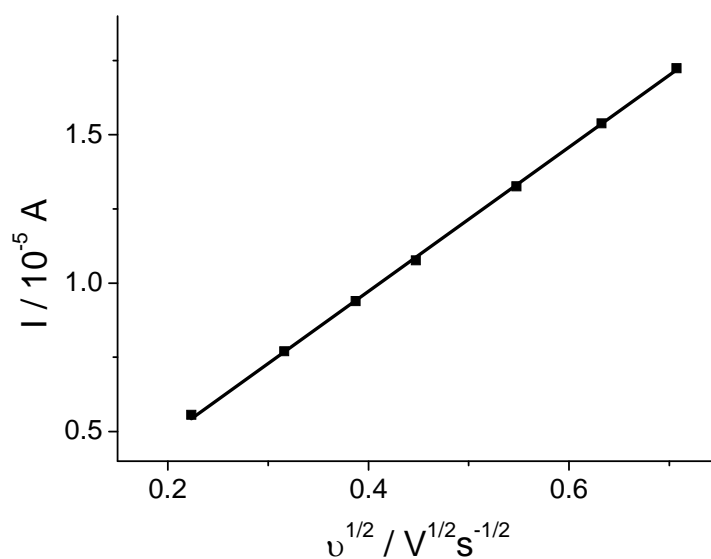


Figure 7.13 Fc in [bmim][BF<sub>4</sub>]



Figure 7.14 TTF in [bmim][PF<sub>6</sub>]Figure 7.15 TCBQ in [omim][BF<sub>4</sub>]

Plots of peak current versus the square root of the scan rates (equation (7.1)) were found to be linear. From the slope of these plots, values of diffusion coefficients have been determined. The linearity of the plots confirms that the heterogeneous electron transfers were reversible and diffusion controlled in all of the investigated RTILs. Additionally, the electron transfer processes are not coupled to any other reactions on this time scale. In Randles-Sevcik equation, there is no intercept and the plot between peak current and square root of scan rate passes through origin. However a non zero value of intercept has also been observed in some compounds. This behaviour is similar to that observed

by Compton<sup>9</sup>. Our cell construction is similar to the one which has been described by this group<sup>10</sup>. The cell size is very small and the viscosity of the ionic liquids is high enough for the slow transportation of the electrode surface layer into the bulk. Thus the conditions are appropriate for the working electrode to respond to the analyte which should have been moved into the bulk but still closer to some extent to the surface of working electrode.

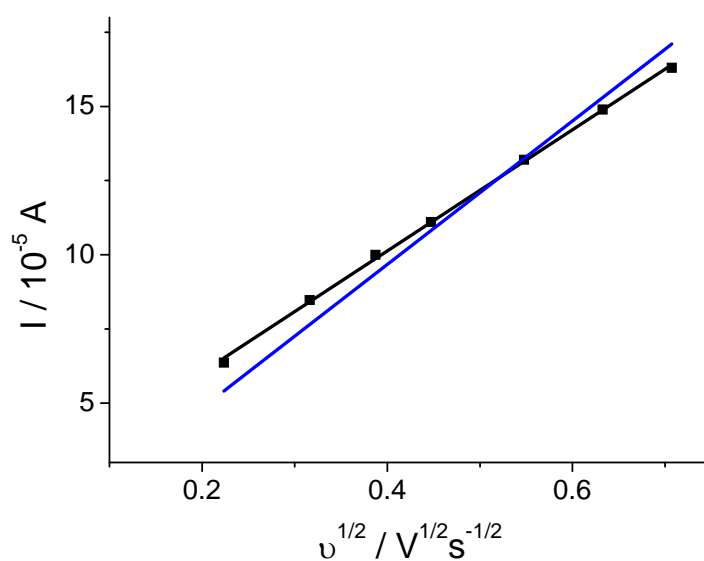


Figure 7.16 TCNE in [emim][BF<sub>4</sub>]

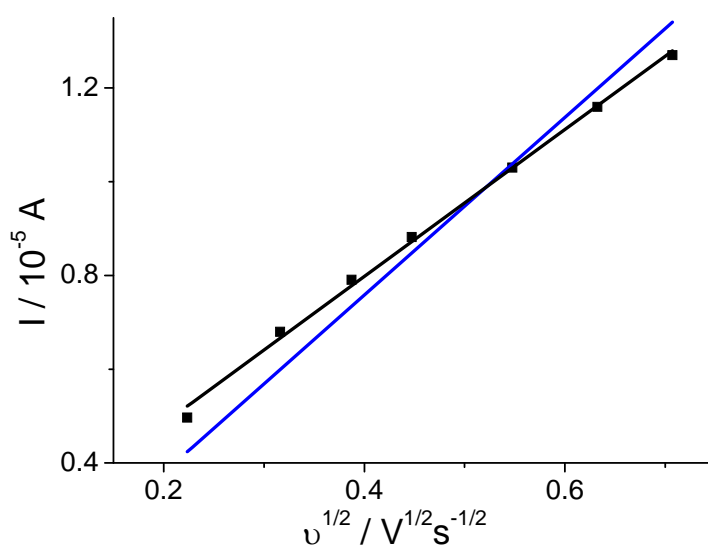
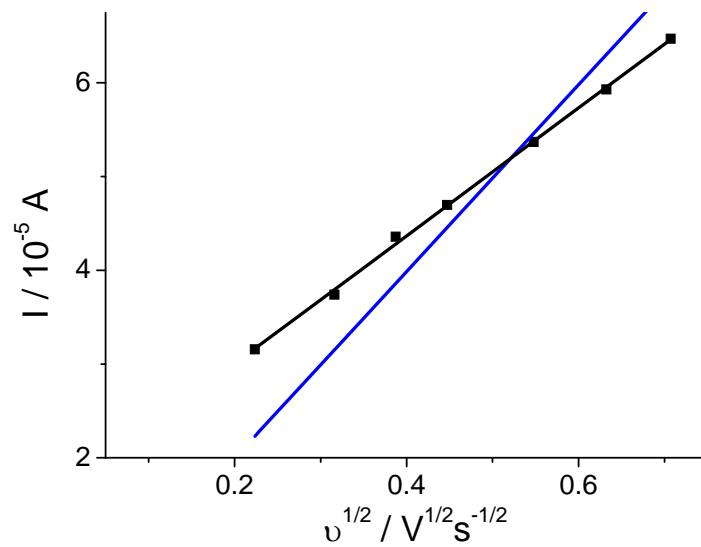
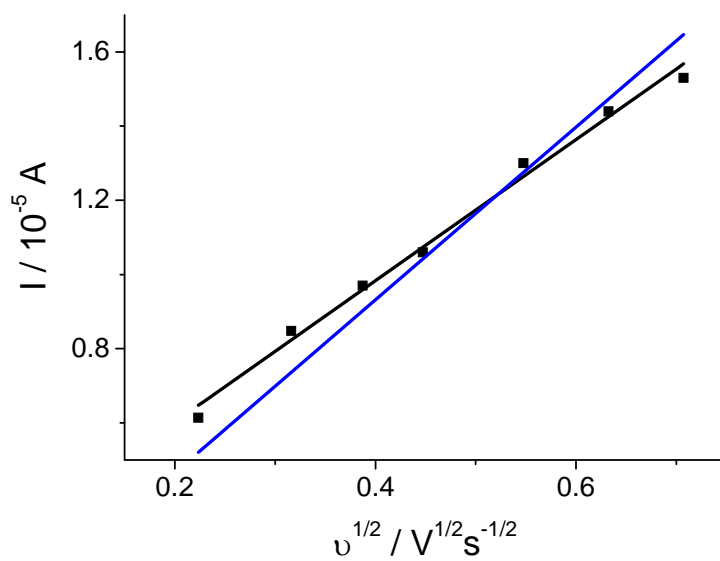


Figure 7.17 TBBQ in [bmim][OTf]

Figure 7.18 TMPPD in [bmim][BF<sub>4</sub>]Figure 7.19 TCBQ in [bmim][PF<sub>6</sub>]

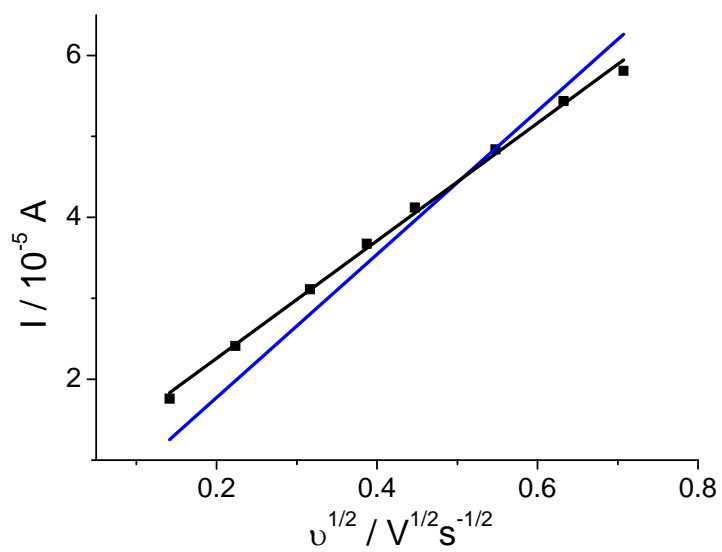


Figure 7.20 TEMPOL in [omim][BF<sub>4</sub>]

The values of the diffusion coefficient obtained in RTILs are 2-3 orders of magnitude lower than the corresponding ones in organic solvents (e.g. acetonitrile, DMF etc). This behaviour is similar to that reported for other redox couples in ionic liquids<sup>11</sup> due to the high viscosity of the RTILs.

Results have been discussed here in two main groups based upon the ionic liquid's cationic and anionic moiety. Each group has been further classified into two sub groups according to the donor and acceptor systems.

- 1a Reduction couples in ionic liquids where the anion is same but the cation is different
- 1b Oxidation couples in ionic liquids where the anion is same but the cation is different
- 2a Reduction couples in ionic liquids where the cation is same but the anion is different
- 2b Oxidation couples in ionic liquids where the cation is same but the anion is different

There are different types of interaction between analyte and ionic liquid's different anionic moiety. First group consists of the data obtained in [emim][BF<sub>4</sub>], [bmim][BF<sub>4</sub>], and [omim][BF<sub>4</sub>]. In these three ionic liquids, only the length of alkyl chain is dissimilar which influences the viscosity of the ionic liquids due to increasing Van der Waal interactions. In the first group, the value of diffusion coefficients decreasing as the viscosity of ionic liquid increases for all oxidation and reduction couples.

Table 7.1 Diffusion coefficient,  $D$ ,  $\text{cm}^2\text{s}^{-1}$  of Reduction couples in the different cationic ILs while anion is same

Compounds	D in [emim][BF <sub>4</sub> ] /10 <sup>-7</sup>	D in [bmim][BF <sub>4</sub> ] /10 <sup>-8</sup>	D in [omim][BF <sub>4</sub> ] /10 <sup>-8</sup>	D in Solvent /10 <sup>-5</sup>
MBQ	1.60	9.92	6.17	
TBBQ	1.30	4.48	2.69	1.25 (MeCN) <sup>12</sup>
TCBQ	36.0	4.59	2.61	1.65
2,5-DMBQ	0.745	6.69		2.14 (MeCN) <sup>13</sup>
2,6-DMBQ	1.28	3.85		0.16 (HMPT) <sup>14</sup>
DQ	13.8	12.2	1.47	
TCNE	1.05	4.76	2.96	
MV <sup>2+</sup>	1.26	2.96		1.0 (DMF) <sup>15</sup>
EV <sup>2+</sup>	0.917	2.51		

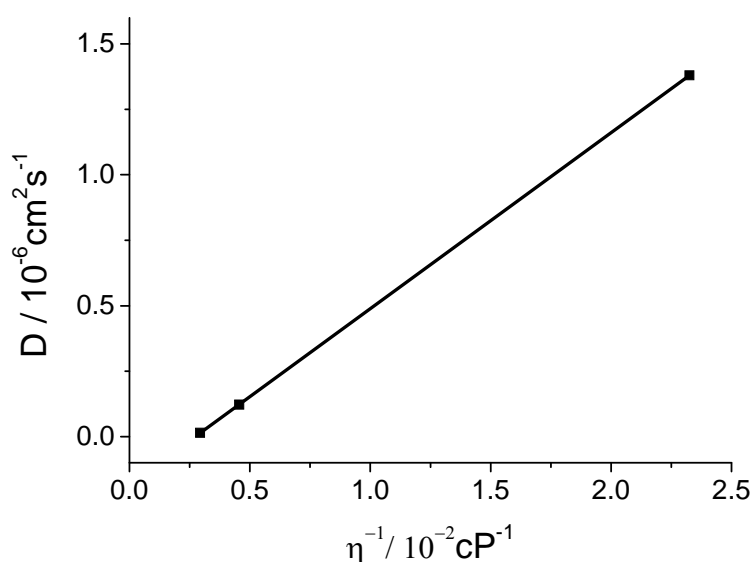


Figure 7.21 DQ in ILs with the same anion [BF<sub>4</sub>] but different cation.

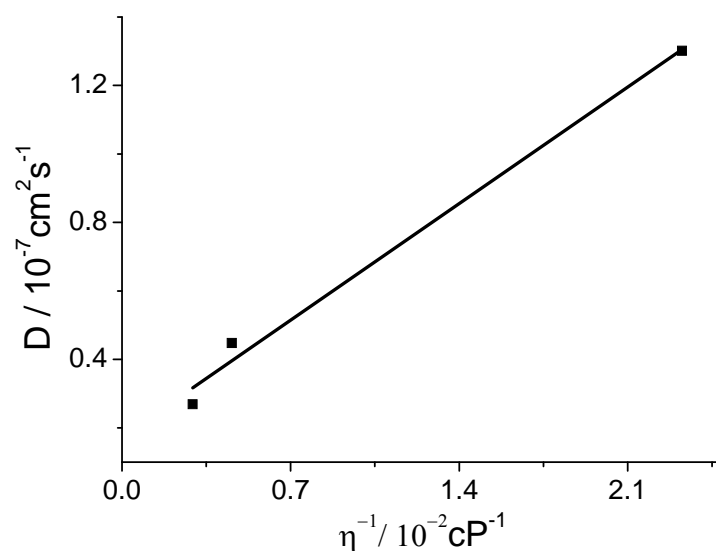


Figure 7.22 TBBQ in ILs with the same anion  $[\text{BF}_4]$  but different cation.

All other acceptor systems are also showing the same linearity linearity.

Table 7.2 Diffusion coefficient  $D$ ,  $\text{cm}^2\text{s}^{-1}$  of oxidation couples in the different cationic ILs where anion is same

Compounds	D in [emim][ $\text{BF}_4$ ] / $10^{-7}$	D in [bmim][ $\text{BF}_4$ ] / $10^{-8}$	D in [omim][ $\text{BF}_4$ ] / $10^{-8}$	D in Solvent / $10^{-5}$
Fc	0.926	2.78		2.37 (MeCN) <sup>16</sup> 1.07 (DMF) <sup>16</sup>
PPD	1.75	3.46		2.06 (MeCN) <sup>17</sup> 0.91 (DMF) <sup>17</sup> 0.15 (HMPT) <sup>18</sup>
TMPPD	10.6	7.05	1.65	1.09(DMF) <sup>17</sup>
TTF	1.91	5.37	2.67	2.7 (MeCN) <sup>19</sup> 0.46 (HMPT) <sup>19</sup>
TEMPO	98.3	78.8	11.5	
TEMPOL	9.90	45.2	33.8	

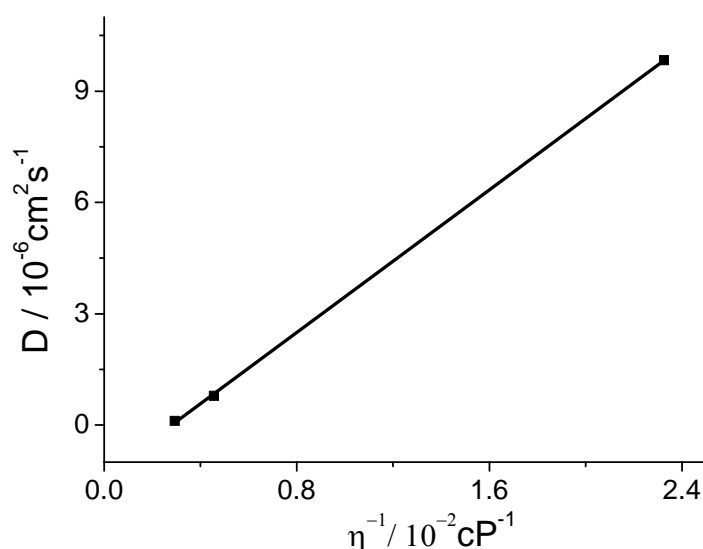


Figure 7.23 TEMPO in ILs with the same anion  $[\text{BF}_4]$  but different cation.

Another set of data pertains to situations wherein the cation of the ionic liquid is the same whereas anion is changing i.e. the case for  $[\text{bmim}][\text{OTf}]$ ,  $[\text{bmim}][\text{BF}_4]$  and  $[\text{bmim}][\text{PF}_6]$ . Here the values of diffusion coefficients are random and the explanation of this is not very straight forward. It seems that one can not understand these results by considering only the viscosity parameter for the different values of diffusion coefficients. It is likely that in addition to viscosity there is some interionic interaction in play between the species with the anionic part of the ionic liquid as has been discussed in literature<sup>20</sup>. The existence of hydrogen bonding has been described for TEMPO in ionic liquids.<sup>21</sup> Interionic interactions due to different anions are able to suppress the effect of viscosity. Therefore a viscosity dependence has not been found in these ionic liquids. By comparing only  $[\text{bmim}][\text{BF}_4]$  and  $[\text{bmim}][\text{PF}_6]$ , it can be said that these data are according to viscosity in the reduction couple i.e 2a. The strange behaviour of  $[\text{bmim}][\text{OTf}]$  is likely caused by the fact that its anion  $[\text{OTf}]$  has a nonzero dipole moment<sup>22</sup>. The others anions do not have dipole moments.



Table 7.3 Diffusion coefficient  $D$ ,  $\text{cm}^2\text{s}^{-1}$  of reduction couples in different anionic ILs while cation is same

Compounds	D in [bmim][OTf]	D in [bmim][BF <sub>4</sub> ]	D in [bmim][PF <sub>6</sub> ]
	/10 <sup>-8</sup>	/10 <sup>-8</sup>	/10 <sup>-8</sup>
MBQ	2.88	9.92	1.87
TBBQ		4.48	2.23
TCBQ	28.1	4.59	0.343
2,5-DMBQ	0.413	6.69	2.73
2,6-DMBQ	9.23	3.85	1.31
DQ		12.2	0.818
TCNE		4.76	2.93
MV <sup>2+</sup>	7.45	2.96	1.27
EV <sup>2+</sup>	5.34	2.51	1.92

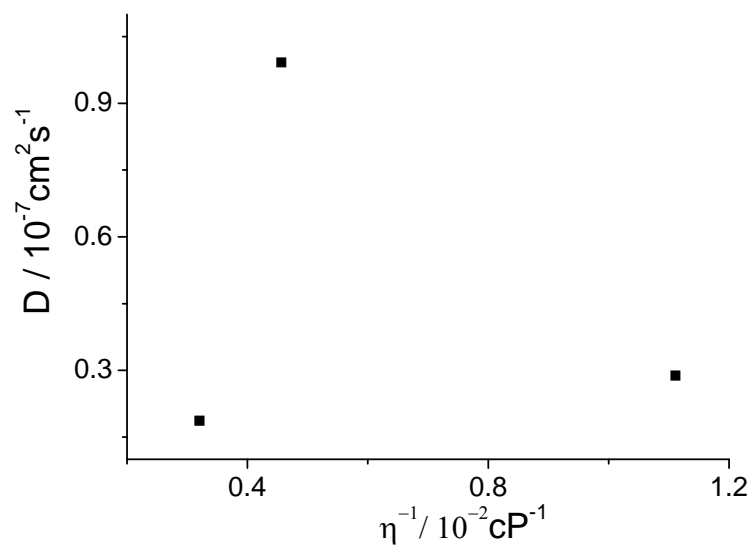


Figure 7.24 MBQ in ILs with the same cation [bmim] but different anion.

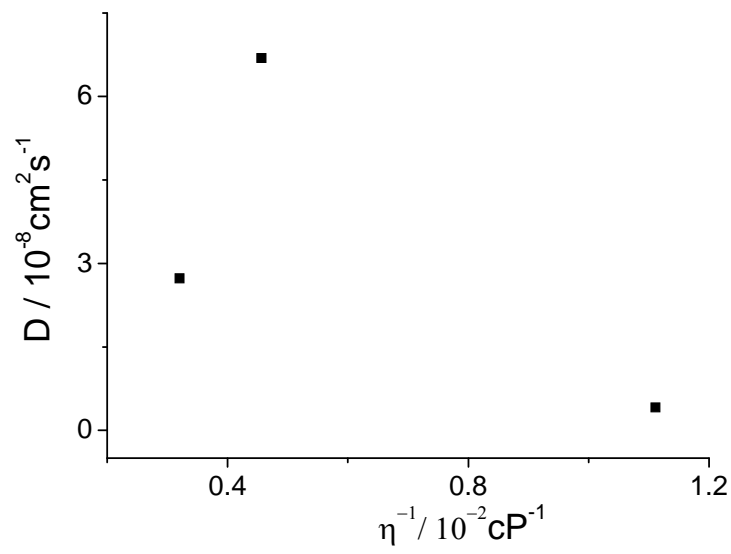


Figure 7.25 2,5-DMBQ in ILs with the same cation [bmim] but different anion

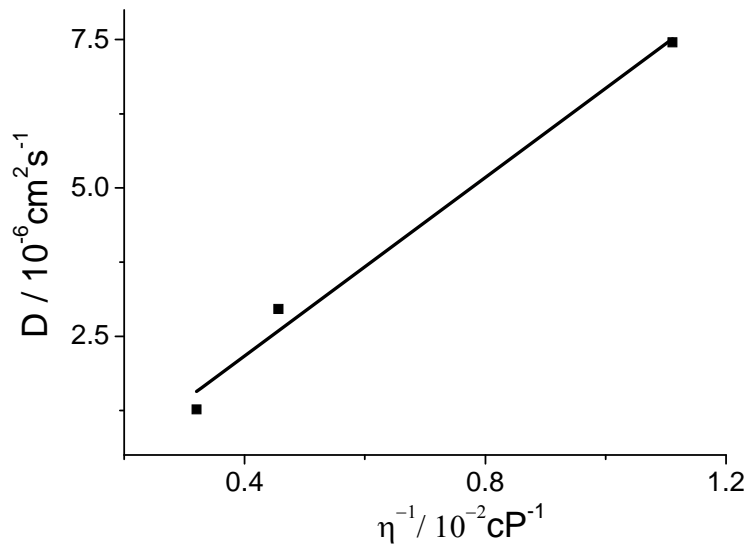


Figure 7.26  $\text{MV}^{2+}$  in ILs with the same cation [bmim] but different anion

For chloranil, 2,6DMBQ,  $MV^{2+}$  and  $EV^{2+}$  straight lines have been obtained, with low values of linear regression factor ( $R^2$ ). It is suggested that interionic interaction completely depends upon the nature of compound and one cannot generalize it to be applicable in all situations.

In group 2b, for various oxidation couple, a similar behaviour has been observed as in 2a. Lower values in [bmim][PF<sub>6</sub>] as compared to [bmim][BF<sub>4</sub>] have been found in all compounds except TMPPD which is within the experimental error. The smaller value of the diffusion coefficient of TEMPOL is due to the hydrogen bonding, which has been discussed by Strehmel<sup>21</sup>.

Table 7.4 Diffusion coefficient  $D$ ,  $cm^2s^{-1}$  of oxidation couples in the different anionic ILs while cation is same

Compounds	D in [bmim][OTf] / $10^{-8}$	D in [bmim][BF <sub>4</sub> ] / $10^{-8}$	D in [bmim][PF <sub>6</sub> ] / $10^{-8}$
Fc	7.56	2.78	2.45
PPD	11.21	3.46	2.63
TMPPD	21	7.05	7.63
TTF	15.2	5.37	3.83
TEMPO	80.3	78.8	2.81
TEMPOL	1.23	45.2	0.876

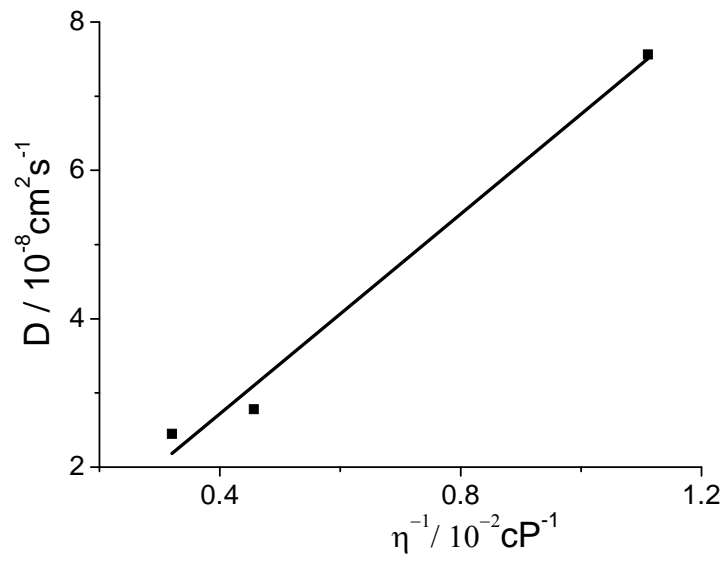
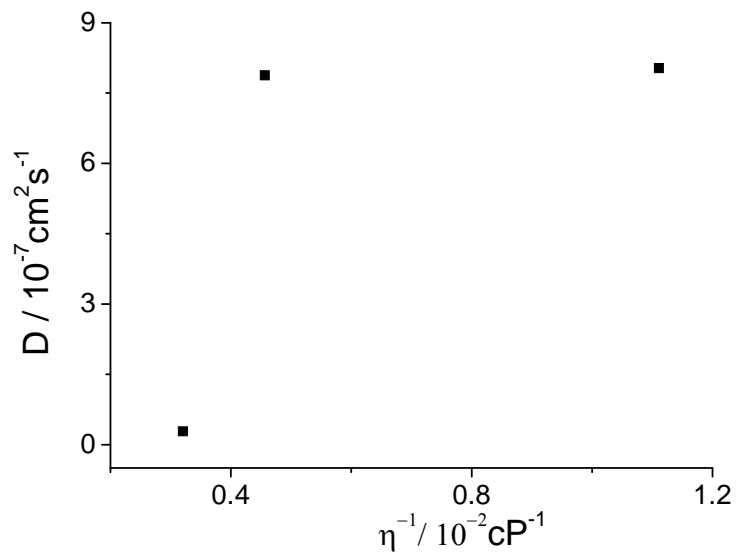


Figure 7.27Fc in ILs with the same cation [bmim] but different anion



7.28 TEMPO in ILs with the same cation [bmim] but different anion

For all data sets the values of diffusion coefficients are smaller than in organic solvent.

It is clear that rates of mass transport to the electrode are slower in more viscous solvents.

The values of the diffusion coefficient have also been compared with published data by Compton which is in same order of magnitude. These values are not exactly similar because of the dissimilar experimental set ups. The values of diffusion coefficient have been determined by Compton through different techniques. Consequently, they used different viscosity values for the same ionic liquids then the values which has been used here.

Table 7.5 Comparison of Diffusion coefficients,  $D$  ( $\text{cm}^2\text{s}^{-1}$ ) data with the data of Compton

Compound	ILs	D in This work / $10^{-8}$	D by Compton / $10^{-8}$
Fc	[bmim][OTf]	7.56	23.6 <sup>23</sup>
Fc	[bmim][BF <sub>4</sub> ]	2.78	1.83 <sup>23</sup>
Fc	[bmim][PF <sub>6</sub> ]	2.45	5.90 <sup>23</sup>
MV <sup>2+</sup>	[bmim][PF <sub>6</sub> ]	1.27	1.1 <sup>24</sup>
MV <sup>2+</sup>	[bmim][BF <sub>4</sub> ]	2.96	1.5 <sup>24</sup>

## 7.2 Heterogeneous Electron Transfer Rate Constants

The well-known Nicholson method<sup>25</sup> is applied to calculate the heterogeneous electron transfer rate constant

$$k_{\text{het}} = \frac{\psi}{\gamma^{\alpha}} \sqrt{\frac{\pi n F \nu D}{RT}} \quad (7.2)$$

Here  $v$  is the scan rate,  $n$  the number of electrons transferred in the electrode reaction,  $\alpha$  the transfer coefficient, which was taken as 0.5 for all electron transfer processes and  $\gamma$  a parameter given by the relationship

$$\gamma = \left( \frac{D_{ox}}{D_{Red}} \right)^{1/2} \quad (7.3)$$

To a good approximation it is assumed that the diffusion coefficients of the reduced and the oxidized species are equal, since the radii do not change very much upon electron transfer, therefore  $D=D_{ox}=D_{red}$  and consequently  $\gamma = 1$ .

Recently, Hapiot et al.<sup>26</sup> pointed out that the ratio  $D_R/D_O$  differs from one in ILs for charge localized radical anions of aromatic nitro compounds, but for charge delocalized radical anions  $D_R/D_O$  tends to unity.

$\psi$  is a dimensionless charge transfer parameter which depends on  $\Delta E_p$ .  $\psi$ -values for various  $\Delta E_p$  at 298 K were tabulated by Nicholson<sup>25</sup>. However, applicability of the original dataset is quite limited. For  $\Delta E_p$ -values close to 59 mV, the percentage error in  $\Psi$  becomes large. An improvement of this dataset was reported by Heinze<sup>27</sup>. In keeping with the times, computer calculations of  $k_{het}$  need an analytical function:  $\Delta E_p = f(\Psi)$ . Such attempts have been published by Parker et al.<sup>28</sup>, but with a limited range of application.

A much better approximation was reported by Swaddle<sup>29</sup>:

$$\ln \psi = 3.69 - 1.16 \ln(\Delta E_p - 59) \quad (7.4)$$

A detailed analysis<sup>30</sup> of the published datasets<sup>25,27</sup> led to the following equation:

$$\Delta E_p = A + \frac{B}{\Psi} + \frac{C}{\Psi^{1/2}} + \frac{D}{\Psi^{1/3}} \quad (7.5)$$

With:  $A = 81.34$  mV,  $B = -3.06$  mV,  $C = 149$  mV and  $D = -145.5$  mV at 298 K.

Over a large range of  $\Delta E_p$ , ( $61 \text{ mV} \leq \Delta E_p \leq 212 \text{ mV}$ ), the error in eq. (7.5) is below 0.9 mV, which is comparable with the accuracy of the electrochemical measurements. At  $\Delta E_p = 60 \text{ mV}$  the error is 1.58 mV. This equation has been used to calculate the value of  $\psi$  in current work. A similar, but mathematically more complicated method using hyperplanes is reported by Speiser et al<sup>31</sup>. It should be taken into account that  $\Delta E_p$ -measurements are useful only over a certain range. For  $\Delta E_p$  of 150 mV or more the CV peaks become broad and difficult to evaluate accurately, since the baseline is often sloping. Also at high scan rates corrections for double-layer charging currents become necessary<sup>29</sup>.

Magno et al<sup>32</sup> has also reported an equation which works up to 200 mV.

$$\Psi = (-0.6288 + 0.0021X) / (1 - 0.017X) \quad (7.6)$$

Where  $X = \Delta E_p \times n$  in mV

Table 7.6 Heterogeneous electron transfer rate constants,  $k_{\text{het}}$ , in  $\text{cm s}^{-1}$  of reduction couples in the different cationic ILs, while anion is the same.

Acceptor Systems	$k_{\text{het}}$ in [emim][BF <sub>4</sub> ]/10 <sup>-4</sup>	$k_{\text{het}}$ in [bmim][BF <sub>4</sub> ]/10 <sup>-4</sup>	$k_{\text{het}}$ in [omim][BF <sub>4</sub> ]/10 <sup>-4</sup>	$k_{\text{het}}$ in solvents
MBQ	7.19	5.45	4.32	
TBBQ	9.95	3.67		0.3 (MeCN) <sup>12</sup>
TCBQ	5.09	2.34	1.26	0.2 (MeCN) <sup>12</sup>
2,5-DMBQ	2.46	1.06		
2,6-DMBQ	6.12	1.29		0.31 (HMPT) <sup>14</sup>
DQ	3.50	2.31	1.98	
TCNE	15.3	10.5	1.86	>1 (MeCN) <sup>33</sup>
MV <sup>2+</sup>	6.41	2.67		0.004 (DMF) <sup>34</sup>
EV <sup>2+</sup>	9.21	2.12		

The values obtained for the heterogeneous electron transfer rate constants for groups 1 and 2, of the various compounds clearly show variation with the viscosity of ILs and are 2-3 orders of magnitude smaller than compared with conventional organic solvents. Similar results are reported for N,N,N',N'-tetramethyl-p-phenylenediamine (TMPPD)<sup>35</sup>,

2,2,6,6-tetramethylpiperidine-1-oxyl (TEMPO)<sup>36</sup>. Hapoit et al. have studied several nitrocompounds<sup>11</sup> and 1,2-dimethoxybenzene as well as methylated benzenes<sup>37</sup>. These results also exhibit reduced rate constants compared to classical organic solvents. Various arenes and substituted anthracenes show the same behaviour<sup>38</sup>.

Table 7.7 Heterogeneous electron transfer rate constants,  $k_{\text{het}}$ , in  $\text{cm s}^{-1}$  of oxidation couples in the different cationic ILs, while anion is same

Donor Systems	$k_{\text{het}}$ in [emim][BF <sub>4</sub> ]/10 <sup>-4</sup>	$k_{\text{het}}$ in [bmim][BF <sub>4</sub> ]/10 <sup>-4</sup>	$k_{\text{het}}$ in [omim][BF <sub>4</sub> ]/10 <sup>-4</sup>	$k_{\text{het}}$ in solvents
Fc	5.47	2.67		0.02 (MeCN) <sup>39</sup> 0.99 (MeCN) <sup>40</sup>
PPD	11.4	5.07		0.22 (MeCN) <sup>18</sup> 0.09 (DMF) <sup>17</sup>
TMPPD	9.01	7.55	2.23	0.175 <sup>41</sup>
TTF	13.2	6.35	1.58	2.2 (MeCN) <sup>19</sup> 0.031 (HMPT) <sup>19</sup>
TEMPO	6.02	4.25	2.77	
TEMPOL	12.5	8.56	4.10	

The results for heterogeneous electron transfer rate constants, in group 2a, have been reported in table 8. These results are similar to the results obtained for diffusion coefficients values.



Table 7.8 Heterogeneous electron transfer rate constants,  $k_{\text{het}}$ , in  $\text{cm s}^{-1}$  of reduction couples in the different anionic ILs, while cation is the same

Acceptor Systems	$k_{\text{het}}$ in [bmim][OTf] / $10^{-4}$	$k_{\text{het}}$ in [bmim][BF <sub>4</sub> ] / $10^{-4}$	$k_{\text{het}}$ in [bmim][PF <sub>6</sub> ] / $10^{-4}$
MBQ	18.1	5.45	1.44
TBBQ		3.67	1.54
TCBQ	3.28	2.34	3.22
2,5-DMBQ	1.09	1.06	2.10
2,6-DMBQ	2.93	1.29	0.75
DQ		2.31	1.30
TCNE		10.5	8.29
MV <sup>2+</sup>	3.61	2.67	2.45
EV <sup>2+</sup>	5.07	2.12	1.82

All compounds are having smaller values for heterogeneous rate constant in [bmim][PF<sub>6</sub>] than those in [bmim][BF<sub>4</sub>] except 2,5-DMBQ which has higher heterogeneous electron transfer rate constant in [bmim][BF<sub>4</sub>]. However, it is lower as compared to [bmim][PF<sub>6</sub>] and that it is in the experimental error range. [OTf]<sup>-</sup> is expected to behave differently from other ionic liquids because of its dipole moment while others possess no dipole moment. It also produces different ionic interactions compared with others.

Table 7.9 Heterogeneous electron transfer rate constants,  $k_{\text{het}}$ , in  $\text{cm s}^{-1}$  of oxidation couples in the different anionic ILs while cation is same

<b>Donor Systems</b>	$k_{\text{het}}$ in <b>bmim][OTf]</b> / $10^{-4}$	$k_{\text{het}}$ in <b>bmim][BF<sub>4</sub>]</b> / $10^{-4}$	$k_{\text{het}}$ in <b>[bmim][PF<sub>6</sub>]</b> / $10^{-4}$
Fc	2.83	2.67	1.78
PPD	7.35	5.07	3.69
TMPPD	4.3	7.55	
TTF	8.56	6.35	2.92
TEMPO	8.38	4.17	3.31
TEMPOL	1.22	8.56	0.878

In group 2b, every compound is following the expected trend of viscosity except TEMPOL which is a likely result of hydrogen bonding.

### 7.3 Formal Potential

Formal potential of all of the investigated compounds have been determined for all compounds by using the following equation,

$$E^{o'} = \frac{E_{pc} + E_{pa}}{2} \quad (7.7)$$

It is nothing else but just an average of anodic ( $E_{pa}$ ) and cathodic ( $E_{pc}$ ) peak potential. This equation works only under assumption of  $D_{\text{ox}}=D_{\text{red}}$ .

Table 7.10 Formal potentials,  $E^{\circ}$  versus Ag/AgCl in V for reduction couples in ionic liquid

Compounds	[emim][BF <sub>4</sub> ]	[bmim][OTf]	[bmim][BF <sub>4</sub> ]	[bmim][PF <sub>6</sub> ]	[omim][BF <sub>4</sub> ]
MBQ	-0.470	-0.504	-0.445	-0.476	-0.435
TBBQ	-0.017	-	-0.028	-0.032	-
TCBQ	0.143	0.119	0.143	0.104	0.121
2,5-DMBQ	-0.690	-0.601	-0.653	-0.588	-
2,6-DMBQ	-0.561	-0.568	-0.563	-0.524	-
DQ	-0.519	-	-0.590	-0.533	-0.467
TCNE	0.235	-	0.118	0.109	0.196
MV <sup>2+</sup>	-0.516	-0.547	-0.563	-0.597	-
EV <sup>2+</sup>	-0.474	-0.539	-0.557	-0.560	-

Table 7.11 Formal potentials,  $E^{\circ}$  versus Ag/AgCl in V for oxidation couples in ionic liquids

Compounds	[emim][BF <sub>4</sub> ]	[bmim][OTf]	[bmim][BF <sub>4</sub> ]	[bmim][PF <sub>6</sub> ]	[omim][BF <sub>4</sub> ]
Fc	0.310	0.270	0.313	0.248	-
PPD	0.214	0.126	0.203	0.141	-
TMPPD	0.243	0.248	0.155	-	0.242
TTF	0.280	0.222	0.310	0.277	-
TEMPO	0.657	0.667	0.601	0.546	0.631
TEMPOL	0.754	0.705	0.645	0.617	0.670

Formal potential of each redox couple in different ionic liquids are similar and the difference is in the range of 0.1 V which is acceptable for different media.

## 7.4 Measurements in Binary Mixture of Ionic Liquids and Acetonitrile

Only one compound Ferrocene has been studied in a binary mixture of Ionic liquids and acetonitrile to observe the effect of solvent on the electron transfer process. Different solutions, based on binary mixtures having compositions 20%, 40%, 60% 80% and 100% by volume, have been prepared from ionic liquids and acetonitrile. Cyclic voltammograms, for each mixture, have been recorded at different scan rates at room temperature cf. Figure 29.

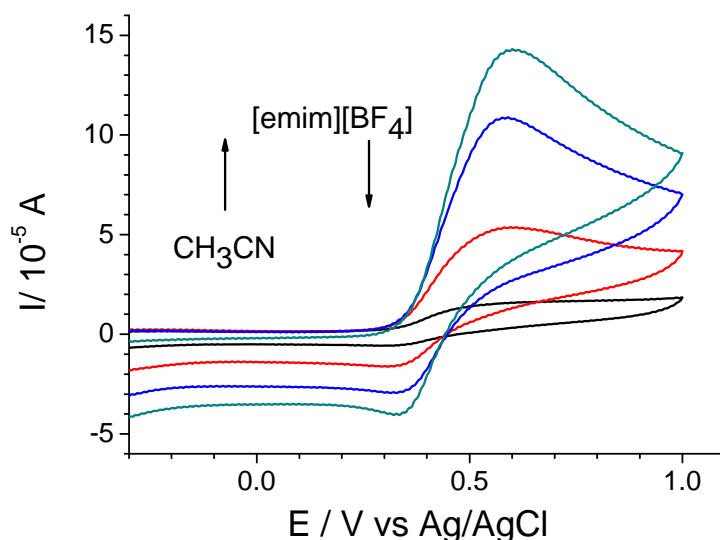


Figure 29 Cyclic voltammograms of ferrocene in a binary mixture of [emim][BF<sub>4</sub>] and acetonitrile at a scan rate of 100 mV sec<sup>-1</sup>

It has been observed that peak current increases as the content of acetonitrile gets enhanced in the solvent mixture. The shapes of cyclic voltammograms appear not to be as reversible as it has been observed in pure ionic liquids or in acetonitrile and that anodic peak current is higher than the cathodic peak current. It may be suggested that differing solvation patterns around the molecule are responsible for this unusual behavior.

Diffusion coefficients and heterogeneous electron transfer rate constants have been calculated for each solvent mixture. The viscosity of the mixture in question is expected to decrease as the fraction of acetonitrile increases. This got substantiated by the observation that diffusion coefficients increase with increasing acetonitrile fraction and that higher heterogeneous rate constants are also obtained.

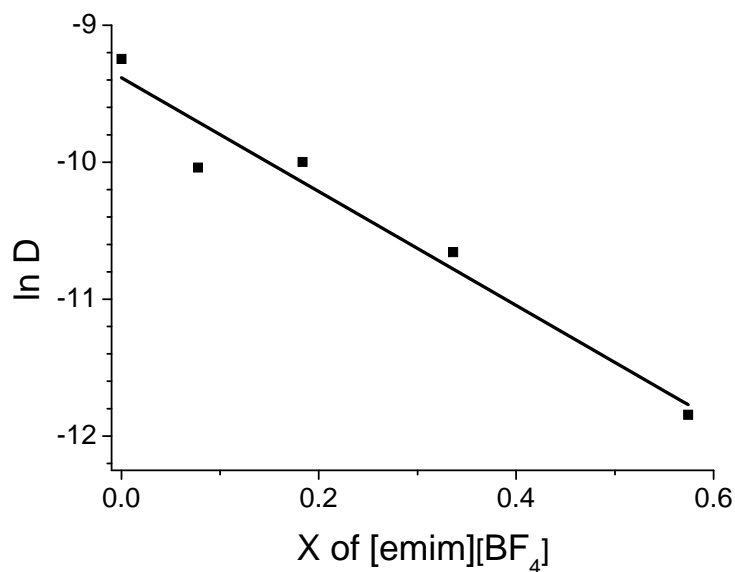


Figure 30 Ferrocene in a mixture of acetonitrile and [emim][BF<sub>4</sub>]

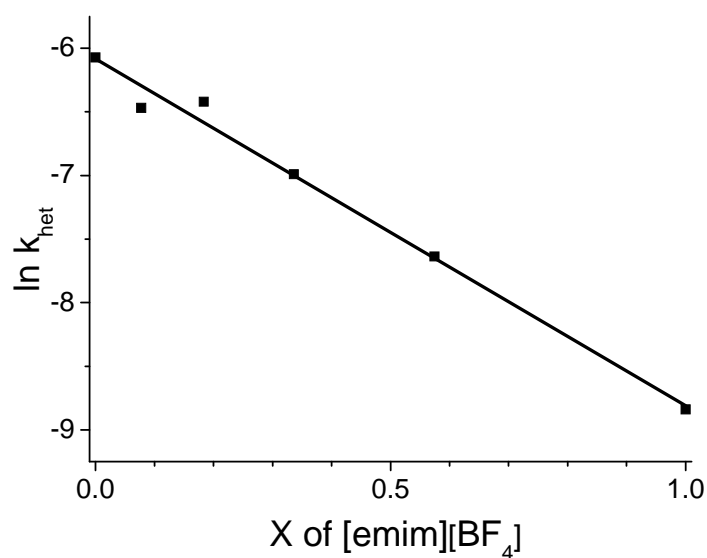


Figure 31 Ferrocene in a mixture of acetonitrile and [emim][BF<sub>4</sub>]

In both plots, pertaining to either of  $\ln D$  or  $\ln K_{\text{het}}$  against mole fraction of [emim][BF<sub>4</sub>] (Figure 30 and Figure 31), straight lines have been achieved. The linear decrease in diffusion coefficients and heterogeneous electron transfer rate constants is, due to the higher content of more viscous ionic liquid [emim][BF<sub>4</sub>], can easily be noticed in these figures.

1. Nishida, T.; Tashiro, Y.; Yamamoto, M. Physical and Electrochemical Properties of 1-Alkyl-3-Methylimidazolium Tetrafluoroborate for Electrolyte. *Journal of Fluorine Chemistry* **2003**, *120*, 135-141.
2. Huddleston, J. G.; Visser, A. E.; Reichert, W. M.; Willauer, H. D.; Broker, G. A.; Rogers, R. D. Characterization and Comparison of Hydrophilic and Hydrophobic Room Temperature Ionic Liquids Incorporating the Imidazolium Cation. *Green Chem.* **2001**, *3*, 156-164.
3. Baker, S. N.; Baker, G. A.; Kane, M. A.; Bright, F. V. The Cybotactic Region Surrounding Fluorescent Probes Dissolved in 1-Butyl-3-Methylimidazolium Hexafluorophosphate: Effects of Temperature and Added Carbon Dioxide. *J. Phys. Chem. B* **2001**, *105*, 9663-9668.
4. Tokuda, H.; Tsuzuki, S.; Susan, M. A. B. H.; Hayamizu, K.; Watanabe, M. How Ionic Are Room-Temperature Ionic Liquids? An Indicator of the Physicochemical Properties. *The Journal of Physical Chemistry B* **2006**, *110*, 19593-19600.
5. McEwen, A. B.; Ngo, H. L.; LeCompte, K.; Goldman, J. L. Electrochemical Properties of Imidazolium Salt Electrolytes for Electrochemical Capacitor Applications. *J. Electrochem. Soc.* **1999**, *146*, 1687-1695.
6. Bonhote, P.; Dias, A.-P.; Papageorgiou, N.; Kalyanasundaram, K.; Gratzel, M. Hydrophobic, Highly Conductive Ambient-Temperature Molten Salts†. *Inorganic Chemistry* **1996**, *35*, 1168-1178.
7. Suarez, P., A.Z.; Einloft, S.; Dullius, J., E.L.; de Souza, R., F.; Dupont, J. Synthesis and Physical-Chemical Properties of Ionic Liquids Based on 1-Butyl-3-Methylimidazolium Cation. *J. Chim. Phys.* **1998**, *95*, 1626-1639.
8. Harris, K. R.; Kanakubo, M.; Woolf, L. A. Temperature and Pressure Dependence of the Viscosity of the Ionic Liquids 1-Methyl-3-Octylimidazolium Hexafluorophosphate and 1-Methyl-3-Octylimidazolium Tetrafluoroborate. *Journal of Chemical & Engineering Data* **2006**, *51*, 1161-1167.
9. Long, J. S.; Silvester, D. S.; Barnes, A. S.; Rees, N. V.; Aldous, L.; Hardacre, C.; Compton, R. G. Oxidation of Several P-Phenylenediamines in Room Temperature Ionic Liquids: Estimation of Transport and Electrode Kinetic Parameters. *J. Phys. Chem. C* **2008**, *112*, 6993-7000.
10. Evans, R. G.; Klymenko, O. V.; Hardacre, C.; Seddon, K. R.; Compton, R. G. Oxidation of N,N,N',N'-Tetraalkyl-Para-Phenylenediamines in a Series of Room Temperature Ionic Liquids Incorporating the Bis(Trifluoromethylsulfonyl)Imide Anion. *J. Electroanal. Chem.* **2003**, *556*, 179-188.
11. Lagrost, C.; Preda, L.; Volanschi, E.; Hapiot, P. Heterogeneous Electron-Transfer Kinetics of Nitro Compounds in Room-Temperature Ionic Liquids. *J. Electroanal. Chem.* **2005**, *585*, 1-7.
12. Rees, N. V.; Clegg, A. D.; Klymenko, O. V.; Coles, B. A.; Compton, R. G. Marcus Theory for Outer-Sphere Heterogeneous Electron Transfer: Predicting Electron-Transfer Rates for Quinones. *J. Phys. Chem. B* **2004**, *108*, 13047-13051.
13. Frontana, C.; Gonzalez, I. Revisiting the Effects of the Molecular Structure in the Kinetics of Electron Transfer of Quinones: Kinetic Differences in Structural Isomers. *J. Mex. Chem. Soc.* **2008**, *52*, 11-18.
14. Kapturkiewicz, A. Rate Constants of the Electrode Reactions of Some Quinones in Hexamethylphosphoramide Solutions at Mercury Electrodes. *J. Electroanal. Chem. Interfacial Electrochem.* **1986**, *201*, 205-209.
15. Aslam, M., Quaid-e-Azam University, 1994.

16. Jacob, S. R.; Hong, Q.; Coles, B. A.; Compton, R. G. Variable-Temperature Microelectrode Voltammetry: Application to Diffusion Coefficients and Electrode Reaction Mechanisms. *J. Phys. Chem. B* **1999**, *103*, 2963-2969.
17. Kapturkiewicz, A.; Jaenicke, W. Comparison between Heterogeneous and Homogeneous Electron Transfer in P-Phenylenediamine Systems. *J. Chem. Soc., Faraday Trans. 1* **1987**, *83*, 2727-2734.
18. Opallo, M. The Solvent Effect on the Electrooxidation of 1,4-Phenylenediamine. The Influence of the Solvent Reorientation Dynamics on the One-Electron Transfer Rate. *J. Chem. Soc., Faraday Trans. 1* **1986**, *82*, 339-347.
19. Grampp, G.; Kapturkiewicz, A.; Jaenicke, W. Homogeneous and Heterogeneous Electron Transfer Rates of the Tetrathiafulvalene-System. *Ber. Bunsen-Ges. Phys. Chem.* **1990**, *94*, 439-447.
20. Tsuzuki, S.; Tokuda, H.; Mikami, M. Theoretical Analysis of the Hydrogen Bond of Imidazolium C2-H with Anions. *Physical Chemistry Chemical Physics* **2007**, *9*, 4780-4784.
21. Strehmel, V.; Rexhausen, H.; Strauch, P.; Görnitz, E.; Strehmel, B. Temperature Dependence of Interactions between Stable Piperidine-1-Yloxy Derivatives and an Ionic Liquid. *ChemPhysChem* **2008**, *9*, 1294-1302.
22. Liu, X.; Zhang, S.; Zhou, G.; Wu, G.; Yuan, X.; Yao, X. New Force Field for Molecular Simulation of Guanidinium-Based Ionic Liquids. *The Journal of Physical Chemistry B* **2006**, *110*, 12062-12071.
23. Rogers, E. I.; Silvester, D. S.; Poole, D. L.; Aldous, L.; Hardacre, C.; Compton, R. G. Voltammetric Characterization of the Ferrocene|Ferrocenium and Cobaltocenium|Cobaltocene Redox Couples in Rtils. *J. Phys. Chem. C* **2008**, *112*, 2729-2735.
24. Schroder, U.; Wadhawan, J. D.; Compton, R. G.; Marken, F.; Suarez, P. A. Z.; Consorti, C. S.; de Souza, R. F.; Dupont, J. Water-Induced Accelerated Ion Diffusion: Voltammetric Studies in 1-Methyl-3-[2,6-(S)-Dimethylocten-2-Yl]Imidazolium Tetrafluoroborate, 1-Butyl-3-Methylimidazolium Tetrafluoroborate and Hexafluorophosphate Ionic Liquids. *New J. Chem.* **2000**, *24*, 1009-1015.
25. Nicholson, R. S. Theory and Application of Cyclic Voltammetry for Measurement of Electrode Reaction Kinetics. *Anal. Chem.* **1965**, *37*, 1351-1355.
26. Zigah, D.; Ghilane, J.; Lagrost, C.; Hapiot, P. Variations of Diffusion Coefficients of Redox Active Molecules in Room Temperature Ionic Liquids Upon Electron Transfer. *J. Phys. Chem. B* **2008**, *112*, 14952-14958.
27. Heinze, J. Theory of Cyclic Voltammetry at Microdisk Electrodes. *Ber. Bunsenges. Phys. Chem.* **1981**, *85*, 1096-1103.
28. Ahlberg, E.; Parker, V. D. The Effect of Heterogeneous Charge Transfer Kinetics on Electrode Measurements. *Acta Chem. Scand., Ser. B* **1980**, *B34*, 109-112.
29. Swaddle, T. W. Homogeneous Versus Heterogeneous Self-Exchange Electron Transfer Reactions of Metal Complexes: Insights from Pressure Effects. *Chem. Rev. (Washington, DC, U. S.)* **2005**, *105*, 2573-2608.
30. Rüssel, C., University of Erlangen, 1984.
31. Speiser, B. Electroanalytical Investigations. Part V. The Simulation of Fast Chemical Reactions in Cyclic Voltammetry by a Combination of the Orthogonal Collocation Method and the Heterogeneous Equivalent Approach. *J. Electroanal. Chem. Interfacial Electrochem.* **1984**, *171*, 95-109.
32. Lavagnini, I.; Antiochia, R.; Magno, F. An Extended Method for the Practical Evaluation of the Standard Rate Constant from Cyclic Voltammetric Data. *Electroanalysis* **2004**, *16*, 505-506.

33. Petersen, R. A.; Evans, D. H. Heterogeneous Electron Transfer Kinetics for a Variety of Organic Electrode Reactions at the Mercury-Acetonitrile Interface Using Either Tetraethylammonium Perchlorate or Tetraheptylammonium Perchlorate Electrolyte. *J. Electroanal. Chem. Interfacial Electrochem.* **1987**, *222*, 129-150.
34. Bhatti, N. K.; Subhani, M. S.; Khan, A. Y.; Qureshi, R.; Rahman, A. Heterogeneous Electron Transfer Rate Constants of Viologen at a Platinum Disk Electrode. *Turk. J. Chem.* **2005**, *29*, 659-668.
35. Silvester, D. S.; Compton, R. G. Electrochemistry in Room Temperature Ionic Liquids: A Review and Some Possible Applications. *Z. Phys. Chem. (Muenchen, Ger.)* **2006**, *220*, 1247-1274.
36. Evans, R. G.; Wain, A. J.; Hardacre, C.; Compton, R. G. An Electrochemical and ESR Spectroscopic Study on the Molecular Dynamics of Tempo in Room Temperature Ionic Liquid Solvents. *ChemPhysChem* **2005**, *6*, 1035-1039.
37. Lagrost, C.; Carrie, D.; Vaultier, M.; Hapiot, P. Reactivities of Some Electrogenerated Organic Cation Radicals in Room-Temperature Ionic Liquids: Toward an Alternative to Volatile Organic Solvents? *J. Phys. Chem. A* **2003**, *107*, 745-752.
38. Belding, S. R.; Rees, N. V.; Aldous, L.; Hardacre, C.; Compton, R. G. Behavior of the Heterogeneous Electron-Transfer Rate Constants of Arenes and Substituted Anthracenes in Room-Temperature Ionic Liquids. *J. Phys. Chem. C* **2008**, *112*, 1650-1657.
39. Abbott, A. P.; Miaw, C. L.; Rusling, J. F. Correlations between Solvent Polarity Scales and Electron Transfer Kinetics and an Application to Micellar Media. *J. Electroanal. Chem.* **1992**, *327*, 31-46.
40. Clegg, A. D.; Rees, N. V.; Klymenko, O. V.; Coles, B. A.; Compton, R. G. Marcus Theory of Outer-Sphere Heterogeneous Electron Transfer Reactions: High Precision Steady-State Measurements of the Standard Electrochemical Rate Constant for Ferrocene Derivatives in Alkyl Cyanide Solvents. *J. Electroanal. Chem.* **2005**, *580*, 78-86.
41. Fernández, H.; Zón, M. A. Solvent Effects on the Kinetics of Heterogeneous Electron Transfer Processes. The Tmpd/Tmpd<sup>•+</sup> Redox Couple. *J. Electroanal. Chem.* **1992**, *332*, 237-255.



## CHAPTER 8. THEORETICAL CALCULATIONS OF REORGANIZATION ENERGIES

Reorganization energies have been explained in details previously (chapter 3). There are different methods to calculate the inner sphere reorganization energy. The Marcus method is an old method and a more modern method is given by Nelsen, which is commonly being used now because the results obtained by using the Nelsen method are more accurate as compared to those of the Marcus method. This method has been used to obtain the inner sphere reorganization energy term in this study.

The basic meaning of outer sphere reorganization energy has been explained in theory chapter. Here different calculations have been done to apply these ideas to ionic liquids. For these theoretical calculations, the Marcus and Hush models have been applied. Two different approximations have been used for the radius of the molecule.

### 8.1 Computational Study for the Inner Sphere Reorganization Energies

The inner sphere reorganization energy ( $\lambda_i$ ) is determined by quantum mechanical calculations which were first describe by Nelsen et al<sup>1</sup>. For self exchange reactions, the inner-sphere reorganization energy can be described by the difference between the vertical ionization potential and the vertical electron affinity.  $\lambda_i^\infty$  can be determined by the energies for the conformations of the oxidized and reduced species with and without electron transfer. One has to calculate the energies of four points e.g. for the acceptor system the four points are: Nng is the neutral geometry, Nag is the neutral molecule at the geometry of the anion, Aag is anion geometry and Ang is the anion at the geometry of neutral molecule. These four point geometries have been used to determined the relaxation energies of the neutral molecule from Nag to Nng i.e.  $\lambda_2$  and relaxation energies of the anion from Ang to Aag i.e.  $\lambda_1$ .

Generally the inner sphere reorganization energy can be correlated with  $\lambda_1$  and  $\lambda_2$  by the following equation:

$$\lambda_i^\infty = \lambda_1 + \lambda_2 \quad (8.1)$$

$\lambda_1$  and  $\lambda_2$  describe the relaxation after a Frank-Condon type excitation of the oxidized and reduced species.  $\lambda_i^\infty$  is the inner sphere reorganization energy where all the vibrations are taken into account.

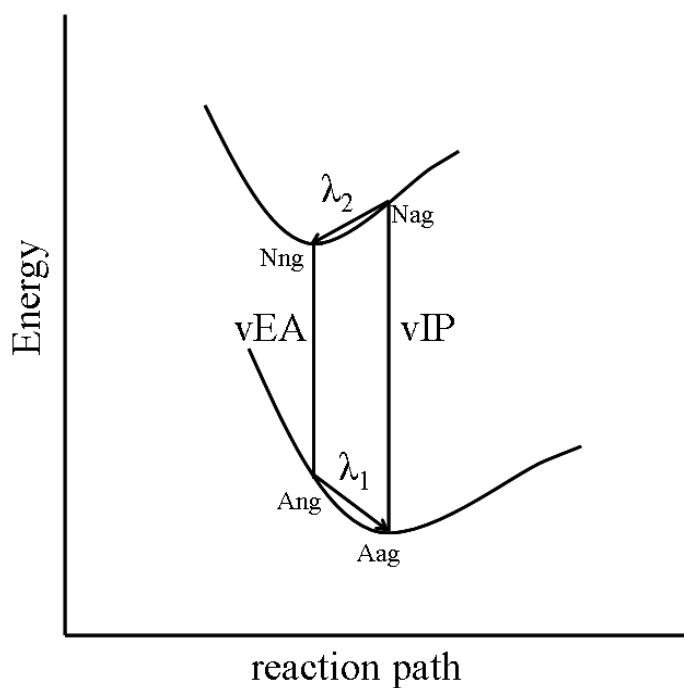


**Figure 8.1** Potential energy curve of the electron transfer reaction for acceptor system

For the donor system, energy of the points Cng (cation at geometry of neutral molecule), Ccg (cation geometry), Ncg (neutral molecule at the geometry of cation) and Nng neutral geometry) have been determined.

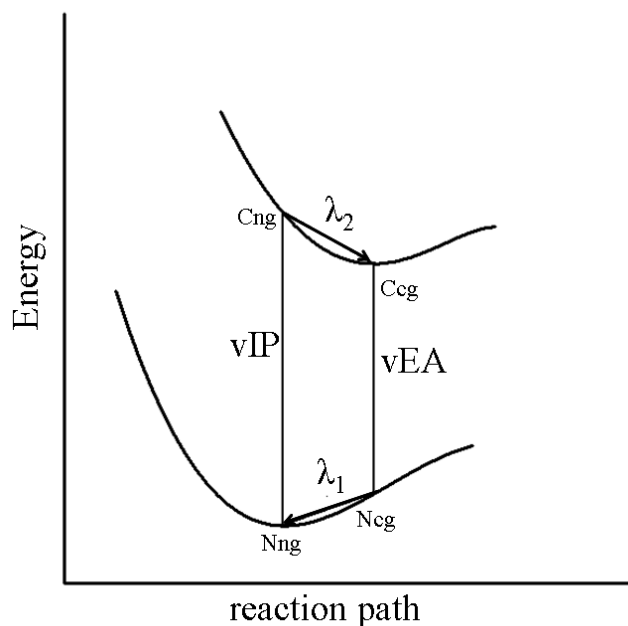


Figure 8.2 Potential energy curve of the electron transfer reaction for donor system

### 8.1.1 Molden Software

The Molden software has been used for the visualization of the structure of the species. The same software has been used to calculate the changes in structure after doing optimization and electron transfer, as changes in bond length and structure can be obtained through this software.

### 8.1.2 ORCA Program

Evaluation of geometries and energies through Density Functional Theory calculations have been performed by employing the molecular modeling software package, ORCA program<sup>2-3</sup> including optimization. B3LYP functional with TZVPP basis set has been used for the geometry optimizations of the oxidized and reduced species. The quality of local minima has been checked by frequency calculations. Also single point calculations were done to receive the vertical ionization potential and vertical electron affinity at the same level of theory.

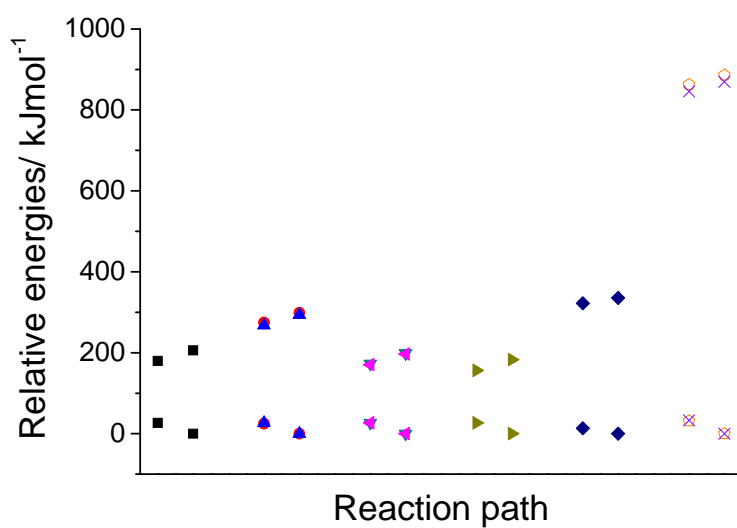


Figure 8.3 Relative four points energies for acceptor system ■ MBQ ● Bromanil ▲ Chloranil

▼ 25DMBQ ◀ 26DMBQ ▶ DQ ◆ TCNE ◻ EV<sup>2+</sup> × MV<sup>2+</sup>

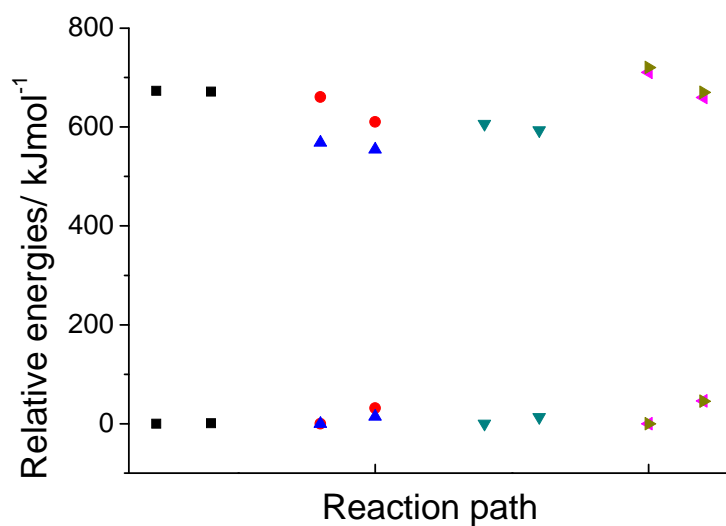


Figure 8.4 Relative four points energies for donor system ■ Fc ● PPD ▲ TMPPD ▼ TTF ◀ TEMPO ▶ TEMPOL

### 8.1.3 Comparison of Ionization potential and Electron Affinity

The quality of the method has been checked by comparing the calculated vertical ionization potential and electron affinities against the published experimental values from the NIST data base. They show a small error of 0.01 to 0.63 eV for the B3LYP/TZVPP method which is appropriate for the calculation of inner sphere reorganization energy.

**Table 8.1 Comparison of ionization potentials and electron affinities with published values (eV)**

	Compounds	I.P	I.P References	E.A	E.A References
Acceptor System	MBQ	2.14		1.59	1.85 <sup>4</sup>
	TBBQ	3.09		2.59	
	TCBQ	3.05		2.50	2.78, 2.45 <sup>5</sup>
	2,5-DMBQ	2.06		1.52	1.76 <sup>4</sup>
	2,6-DMBQ	2.04		1.49	1.76 <sup>4</sup>
	DQ	1.89		1.34	1.60 <sup>4</sup>
	TCNE	3.48		3.20	3.17 <sup>6</sup>
	MV <sup>2+</sup>	9.18	9.19 <sup>7</sup>	8.61	
	EV <sup>2+</sup>	9.01		8.42	
Donor System	Fc	6.98	6.90 <sup>8</sup>	6.95	
	PPD	6.85	6.84 <sup>9</sup>	6.00	
	TMPPD	5.89	6.10 <sup>10</sup>	5.60	
	TTF	6.28	6.30 <sup>11</sup>	6.01	
	TEMPO	7.36	6.73 <sup>12</sup>	6.36	
	TEMPOL	7.47	7.40 <sup>13</sup>	6.48	

### 8.1.4 Relation between Homogeneous and Heterogeneous $\lambda_I$ Values

The inner sphere reorganization energy for homogeneous reaction can be correlated with heterogeneous electron transfer reaction by the following expression<sup>14-15</sup>:

$$\lambda_i(\text{heterogeneous}) = \frac{1}{2} \lambda_i(\text{homogeneous}) \quad (8.2)$$

Only one molecule must be activated at the surface of the electrode.

### 8.1.5 Temperature Correction

The Holstein equation<sup>16</sup> has been employed to get the corrected value of  $\lambda_i$  at room temperature.

$$\lambda_i(T) = \sum_j \lambda_i^\infty \left[ \frac{4kT}{h\nu_j} \tanh \frac{h\nu_j}{4kT} \right] \quad (8.3)$$

with a mean value for the vibrations of:  $\nu_j = 5 \times 10^{13} \text{ s}^{-1}$ .

The calculated inner-sphere reorganization energies calculated with the Nelsen method represent  $\lambda_i^\infty$ -values. The temperature-corrected values, according to eq. (8.3) are listed in

Table 8.2. The value from literature have been recalculated in  $\text{kJmol}^{-1}$  but temperature correction has not been taken into account unless it is already in reference.

Table 8.2 Calculated inner sphere reorganization energies,  $\lambda_i$  kJmol<sup>-1</sup>

	Compounds	This work	Literature
Acceptor System	MBQ	12.6	7.6 <sup>17b,d</sup>
	TBBQ	11.7	9.6 <sup>17b,d</sup>
	TCBQ	12.6	9.7 <sup>17b,d</sup>
	2,5-DMBQ	12.6	10.3 <sup>17b,d</sup>
	2,6-DMBQ	12.7	10.3 <sup>17b,d</sup>
	DQ	12.7	10.3 <sup>17b,d</sup>
	TCNE	6.4	14 <sup>18a,b,e</sup>
	MV <sup>2+</sup>	13.2	32 <sup>19a,c,e</sup>
	EV <sup>2+</sup>	13.6	
Donor System	Fc	0.6	1.4 <sup>20a,b,d</sup>
	PPD	19.5	16 <sup>18,b,e</sup>
	TMPPD	6.7	23 <sup>18a,b,e</sup>
	TTF	6.3	17 <sup>18a,b,e</sup>
	TEMPO	23.1	33.5 <sup>21a,c,e</sup>
	TEMPOL	22.9	

a is inner sphere reorganization energy for homogeneous electron transfer

b by Marcus equation

c by Nelsen method

d without temperature correction

e with temperature correction

### 8.1.6 Discussion

The results of  $\lambda_i$  obtained by the calculations can not be compared with the published data values because these values are determined by different methods as reported in literature. In the published value, some time similar Nelsen method was employed but when quantum mechanical calculation was done but by using AM-1 method with different basis set. The present values have been calculated with the more appropriate DFT method with good basis set B3LYP/TZVPP.



Ferrocene was our benchmark molecule, and both oxidized and reduced species were found in the eclipsed conformation confirming the published value of  $\lambda_i$ . Ferrocene is a metallocene compound which usually doesn't change the structure much during the electron transfer reaction. Therefore it has the smallest value of inner sphere reorganization energy.

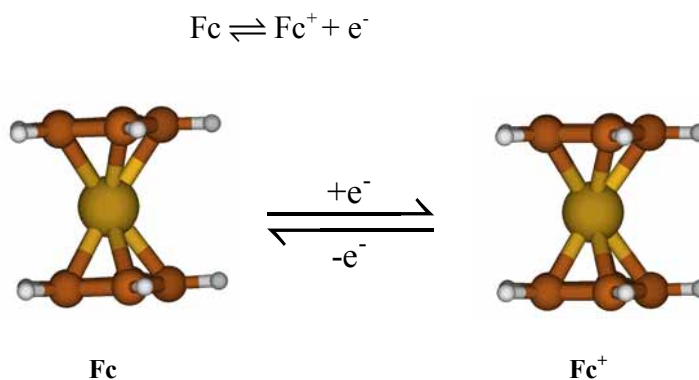


**Figure 8.5 Geometrical changes in Ferrocene after electron transfer**

For  $\text{MV}^{2+}$  and  $\text{EV}^{2+}$  (Figure 8.6 Geometrical changes in Ethylviologen after electron transfer Figure 8.6), inner reorganization energy comes from the change of its twisted conformation to planer structure during electron transfer<sup>22</sup>.

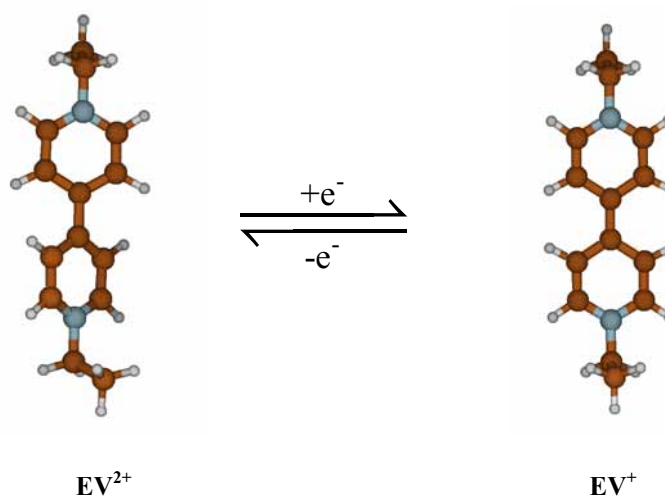


**Figure 8.6 Geometrical changes in Ethylviologen after electron transfer**

For PPD the calculated bond lengths were checked and a good agreement is found<sup>23</sup>. The published data were mainly based on simple Huckle (HMO)-calculations.



Figure 8.7 PPD

Table 8.3 Geometrical Parameters of PPD optimized structure

	Literature <sup>23</sup>	Calculated Neutral	Calculated cation
C1-N (BL)	1.408	1.40604	1.33993
C1-C2	1.389	1.39674	1.42432
C2-C3	1.377	1.38825	1.36192
H-N-H (BA)		110.545°	116.994°
C1-N-H		114.207°	121.502°
C2-C1-N-H		27.359°	0.148°

However, the literature values for bond length agree well with the calculated values but  $\lambda_i$  does not correspond from this calculation to the literature.

Neutral PPD has a permanent dipole moment of 1.51 Db<sup>24</sup>, which agrees with the non-planar structure. The calculated IP (6.84 eV) corresponds well with the published NIST data for IP (6.87 eV).

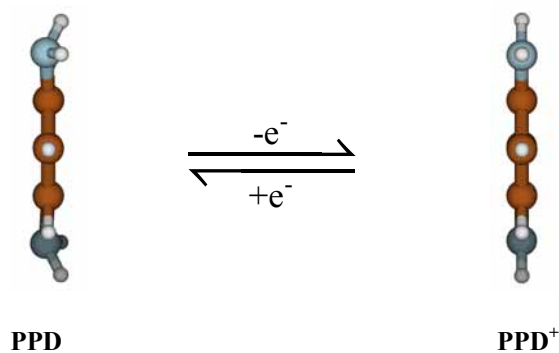


Figure 8.8 Geometrical changes in PPD after electron transfer

Larger geometry changes result in larger inner sphere reorganization energies and it can be either a torsional rotation ( $EV^{2+}$ ,  $MV^{2+}$ ) in Figure 8.6, or a summation of many small bond length changes (DBBQ, 26DMBQ).

## 8.2 Theoretical Calculations of the Outer Sphere Reorganization Energy

Outer sphere reorganization energies have been calculated theoretically using the following equation for those ionic liquids for which data for dielectric constant and refractive index is available.

$$\lambda_o = \frac{e_o^2 \cdot N_L}{8 \cdot \pi \cdot \epsilon_o} \left( \frac{1}{r} - \frac{1}{d_{het}} \right) \cdot \gamma \quad (8.4)$$

Here  $e_o$  is the electronic charge,  $N_L$  is Avogadro's constant,  $\epsilon_o$  is the permittivity of vacuum,  $r$  is the radius of the molecule,  $d_{het}$  is the distance from the reactant to the metal surface and  $\gamma$  the Pekar factor.

In the spherical model  $r$  has been calculated from the molar mass of the substance studied, see eq. 3.10 in chapter 3. The radius of molecule has also been taken from literature where it was determined by considering organic molecules as ellipsoid. It has been discussed earlier in chapter 3.

Table 8.4 Radii of compounds from the spherical and ellipsoidal model

Compounds	r (spherical model) /	r (ellipsoidal model) /
MBQ	3.65	3.19 <sup>25</sup>
TBBQ	5.52	3.85 <sup>25</sup>
TCBQ	4.60	3.68 <sup>25</sup>
2,5-DMBQ	3.78	3.48 <sup>25</sup>
2,6-DMBQ	3.78	3.51 <sup>25</sup>
DQ	4.02	2.77 <sup>25</sup>
TCNE	3.70	3.1 <sup>18</sup>
MV <sup>2+</sup>	5.74	5 <sup>26</sup> 6 <sup>27</sup>
EV <sup>2+</sup>	5.85	
FC	4.19	2.7 <sup>28</sup> 3.5 <sup>26</sup>
PPD	3.50	2.85 <sup>18</sup>
TMPPD	4.02	4.06 <sup>18</sup>
TTF	4.33	3.04 <sup>18</sup>
TEMPO	3.96	3.11 <sup>21</sup>
TEMPOL	4.09	

### 8.2.1 Pekar Factor

The Pekar factor has been calculated using the published data values of dielectric constant,  $\epsilon_s$  and refractive index,  $n$  at room temperature. There is more than one refractive index for one ionic liquid. Although the calculated values of Pekar factors from different values of  $n$  and  $\epsilon_s$  are not changing very much. Only few values are reported for refractive index but the bold values are used (where more than one  $n$ ) for the calculation of Pekar factor which is further used for the outer sphere reorganization energy.

**Table 8.5 Solvent properties of Ionic Liquids**

RTILs	$n$	$\epsilon$	$\gamma$
[emim][BF <sub>4</sub> ]	1.4109 <sup>29</sup>	12.9 <sup>30</sup>	0.425
[bmim][OTf]	1.4380 <sup>31</sup> <b>1.4368</b> <sup>32</sup>	13.2 <sup>30</sup>	0.408 <b>0.409</b>
[bmim][BF <sub>4</sub> ]	1.4218 <sup>32</sup>	11.7 <sup>30</sup>	0.409
[bmim][PF <sub>6</sub> ]	<b>1.4095</b> <sup>32</sup> 1.4079 <sup>33</sup> 1.40937 <sup>34</sup>	11.4 <sup>30</sup>	<b>0.416</b> 0.417 0.416

### 8.2.2 Marcus Approach for Outer Sphere Reorganization Energy

There are two different approaches for  $d_{\text{het}}$  which have been used to determine  $\lambda_o$ .  $d_{\text{het}}$  is assumed by Marcus to be  $2r^{35}$ , based on the classical electro-dynamical picture of a reactant-electrode image interaction.

**Table 8.6 Theoretical values of outer sphere reorganization energy according to Marcus using ellipsoidal radius of molecule**

Compounds	[emim][BF <sub>4</sub> ]	[bmim][OTf]	[bmim][BF <sub>4</sub> ]	[bmim][PF <sub>6</sub> ]
MBQ	46.26	44.50	44.56	45.26
TBBQ	38.33	36.87	36.92	37.50
TCBQ	40.10	38.58	38.63	39.24
2,5-DMBQ	42.41	40.79	40.85	41.49
2,6-DMBQ	42.05	40.44	40.50	41.14
DQ	53.28	51.25	51.32	52.13
TCNE	47.61	45.79	45.86	46.58
MV <sup>2+</sup>	29.52	28.39	28.43	28.88
EV <sup>2+</sup>				
FC	54.66	52.58	52.65	53.48
PPD	51.78	49.81	49.88	50.66
TMPPD	36.35	34.97	35.01	35.56
TTF	48.55	46.70	46.76	47.50
TEMPO	47.45	45.65	45.71	46.43
TEMPOL				

The outer sphere reorganization energies are similar for all these ionic liquids because the Pekar factor is not very different. The difference in viscosity data are about one order of magnitude (range of viscosity is 32 cP to 312 cP).

**Table 8.7** Theoretical values of outer sphere reorganization energy in  $\text{kJmol}^{-1}$  according to Marcus using spherical radius of molecule

Compounds	[emim][BF <sub>4</sub> ]	[bmim][OTf]	[bmim][BF <sub>4</sub> ]	[bmim][PF <sub>6</sub> ]
MBQ	40.48	38.94	38.99	39.61
TBBQ	26.74	25.72	25.76	26.16
TCBQ	32.06	30.84	30.88	31.36
2,5-DMBQ	39.04	37.55	37.61	38.20
2,6-DMBQ	39.04	37.55	37.61	38.20
DQ	36.68	35.28	35.33	35.88
TCNE	39.84	38.33	38.38	38.98
MV <sup>2+</sup>	25.72	24.74	24.77	25.16
EV <sup>2+</sup>	25.23	24.27	24.31	24.69
FC	35.18	33.84	33.89	34.42
PPD	42.16	40.55	40.61	41.24
TMPPD	36.67	35.28	35.33	35.88
TTF	34.10	32.80	32.84	33.36
Tempo	37.29	35.87	35.92	36.48
Tempol	36.10	34.72	34.77	35.32

### 8.2.3 Hush Approach for Outer Sphere Reorganization Energy

In contrast to Marcus, Hush<sup>14</sup> argues that  $d_{\text{het}}$  is larger than  $2r$  since the molecules react in the outer Helmholtz plane. This idea is expressed by  $d_{\text{het}} = \infty$ . A similar calculation has been done to get the value of  $\lambda_o$  by Hush. These values are doubled of the ones obtained by Marcus.

**Table 8.8** Theoretical values of outer sphere reorganization energy,  $\lambda_0$  in  $\text{kJmol}^{-1}$  by Hush using ellipsoidal model for radius

Compounds	[emim][BF <sub>4</sub> ]	[bmim][OTf]	[bmim][BF <sub>4</sub> ]	[bmim][PF <sub>6</sub> ]
MBQ	92.53	89.00	89.13	90.52
TBBQ	76.67	73.75	73.85	75.01
TCBQ	80.21	77.15	77.26	78.47
2,5-DMBQ	84.82	81.59	81.70	82.98
2,6-DMBQ	84.09	80.89	81.00	82.27
DQ	106.56	102.50	102.64	104.25
TCNE	95.21	91.59	91.71	93.15
MV <sup>2+</sup>	59.03	56.78	56.86	57.75
EV <sup>2+</sup>				
FC	109.32	105.16	105.30	106.95
PPD	103.57	99.62	99.76	101.32
TMPPD	72.70	69.93	70.03	71.13
TTF	97.09	93.39	93.52	94.99
TEMPO	94.91	91.29	91.42	92.85
TEMPOL				



**Table 8.9** Theoretical values of outer sphere reorganization energy,  $\lambda_o$  in  $\text{kJmol}^{-1}$  by Hush using spherical model for radius

Compounds	[emim][BF <sub>4</sub> ]	[bmim][OTf]	[bmim][BF <sub>4</sub> ]	[bmim][PF <sub>6</sub> ]
MBQ	80.96	77.88	77.99	79.21
TBBQ	53.48	51.44	51.52	52.32
TCBQ	64.12	61.68	61.76	62.73
2,5-DMBQ	78.08	75.11	75.21	76.39
2,6-DMBQ	78.08	75.11	75.21	76.39
DQ	73.36	70.56	70.66	71.77
TCNE	79.69	76.65	76.76	77.96
MV <sup>2+</sup>	51.44	49.48	49.55	50.33
EV <sup>2+</sup>	50.47	48.54	48.61	49.37
FC	70.37	67.68	67.78	68.84
PPD	84.31	81.10	81.21	82.49
TMPPD	73.35	70.55	70.65	71.76
TTF	68.20	65.60	65.69	66.72
TEMPO	74.58	71.74	71.84	72.96
TEMPOL	72.20	69.44	69.54	70.63

## 8.2.4 Experimental Outer Sphere Reorganization Energies

Outer sphere reorganization energy has been estimated experimentally using the Marcus equation for heterogeneous electron transfer reaction.

$$k_{\text{het}} = Z_{\text{het}} \exp\left(\frac{-\Delta G^*}{RT}\right) \quad (8.5)$$

After substituting reorganization parameters in place of  $\Delta G^*$  and then rearrangements give the following equation(8.6) which has been used to deduce the value of  $\lambda_o$

$$\lambda_o = 4RT \ln \left( \frac{Z_{\text{het}}}{k_{\text{het}}} \right) - \lambda_i \quad (8.6)$$

The collision frequency  $Z_{\text{het}}$  can easily be calculated by molar mass. It has been explained in chapter 3. The results of heterogeneous electron transfer rate constant obtained at room temperature has been used here.

Table 8.10  $\lambda_0$  values in  $\text{kJ mol}^{-1}$  using experimental data in all ionic liquids at room temperature<sup>a</sup>

Compounds	Molar mass / $\text{g mol}^{-1}$	$Z_{\text{het}}^b / 10^3 \text{ cms}^{-1}$	[emim][BF <sub>4</sub> ]	[bmim][OTf]	[bmim][BF <sub>4</sub> ]	[bmim][PF <sub>6</sub> ]	[omim][BF <sub>4</sub> ]
MBQ	122.12	5.7	145	136	148	161	150
TBBQ	423.68	3.1	136	-	146	155	-
TCBQ	245.88	4.0	145	149	152	149	159
2,5-DMBQ	136.15	5.4	155	163	163	156	-
2,6-DMBQ	136.15	5.4	146	153	161	167	-
DQ	164.20	4.9	150	-	154	160	156
TCNE	128.09	5.5	143	-	147	149	164
MV <sup>2+</sup>	476.18	2.9	139	144	147	148	-
EV <sup>2+</sup>	504.24	2.8	134	140	149	150	-
Fc	186.03	4.6	157	164	165	169	-
PPD	108.14	6.0	134	138	142	145	-
TMPPD	164.25	4.9	151	154	160	-	165
TTF	204.36	4.4	143	147	150	157	-
TEMPO	156.25	5.0	135	132	138	141	149
TEMPOL	172.24	4.8	127	150	151	154	138

a- from equation (8.5)

b- from equation (3.5)

## 8.2.5 Discussion

These experimental values for  $\lambda_0$  are very different from the theoretical values. It means that theoretical values are very questionable by using deduced dielectric constants for ionic liquids.

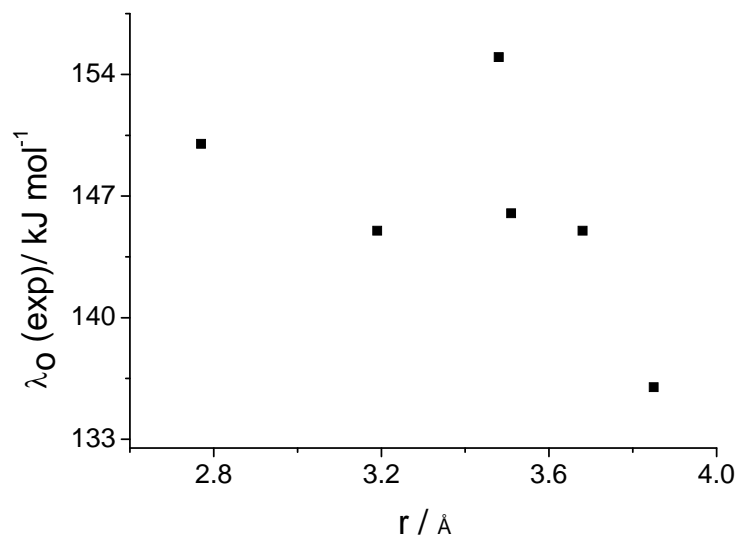


Figure 8.9 Quinones in [emim][BF<sub>4</sub>]

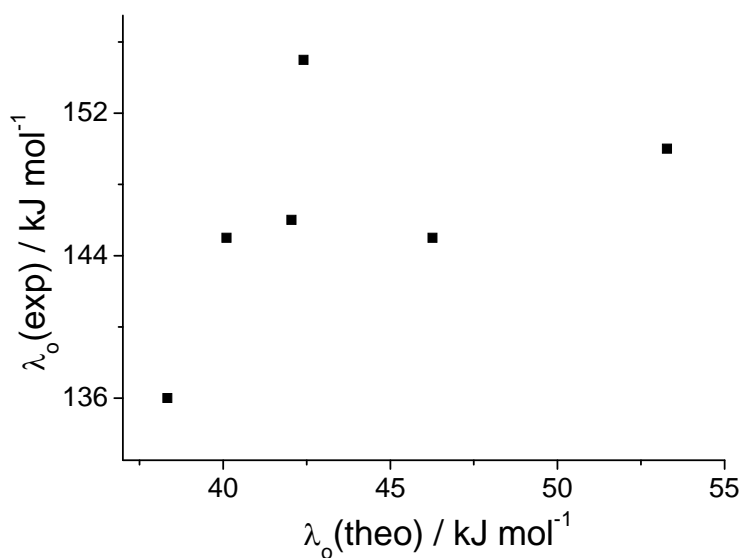
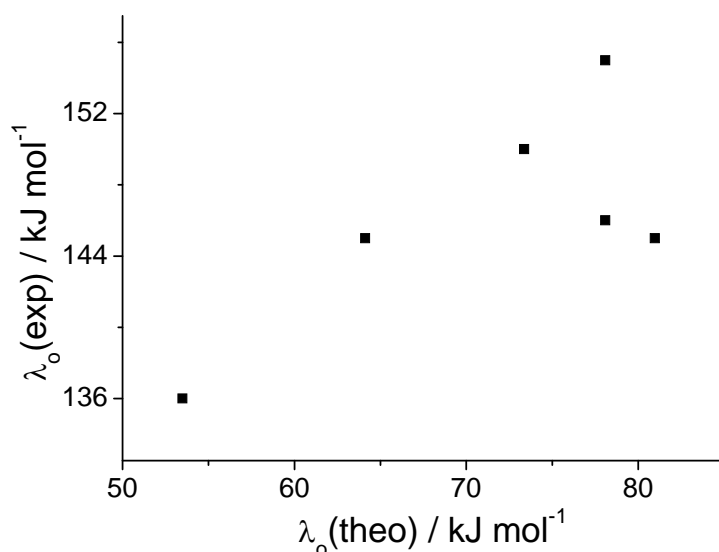


Figure 8.10 Quinones in [emim][BF<sub>4</sub>] theoretical  $\lambda_0$  calculated by Marcus model using ellipsoidal radius



**Figure 8.11** Quinones in [emim][BF<sub>4</sub>], theoretical  $\lambda_o$  calculated by Hush model using spherical radius

All these plot show that experimental values of outer sphere reorganization energies are not fitting well with any theoretical approximation.

Dielectric constants of ionic liquids are not directly measurable as for classical organic solvent. Dielectric constant values are deduced from various experimental methods like Stokes shift, Reichert scale etc. The use of the Pekar factor to calculate  $\lambda_o$  is questionable for ILs because a Marcus concept of dielectric polarization of the solvent is not applicable to ILs. The  $\lambda_o$  for ILs also exists, but the origin is different from the classical Marcus theory describing the change of polarization by the dielectric constant and refractive index. Marcus relation of  $\lambda_o$  is based on Born equation which includes a  $1/r$  distance dependence of the Coulomb potential of the charge reacting species<sup>36</sup>.

All these results indicate that the classical Marcus relation for  $\lambda_o$  is not applicable to ionic liquids as solvents. In a series of remarkable papers, Kobra et al<sup>37-38</sup> et al. indicate that it is dangerous to use classical dipole and dielectric descriptions for ionic liquids. They pointed out that the use of dipolar description on an ionic charge distribution or the use of the dielectric continuum model for the medium is questionable on fundamental physical reasons<sup>39</sup>. This is in contrast to recent theoretical calculations published by R. M. Lynden-

Bell<sup>40-41</sup>, indicating that the outer sphere reorganization energies in ILs should be similar to those calculated from equation (8.4).

1. Nelsen, S. F.; Blackstock, S. C.; Kim, Y. Estimation of inner shell Marcus terms for amino nitrogen compounds by molecular orbital calculations. *J. Am. Chem. Soc.* **1987**, *109*, 677-682.
2. Neese, F. Sum-over-states based multireference ab initio calculation of EPR spin Hamiltonian parameters for transition metal complexes. A case study. *Magnetic Resonance in Chemistry* **2004**, *42*, S187-S198.
3. Neese, F. Correlated ab initio calculation of electronic g-tensors using a sum over states formulation. *Chemical Physics Letters* **2003**, *380*, 721-728.
4. Heinis, T.; Chowdhury, S.; Scott, S. L.; Kebarle, P. Electron affinities of benzo-, naphtho-, and anthraquinones determined from gas-phase equilibria measurements. *J. Am. Chem. Soc.* **1988**, *110*, 400-407.
5. Farragher, A. L.; Page, F. M. Experimental determination of electron affinities: Part 9. - Benzoquinone, chloranil and related compounds. *Transactions of the Faraday Society* **1966**, *62*, 3072-3080.
6. Chowdhury, S.; Kebarle, P. Electron affinities of di- and tetracyanoethylene and cyanobenzenes based on measurements of gas-phase electron-transfer equilibria. *J. Am. Chem. Soc.* **1986**, *108*, 5453-5459.
7. Peon, J.; Tan, X.; Hoerner, J. D.; Xia, C.; Luk, Y. F.; Kohler, B. Excited state dynamics of methyl viologen. Ultrafast photoreduction in methanol and fluorescence in acetonitrile. *J. Phys. Chem. A* **2001**, *105*, 5768-5777.
8. Barfuss, S.; Grade, M.; Hirschwald, W.; Rosinger, W.; Boag, N. M.; Driscoll, D. C.; Dowben, P. A. The stability and decomposition of gaseous chloroferrocenes. *Journal of Vacuum Science & Technology A: Vacuum, Surfaces, and Films* **1987**, *5*, 1451-1455.
9. Tsuji, K.; Saito, M.; Tani, T. Ionization potentials of phenylenediamines and steric effect in the ortho isomer. *Denki Kagaku oyobi Kogyo Butsuri Kagaku* **1973**, *41*, 668.
10. Egdell, R.; Green, J. C.; Rao, C. N. R. Photoelectron spectra of substituted benzenes. *Chemical Physics Letters* **1975**, *33*, 600-607.
11. KOBAYASHI; #160; T.; YOSHIDA; Z.; AWAJI; H.; KAWASE; YONEDA; S. *Intramolecular orbital interactions in 6,6'-bi(1,4-dithiafulvenyl) studied by photoelectron spectroscopy*; Chemical Society of Japan: Tokyo, JAPON, 1984; Vol. 57.
12. Morishima, I.; Yoshikawa, K.; Yonezawa, T.; Matsumoto, H. Photoelectron spectra studies of organic free radicals. The nitroxide radical. *Chemical Physics Letters* **1972**, *16*, 336-339.
13. Sümmermann, W.; Deffner, U. Die elektrochemische oxidation aliphatischer nitroxyl-radikale. *Tetrahedron* **1975**, *31*, 593-596.

14. Hush, N. S. Homogeneous and heterogeneous optical and thermal electron transfer. *Electrochim. Acta* **1968**, *13*, 1005-1023.
15. Grampp, G.; Kapturkiewicz, A.; Jaenicke, W. Homogeneous and heterogeneous electron transfer rates of the tetrathiafulvalene-system. *Ber. Bunsen-Ges. Phys. Chem.* **1990**, *94*, 439-447.
16. Holstein, T. Reaction-rate treatment of small-polaron hopping. The role of vibrational relaxation. *Philos. Mag., [Part] B* **1978**, *37*, 499-526.
17. Rüssel, C.; Jaenicke, W. Heterogeneous electron exchange of quinones in aprotic solvents. Part IV. Influence of molecular structure and size on the exchange rate constants both reductions steps. *J. Electroanal. Chem.* **1986**, *200*, 249-260.
18. Grampp, G.; Jaenicke, W. Kinetics of Diabatic and Adiabatic Electron Exchange in Organic Systems Comparison of Theory and Experiment. *Berichte der Bunsengesellschaft für physikalische Chemie* **1991**, *95*, 904-927.
19. Grampp, G.; Kattinig, D.; Mladenova, B. ESR-spectroscopy in ionic liquids: Dynamic linebroadening effects caused by electron-self exchange reactions within the methylviologene redox couple. *Spectrochim Acta A Mol Biomol Spectrosc* **2006**, *63*, 821-825.
20. Richardson, D. E. Potential surfaces for gas-phase electron-transfer reactions. *J. Phys. Chem.* **1986**, *90*, 3697-3700.
21. Grampp, G.; Rasmussen, K. Solvent dynamical effects on the electron self-exchange rate of the TEMPO<sup>•</sup>/TEMPO<sup>+</sup> couple (TEMPO = 2,2,6,6-tetramethyl-1-piperidinyloxy radical): Part I. ESR-linebroadening measurements at T = 298 K. *Physical Chemistry Chemical Physics* **2002**, *4*, 5546-5549.
22. Yasui, S.; Itoh, K.; Ohno, A.; Tokitoh, N. Effect of structural change in viologen acceptors on the rate of single electron transfer from tributylphosphine. *Organic and Biomolecular Chemistry* **2006**, *4*, 2928-2931.
23. Poveteva, Z. P.; Zvonkova, Z. V. *Kristallografiya* **1975**, *20*, 839.
24. McClellan, A. L. *Tables of Experimental Dipole Moments*; Freeman & Co.: San Francisco, 1963.
25. Rüssel, C., University of Erlangen, 1984.
26. Howes, K. R.; Pippin, C. G.; Sullivan, J. C.; Meisel, D.; Espenson, J. H.; Bakac, A. Kinetics of electron-transfer reactions between transition-metal complexes and the methyl viologen radical cation. *Inorganic Chemistry* **1988**, *27*, 2932-2934.
27. Tsukahara, K.; Wilkins, R. G. Kinetics of reduction of cobalt(III) complexes by viologen radicals. *Inorganic Chemistry* **1985**, *24*, 3399-3402.
28. Longinotti, M. P.; Corti, H. R. Diffusion of ferrocene methanol in super-cooled aqueous solutions using cylindrical microelectrodes. *Electrochem. Commun.* **2007**, *9*, 1444-1450.
29. Soriano, A. N.; Doma, B. T., Jr.; Li, M.-H. Density and refractive index measurements of 1-ethyl-3-methylimidazolium-based ionic liquids. *J. Taiwan Inst. Chem. Eng.* **2010**, *41*, 115-121.
30. Weingaertner, H. The static dielectric constant of ionic liquids. *Z. Phys. Chem. (Muenchen, Ger.)* **2006**, *220*, 1395-1405.
31. Bonhote, P.; Dias, A.-P.; Papageorgiou, N.; Kalyanasundaram, K.; Gratzel, M. Hydrophobic, Highly Conductive Ambient-Temperature Molten Salts†. *Inorganic Chemistry* **1996**, *35*, 1168-1178.

32. Soriano, A. N.; Doma Jr, B. T.; Li, M. H. Measurements of the density and refractive index for 1-n-butyl-3-methylimidazolium-based ionic liquids. *J. Chem. Thermodyn.* **2009**, *41*, 301-307.
33. Jaitely, V.; Karatas, A.; Florence, A. T. Water-immiscible room temperature ionic liquids (RTILs) as drug reservoirs for controlled release. *International Journal of Pharmaceutics* **2008**, *354*, 168-173.
34. Pereiro, A. B.; Rodríguez, A. Thermodynamic properties of ionic liquids in organic solvents from (293.15 to 303.15) K. *Journal of Chemical and Engineering Data* **2007**, *52*, 600-608.
35. Marcus, R. A. The theory of oxidation-reduction reactions involving electron transfer. V. Comparison and properties of electrochemical and chemical rate constants. *J. Phys. Chem.* **1963**, *67*, 853-857.
36. Marcus, R. A. Tutorial on rate constants and reorganization energies. *J. Electroanal. Chem.* **2000**, *483*, 2-6.
37. Kobrak, M. N. Electrostatic interactions of a neutral dipolar solute with a fused salt: A new model for solvation in ionic liquids. *J. Phys. Chem. B* **2007**, *111*, 4755-4762.
38. Kobrak, M. N. The relationship between solvent polarity and molar volume in room-temperature ionic liquids. *Green Chem.* **2008**, *10*, 80-86.
39. Kobrak, M. N.; Li, H. Electrostatic interactions in ionic liquids: the dangers of dipole and dielectric descriptions. *Physical Chemistry Chemical Physics* **2010**, *12*, 1922-1932.
40. Lynden-Bell, R. M. Can Marcus Theory Be Applied to Redox Processes in Ionic Liquids? A Comparative Simulation Study of Dimethylimidazolium Liquids and Acetonitrile. *J. Phys. Chem. B* **2007**, *111*, 10800-10806.
41. Lynden-Bell, R. M. Does Marcus theory apply to redox processes in ionic liquids? A simulation study. *Electrochem. Commun.* **2007**, *9*, 1857-1861.



## CHAPTER 9. TEMPERATURE DEPENDENT MEASUREMENTS

All oxidation and reduction couples which have been studied at room temperature, were also studied at various temperatures in all five dried RTILs. Each experiment have been done at various temperatures from 288K to 353 K with 5K or sometimes 10K interval, by using a temperature controlled cell which is specially designed in our lab. At each temperature, cyclic voltammograms have been recorded at different scan rates from 20 to 500  $\text{mV sec}^{-1}$ . It has been observed that the peak current is increasing with increase in scan rate as well as with increase in temperature cf. Figure 9.1-Figure 9.5. By increasing temperature, the viscosity of the medium is decreasing resulting in faster diffusion.

Only a few electrochemical temperature dependent studies in ionic liquids have been published in literature<sup>1-2</sup>.

Diffusion coefficients and heterogeneous electron transfer rate constant have been calculated at each temperature. Corresponding values of activation energy has also been determined for each oxidation and reduction couple.

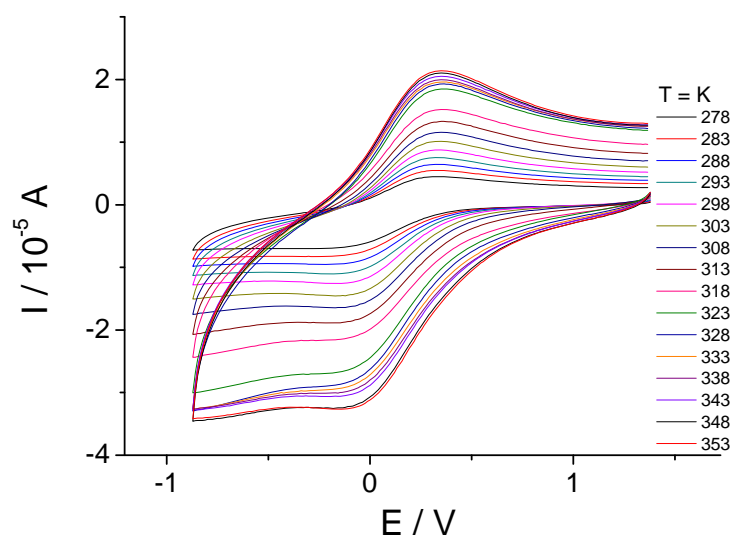


Figure 9.1 TCBQ in [emim][BF<sub>4</sub>]

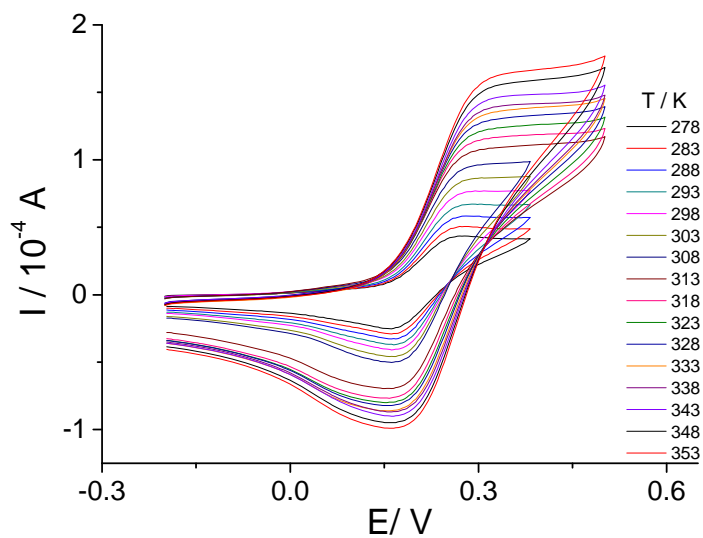


Figure 9.2 TTF in [bmim][OTf]

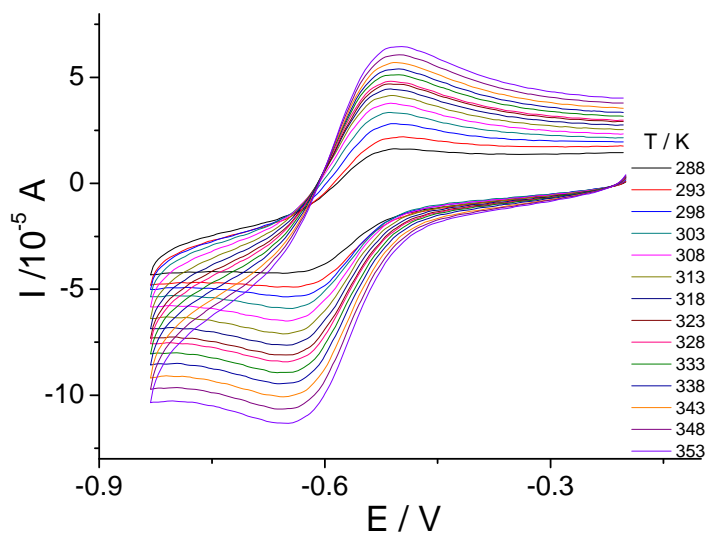


Figure 9.3  $\text{EV}^{2+}$  in [bmim][BF<sub>4</sub>]

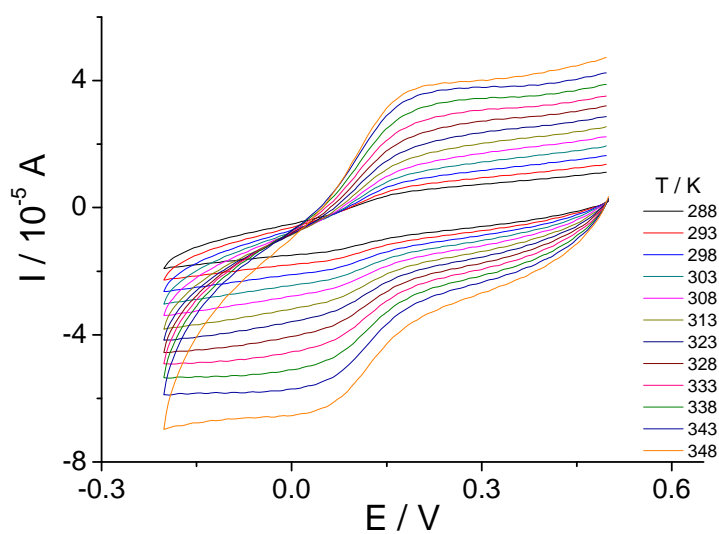


Figure 9.4 TCNE in [bmim][PF<sub>6</sub>]

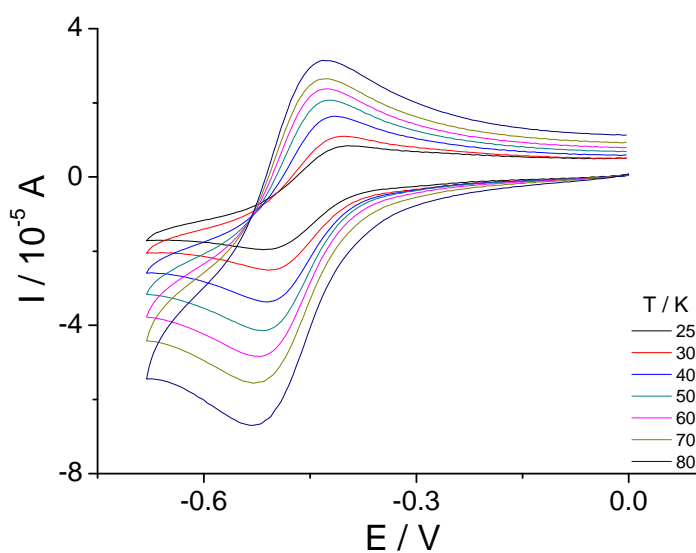


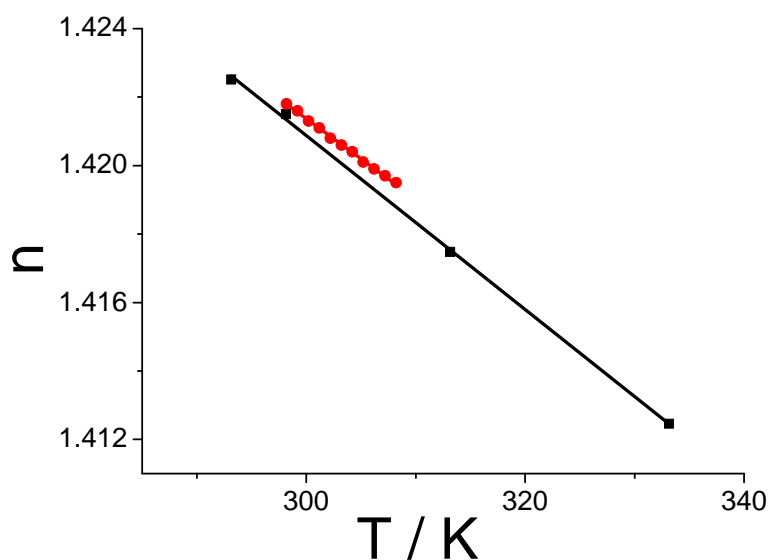
Figure 9.5 DQ in [omim][BF<sub>4</sub>]

## 9.1 Temperature Dependent Properties

It is not simple to interpret temperature dependent results, since many physicochemical properties are affected by temperature e.g. viscosity, refractive index, dielectric constant, conductivity etc.

### 9.1.1 Refractive Index

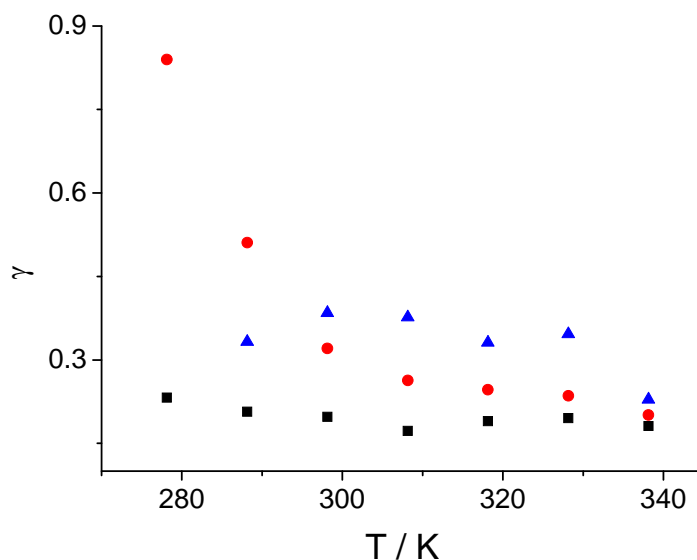
Temperature<sup>3-4</sup> dependent refractive indices have been reported before for all the used RTILs [emim][BF<sub>4</sub>], [bmim][OTf], [bmim][BF<sub>4</sub>], [bmim][PF<sub>6</sub>] and [omim][BF<sub>4</sub>]. Refractive indices is not greatly changing with temperature (e.g for [bmim][BF<sub>4</sub>]<sup>5</sup> the range is 1.4218 to 1.4195 from 298.2 K to 308.2 K, for [bmim][PF<sub>6</sub>]<sup>5</sup> the refractive index is 1.4095 at 298.2K and at 308.2K the value is 1.4075, the change in refractive index for [bmim][OTf]<sup>5</sup> is from 1.4368 to 1.4346 in a temperature range of 298.2 K to 308.2 K and for [emim][BF<sub>4</sub>]<sup>3</sup>, n is 1.4123 at 293.2 and 1.4087 at 308.2K).



9.6 Refractive index for [bmim][BF<sub>4</sub>] from two papers • Soriano<sup>5</sup> ■ Tariq<sup>6</sup>

### 9.1.2 Pekar Factor

Temperature dependence of the dielectric properties for different ILs has been studied by Buchner<sup>7</sup>. These data has been used to evaluate Pekar factor.  $\gamma = \left( \frac{1}{\epsilon_{\infty}} - \frac{1}{\epsilon_s} \right)$



9.7 Pekar factor at different temperature ■ [emim][BF<sub>4</sub>] ● [bmim][BF<sub>4</sub>] ▲ [bmim][PF<sub>6</sub>]

These Pekar factor values are showing very scattered results against temperature. No general criteria can be set by using Pekar factor at different temperature for ILs because different ionic liquids are behaving differently.

### 9.1.3 Viscosity

The viscosity is greatly affected by changes in temperature. Arrhenius type equations are not the best models to fit the temperature dependence of the viscosity of ionic liquids. The traditional plot does not give a straight line but a slight curve. Viscosities of RTILs as a function of temperature are very challenging properties because of the drastic increase at low temperature and a smooth decrease at high temperature. Different equations have been used to fit the temperature dependent viscosity data of ionic liquids in literature.

The Vogel-Fulcher-Tamman (VFT) equation has been used to fit the viscosity data at different temperature for different RTILs. The data for the viscosity has been taken from literature.

$$\eta = \eta_0 \exp\left(\frac{B}{T-T_0}\right) \quad (9.1)$$

Here,  $\eta_0$ , B and  $T_0$  are the constants

Table 9.1. VFT equation parameters for viscosity data

RTILs	$\eta_0/10^{-1}$ mPas	B/ $10^2$ K	T <sub>0</sub> / $10^2$ K
[emim][BF <sub>4</sub> ] <sup>8</sup>	2.0	7.5	1.5
[bmim][BF <sub>4</sub> ] <sup>9</sup>	0.0378	19.70	0.896
[bmim][PF <sub>6</sub> ] <sup>9</sup>	0.2956	13.20	1.48

Ghatee<sup>10</sup> also gave an equation which gives a good fit of viscosity as a function of temperature but there is no value for the constants in the equation. Nevertheless, It is OK to know that there is an equation which gives a perfect straight line for the temperature dependent viscosity in RTILs but it does not have any physical meaning. It is strictly empirical.

$$\left(\frac{1}{\eta}\right)^{\phi} = a + bT \quad (9.2)$$

Where a and b are constant and  $\phi$  is a characteristic exponent which is commonly taken as 0.300.

An Arrhenius type law equation was used to determine the activation energies for viscosities which were calculated from VFT equation.

$$\eta = \eta_{\infty} \exp\left(-\frac{E_{\eta}}{RT}\right) \quad (9.3)$$

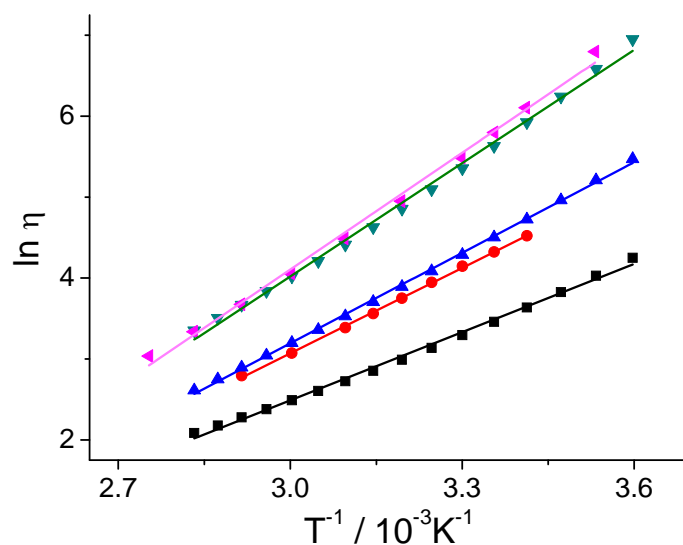


Figure 9.8 Plot of  $\ln \eta$  against  $1/T$  for ■ [emim][BF<sub>4</sub>], ● [bmim][OTf], ▲ [bmim][BF<sub>4</sub>], ▼ [bmim][PF<sub>6</sub>] and ▲ [omim][BF<sub>4</sub>]

The activation energy of viscosity which has been obtained from the slope of plot between  $\ln \eta$  and inverse of temperature, is 23.34 kJmol<sup>-1</sup>, 29.26 kJmol<sup>-1</sup>, 31.0 kJmol<sup>-1</sup> and 38.77 kJmol<sup>-1</sup> 39.98 kJmol<sup>-1</sup> for [emim][BF<sub>4</sub>], [bmim][OTf], [bmim][BF<sub>4</sub>], [bmim][PF<sub>6</sub>] and [omim][BF<sub>4</sub>] respectively. A reason to choose Arrhenius plot is to determine the activation energy of viscosity which is not possible from VFT equation. This values will be used later to discuss the results.

## 9.2 Diffusion Coefficient

Using the Randles Sevcik's equation, from the slope of the plot between peak current and the square root of scan rate, the diffusion coefficient has been determined.

$$I_p = 0.4463nF \left( \frac{nF}{RT} \right)^{1/2} AD^{1/2}Cv^{1/2} \quad (9.4)$$

Diffusion coefficients have been determined at each temperature. The rate of mass transport is higher at higher temperature because of the decrease in viscosity. It is showing linear dependency with inverse of temperature.

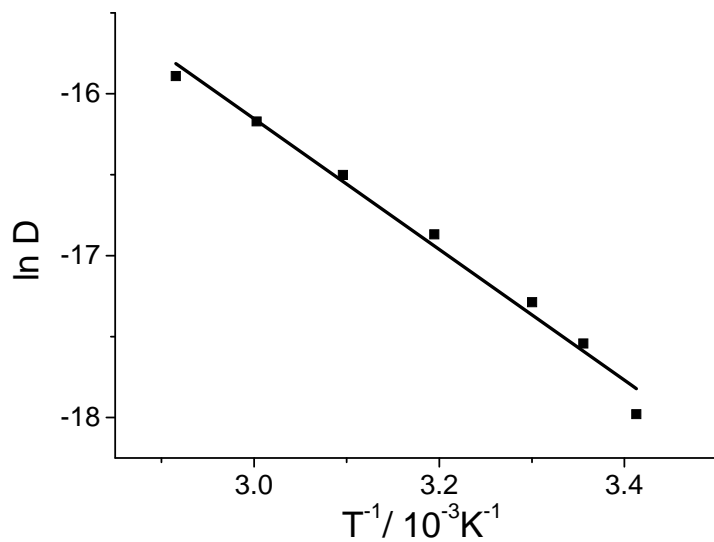


Figure 9.9  $MV^{2+}$  in [emim][ $BF_4$ ]

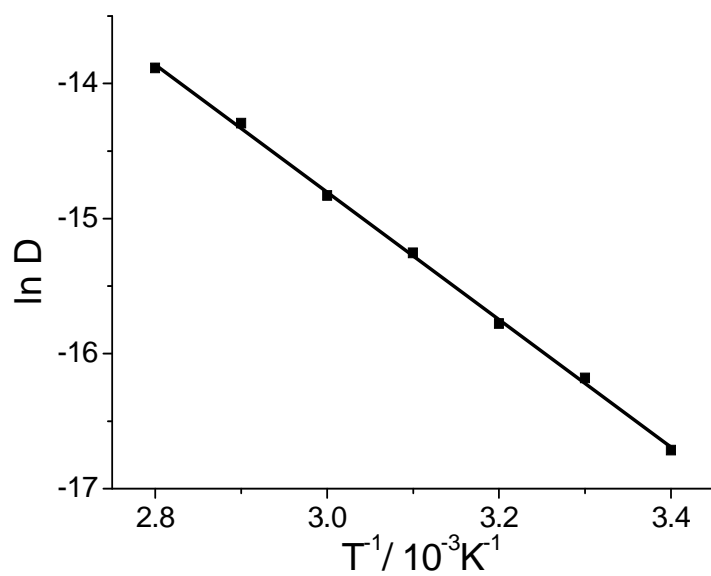
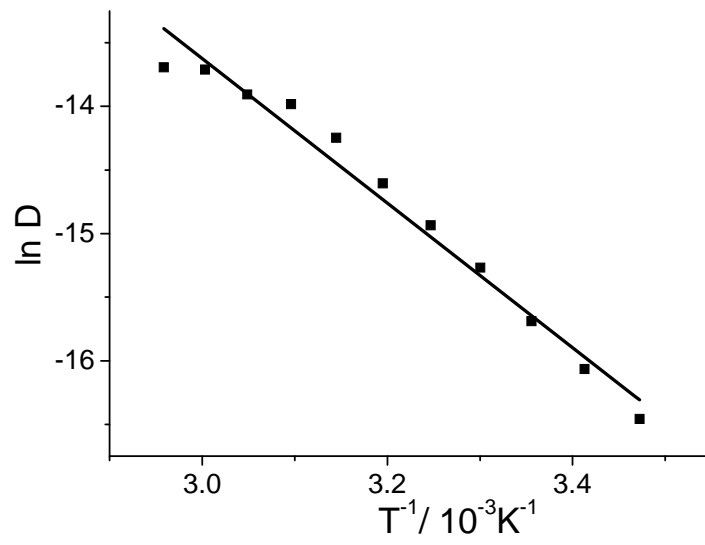
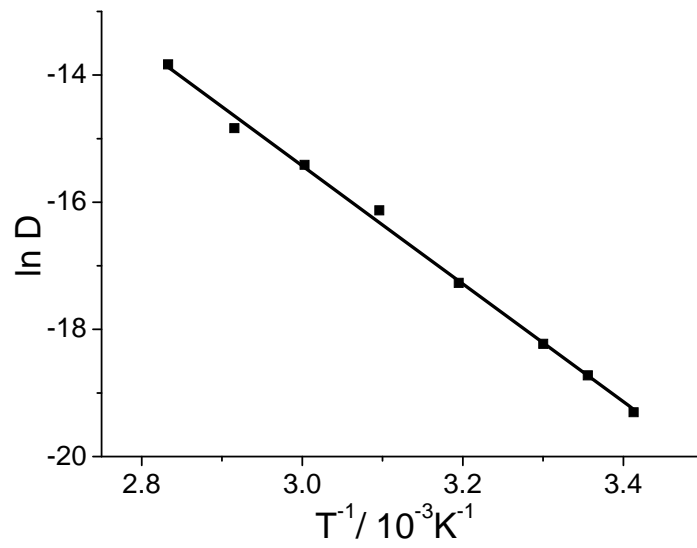


Figure 9.10 TEMPOL in [bmim][OTf]



Figure 9.11 TCNE in [bmim][BF<sub>4</sub>]Figure 9.12 TCNQ in [bmim][PF<sub>6</sub>]

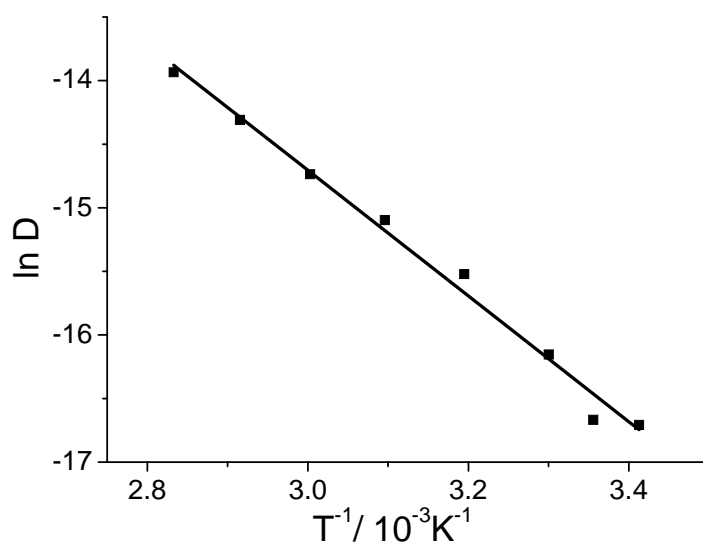


Figure 9.13 TTF in [omim][BF<sub>4</sub>]

The activation energy for diffusion can easily be determined from the slope of the plot of  $\ln D$  versus  $1/T$  by using the following equation.

$$D = D_0 \exp\left(-\frac{E_D}{RT}\right) \quad (9.5)$$

Linear plot between  $\ln D$  against  $1/T$  have been obtained. There is a linear dependence between diffusion coefficient and inverse of viscosity. Non-zero value of the intercept have been obtained which makes it difficult to talk about the validation of Stokes-Einstein equation. The Stokes-Einstein equation is given below,

$$D = \frac{k_B T}{c \pi \eta r} \quad (9.6)$$

Where  $T$  is the absolute temperature,  $\eta$  is the viscosity,  $r$  is the effective spherical radius of the diffusing specie, and  $c$  is a constant with a value of 4 and 6 for the “slip” and “stick” hydrodynamic boundary conditions, respectively. There should be no appearance of an intercept in this equation when one plots the diffusion coefficients versus inverse of viscosity. In literature, there is a big discussion upon the applicability or non validity of the Stokes-Einstein equation. There are few reports about the non-stokes Einstein behaviour in ionic liquid<sup>11-13</sup>. There is also a paper about fractional

Stokes-Einstein behaviour in ionic liquids<sup>14</sup>. In contrast, Compton et al. have been observed that larger molecules closely follow the Stokes-Einstein behaviour, where as solute of smaller radii like H<sub>2</sub>S and SO<sub>2</sub> did not follow Stokes-Einstein at all<sup>1,15</sup>. However they have also observed an intercept in a plot of diffusion coefficient versus inverse of viscosity. Our results are similar to the one observed by Compton.

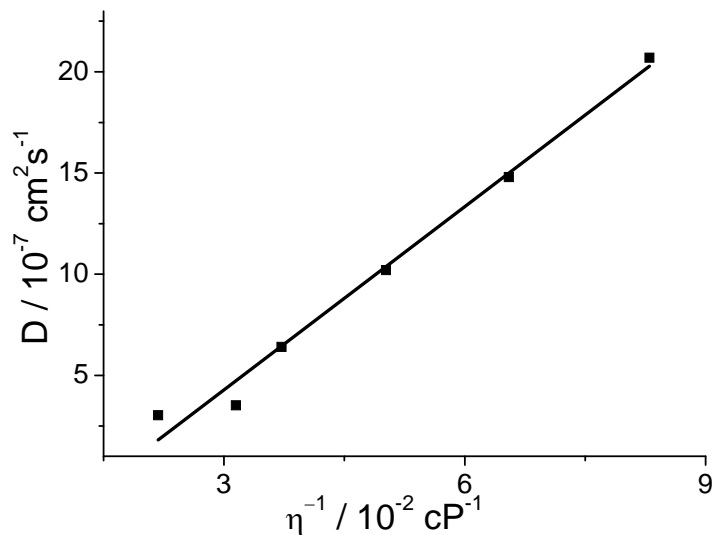


Figure 9.14 DQ in [emim][BF<sub>4</sub>]

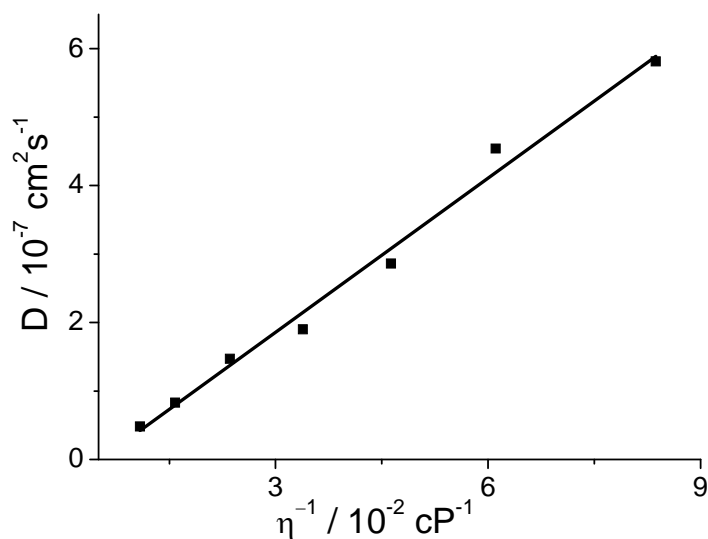
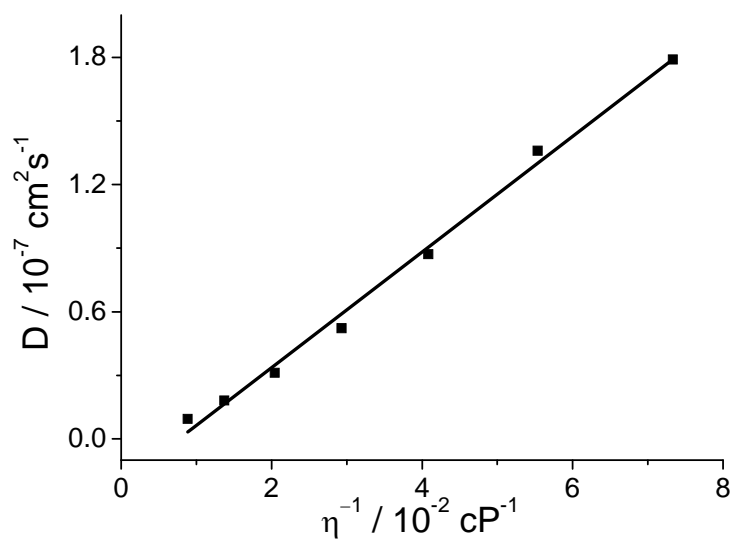
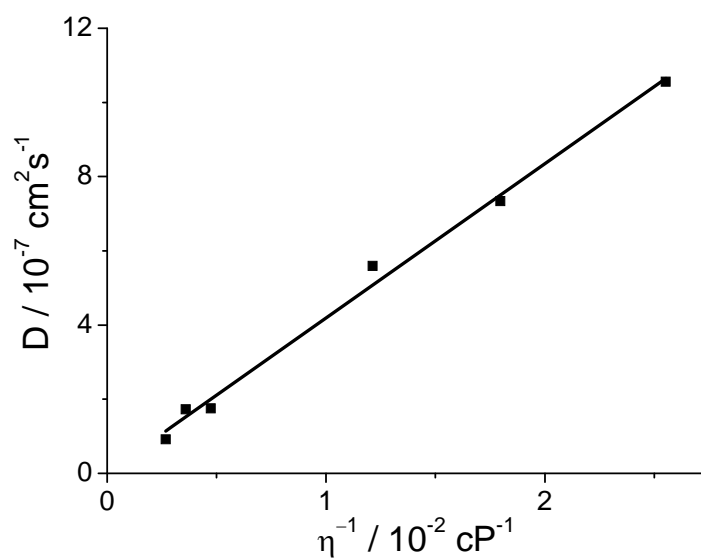


Figure 9.15 EV<sup>2+</sup> in [bmim][OTf]

Figure 9.16 TMPPD in [bmim][BF<sub>4</sub>]Figure 9.17 PPD in [bmim][PF<sub>6</sub>]

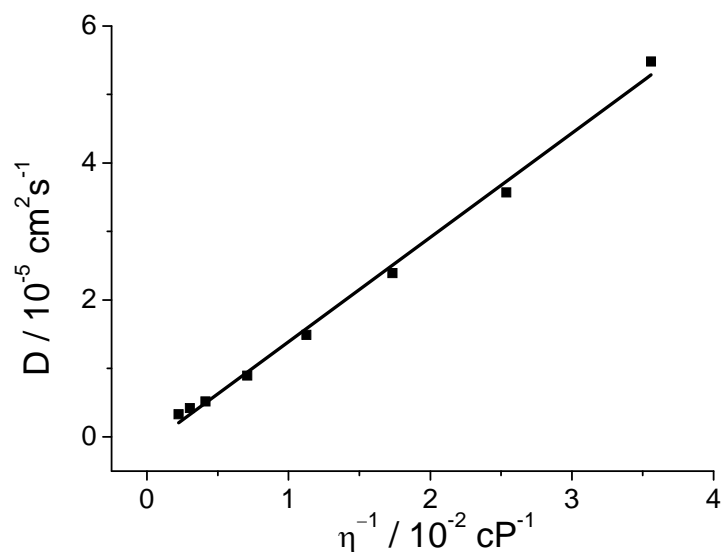


Figure 9.18 TEMPO in [omim][BF<sub>4</sub>]

### 9.3 The Heterogeneous Electron Transfer Rate Constant

Nicholson method<sup>16</sup> has been used to determine the heterogeneous electron transfer rate constant at various temperatures.

$$k_{\text{het}} = \frac{\psi}{\gamma^{\alpha}} \sqrt{\frac{\pi n F \nu D}{RT}} \quad (9.7)$$

All the parameters were explained in chapter 7.  $\psi$  is a dimensionless charge transfer parameter depending on  $\Delta E_p$ .  $\psi$ -values for various  $\Delta E_p$  at 298 K are tabulated by Nicholson<sup>16</sup>, but another equation has been used here to get the corresponding value of  $\psi$  at particular  $\Delta E_p$  at room temperature<sup>17</sup>.

A correction in  $\Delta E_p$  is needed to get the correct value of  $\psi$  at different temperatures<sup>18</sup>. It can be done by using:

$$\Delta E_p^{298} = \Delta E_p^T \left( \frac{298}{T} \right) \quad (9.8)$$

Here,  $T$  is the temperature at which cyclic voltammogram has been recorded,  $\Delta E_p^T$  is the difference in anodic and cathodic peak at that temperature from the cyclic

voltammogram and  $\Delta E_p^{298}$  is the corresponding value of  $\Delta E_p$  at 298 K which itself, can be used to determine the value of  $\psi$  at 298 K.

Heterogeneous electron transfer rate constant have been calculated at each temperature for every scan rate. The heterogeneous electron transfer rate constant increased systematically with temperature due to decrease in viscosity of the ionic liquids at higher temperature, which also give rise high peak current at high temperature. cf. Table 9.2

**Table 9.2 Diffusion coefficients and heterogeneous electron transfer rate constants at different temperature for  $EV^{2+}$  in [bmim][BF<sub>4</sub>]**

T / K	D / $10^{-7} \text{cm}^2 \text{s}^{-1}$	$k_{\text{het}} / 10^{-4} \text{cms}^{-1}$
293	0.250	1.24
298	0.917	2.12
303	1.45	2.59
308	2.40	3.35
313	3.23	4.37
318	4.23	5.13
323	6.30	6.23
328	7.20	6.82
333	8.30	7.51
338	9.77	8.06
343	11.1	9.14
348	12.7	9.99

## 9.4 Activation Energy

According to Marcus, the heterogeneous electron transfer rate constant can be written as,

$$k_{\text{het}} = Z_{\text{het}} \exp\left(\frac{-\Delta G^*}{RT}\right) \quad (9.9)$$

$Z_{\text{het}}$  denotes the collision frequency of reactant molecules upon the electrode surface, which is often estimated by kinetic molecular theory, as given in eq.(5).

$$Z_{\text{het}} = \left(\frac{k_B T}{2\pi m}\right)^{1/2} \quad (9.10)$$

$k_B$  is the Boltzmann constant and  $m$  is the reduced mass of the reactant.

After substituting the  $Z_{\text{het}}$  term into equation (9.9) one can get,

$$\frac{k_{\text{het}}}{T^{1/2}} = \left(\frac{k_B}{2\pi m}\right)^{1/2} \exp\left(\frac{-\Delta G^*}{RT}\right) \quad (9.11)$$

By rewriting equation (9.11)

$$\ln \frac{k_{\text{het}}}{T^{1/2}} = \left(\frac{k_B}{2\pi m}\right)^{1/2} - \frac{\Delta G^*}{RT} \quad (9.12)$$

Activation energy can thus easily be determined by plotting  $\ln k_{\text{het}} \cdot T^{-1/2}$  against inverse of temperature.

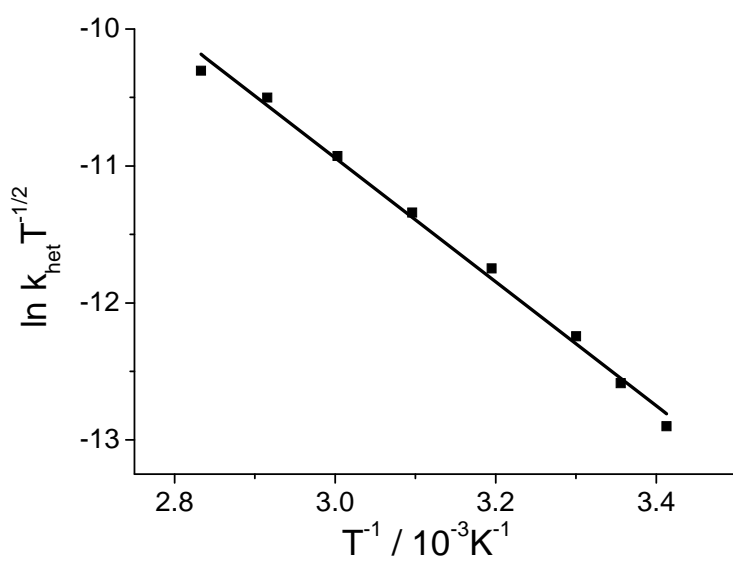
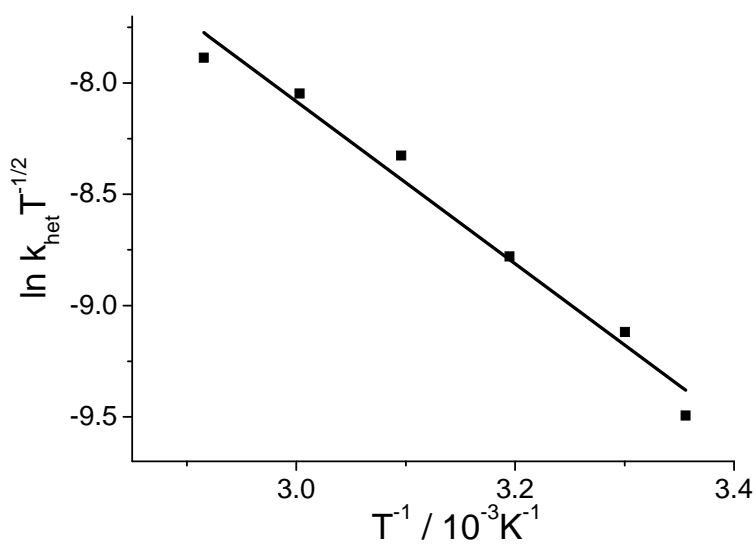
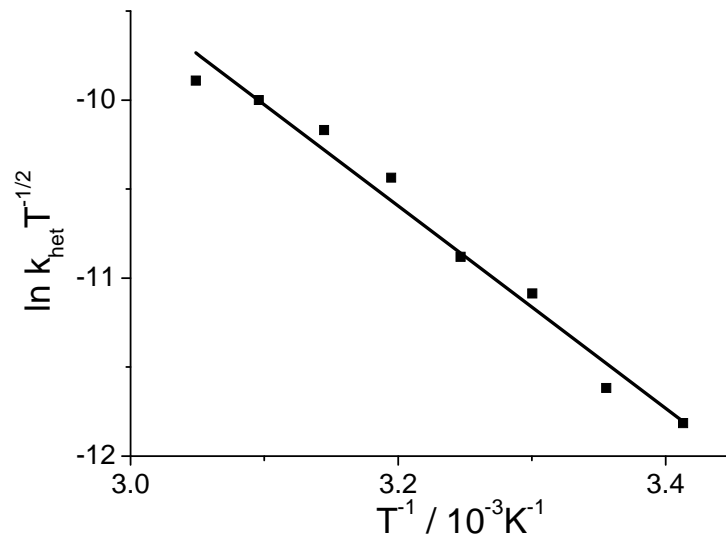
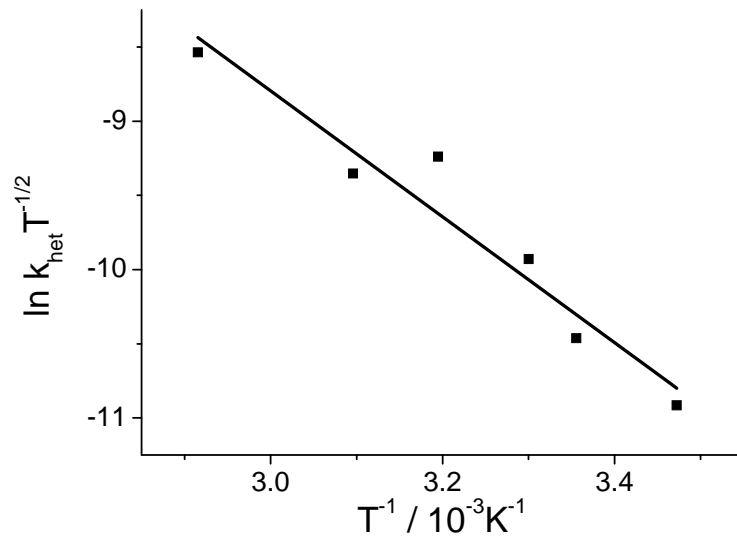
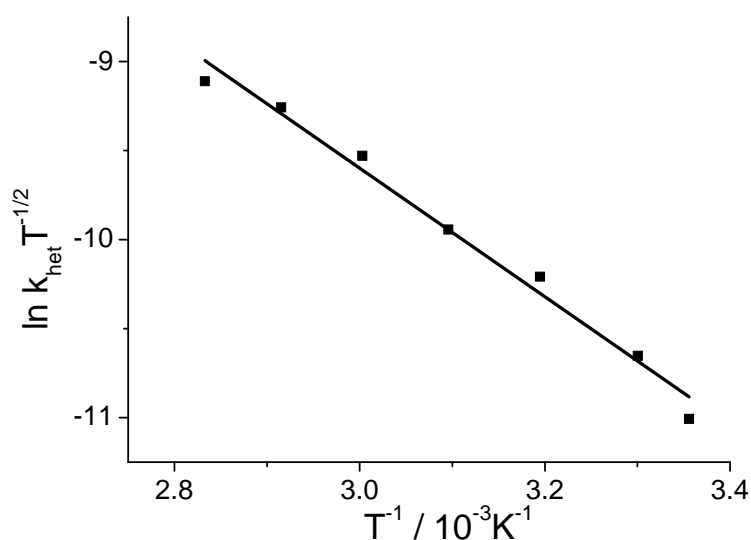
Figure 9.19 TCBQ in [emim][BF<sub>4</sub>]

Figure 9.20 TEMPO in [bmim][OTf]



Figure 9.21  $\text{MV}^{2+}$  in  $[\text{bmim}][\text{BF}_4]$ Figure 9.22 TBBQ in  $[\text{bmim}][\text{PF}_6]$

Figure 9.23 TTF in [omim][BF<sub>4</sub>]

Straight lines have been obtained by plotting  $\ln k_{\text{het}} T^{-1/2}$  against  $1/T$  for all compounds in all of the five different ILs. Activation energies have been determined from the slope of these plot by using Marcus equation (9.12)

Table 9.3 Activation energies,  $\Delta G^*$  (kJ mol<sup>-1</sup>) for reduction couples in different cationic ILs with the same anion.

Acceptor System	[emim][BF <sub>4</sub> ]	[bmim][BF <sub>4</sub> ]	[omim][BF <sub>4</sub> ]
MBQ	32.14	45.42	
TBBQ	44.09	39.01	
TCBQ	38.96	27.33	19.27
2,5-DMBQ		22.91	
2,6-DMBQ	28.88		
DQ	34.57	36.19	33.18
TCNE		25.30	35.39
MV <sup>2+</sup>	33.55	35.97	
EV <sup>2+</sup>		24.47	

The methyl derivatives of quinones show an increase of activation energy as the alkyl chain length of ILs is increasing. It can be explained that greater amount of energy is

required because of the slow diffusion in the more viscous medium. The activation energy of viscosity is also increasing. A totally reversed behaviour has been observed for the bromanil and chloranil compounds. These compounds showing the greatest activation energy in [emim][BF<sub>4</sub>] which is less viscous. However the value of activation energy is smaller in the most viscous ILs i.e. [omim][BF<sub>4</sub>]. The different behaviour of bromanil and chloranil from all the other quinones may be explained with the presence of the heavy electronegative atoms bromine and chlorine in bromanil and chloranil respectively in comparison to methyl group.

Imidazolium rings in ILs can form hydrogen bonds and different other interactions have also been discussed by Strehmel<sup>19,20</sup>. It has been reported that the hydrogen bonding is weaker as the size of alkyl chain increases in the ILs<sup>20</sup>. Hence hydrogen bonding is stronger in [emim][BF<sub>4</sub>] as compared with [bmim][BF<sub>4</sub>] and [omim][BF<sub>4</sub>] because of the less steric effect (small radius<sup>21</sup> of emim (0.303 nm) as compared to bmim (0.330 nm<sup>21</sup> and 0.357 nm<sup>22</sup>) and omim (0.373 nm<sup>21</sup>)).

Table 9.4 Activation energies,  $\Delta G^*$  (kJmol<sup>-1</sup>) for oxidation couples in different cationic ILs while anion is same

Donor Systems	[emim][BF <sub>4</sub> ]	[bmim][BF <sub>4</sub> ]	[omim][BF <sub>4</sub> ]
PPD		34.72	31.32
TMPPD	10.43	23.61	64.74
TTF	26.56		30.01
TEMPO	23.52	26.10	39.27
TEMPOL	22.52	44.53	38.32

The remaining acceptor systems other than the quinones and the donor systems in the ionic liquids with the same anionic part but different alkyl chain in the cationic moiety show that the activation energies are increasing with the activation energy of the viscosity of RTILs.

All reduction and oxidation couples have been studied in those ionic liquids where cationic moiety is same but anions are different. In all quinones except bromanil and chloranil, the values of activation energies are higher in [bmim][PF<sub>6</sub>] as compared to

[bmim][BF<sub>4</sub>]. The different behaviour of [bmim][OTf] can be suggested by its dipole moment which is 4.1808<sup>23</sup>, while others anion does not have dipole moment. However all the other compounds are showing random value of activation energy.

No trend of viscosity, radius of anion (  $r^-$  [BF<sub>4</sub>] = 2.29 Å,  $r^-$  [PF<sub>6</sub>] = 2.72 Å<sup>24</sup>), and  $\beta$  values (hydrogen bond accepting values ) ([OTf] = 0.57, [BF<sub>4</sub>] = 0.55 and [PF<sub>6</sub>] = 0.44) can help to explain the situation.

Table 9.5 Activation energies,  $\Delta G^*$  (kJ mol<sup>-1</sup>) for reduction couples in different anionic ILs while the cations is the same

Acceptor Systems	[bmim][OTf]	[bmim][BF <sub>4</sub> ]	[bmim][PF <sub>6</sub> ]
MBQ	21.26	45.42	44.04
TBBQ	36.79	39.01	36.59
TCBQ	35.26	27.33	33.13
2,5-DMBQ		22.91	39.01
2,6-DMBQ		20.59	31.32
DQ	23.34	36.19	40.27
TCNE		25.30	21.43
MV <sup>2+</sup>		35.97	24.27
EV <sup>2+</sup>		24.47	26.42

Table 9.6 Activation energies,  $\Delta G^*$  (kJ mol<sup>-1</sup>) for oxidation couples in different anionic ILs while the cation is the same

Donor Systems	[bmim][OTf]	[bmim][BF <sub>4</sub> ]	[bmim][PF <sub>6</sub> ]
PPD		34.72	53.18
TMPPD	17.49	23.61	46.48
TEMPO	31.66	26.10	32.75
TEMPOL	24.90	44.53	54.38

Solvatochromic polarity parameter has also been published for most of these ionic liquids which has been studied here. But these results can not be explained by these parameters.

Table 9.7 Solvatochromic polarity parameters of Ionic Liquids

RTILs	ET(30) / kcal mol <sup>-1</sup>	$\pi^*$	$\alpha$
emimBF <sub>4</sub> <sup>25</sup>	53.5	-	-
bmimOTf <sup>26</sup>	51.7	1.01	0.597
bmimBF <sub>4</sub> <sup>26</sup>	52.5	1.04	0.610
bmimPF <sub>6</sub> <sup>26</sup>	52.4	1.02	0.636

## 9.5 Co-relation with Radius

By rewriting eq (9.9) into logarithmic form, one gets

$$\ln\left(\frac{Z_{\text{het}}}{k_{\text{het}}}\right) = \frac{\Delta G^*}{RT} \quad (9.13)$$

The free energy of activation  $\Delta G^*$  is related to the reorganization parameter  $\lambda_i$  and  $\lambda_o$ , neglecting the resonance energy gap

$$\Delta G^* = \frac{\lambda_i + \lambda_o}{4} \quad (9.14)$$

$\lambda_i$  is the inner sphere reorganization energy and  $\lambda_o$  is the outer sphere reorganization energy

After substituting reorganization terms in the above equation one obtains

$$4RT \ln\left(\frac{Z_{\text{het}}}{k_{\text{het}}}\right) - \lambda_i = \frac{e_o^2 \cdot N_L}{8 \cdot \pi \cdot \epsilon_o} \left(\frac{1}{r} - \frac{1}{d_{\text{het}}}\right) \cdot \left(\frac{1}{n^2} - \frac{1}{\epsilon_s}\right) \quad (9.15)$$

Assuming that  $d_{\text{het}}$  is infinity (Hush model), then this suggests that  $4RT \ln(Z_{\text{het}}/k_{\text{het}}) - \lambda_i$  should be a linear function of  $1/r$  in an ionic liquid at constant temperature, because the Pekar factor is also not changing. In the case of Marcus a similar linearity is expected but only half the slope of the Hush slope. Such behavior has not been found in ILs, which is in contrast to classical organic solvents<sup>27</sup>.

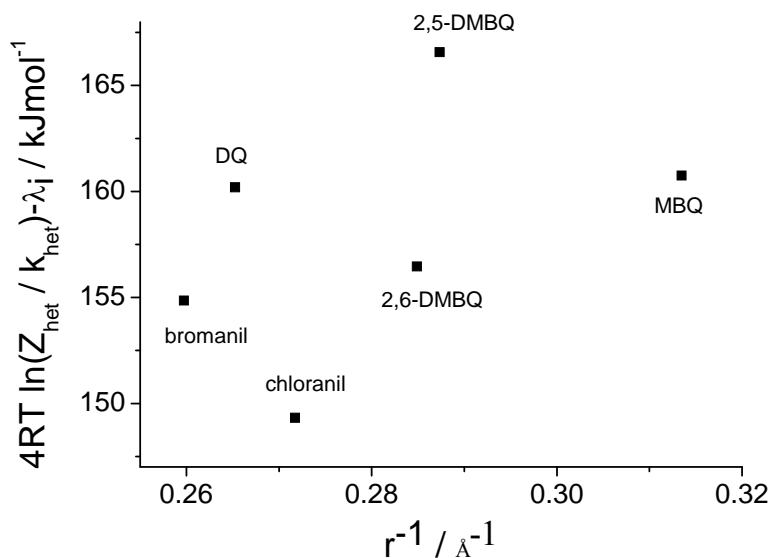


Figure 9.24 Quinones derivative at 298 K in [bmim][PF<sub>6</sub>]

The expected linearity has been drawn here using theoretical values of outer sphere reorganization energies by Hush model using ellipsoidal radius.

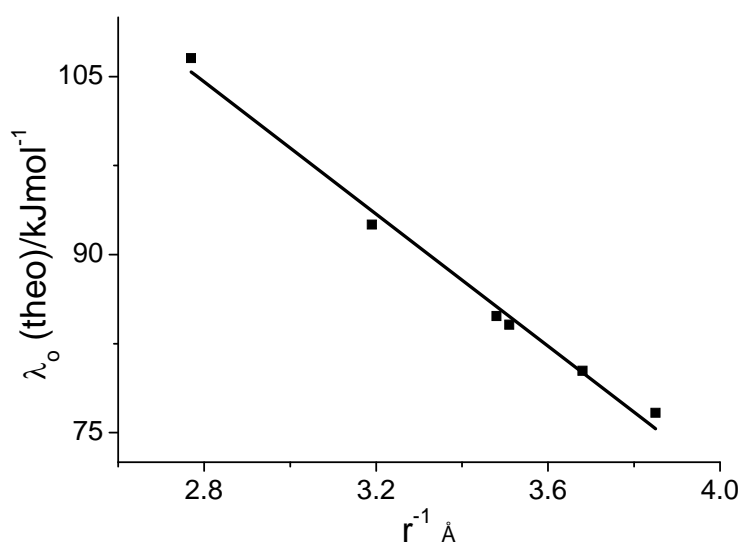


Figure 9.25 Quinone derivatives in [emim][BF<sub>4</sub>] (theoretical)

## 9.6 Temperature Dependent Measurement in Undried ILs

The water content strongly affects the electrochemical reaction in ionic liquids. It affects the interaction between the used compounds and the ionic liquids.

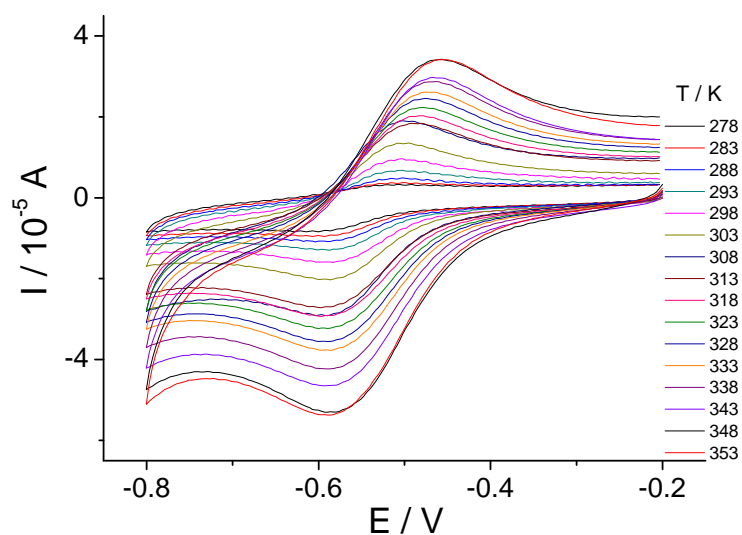


Figure 9.26  $MV^{2+}$  in undried  $[bmim][OTf]$

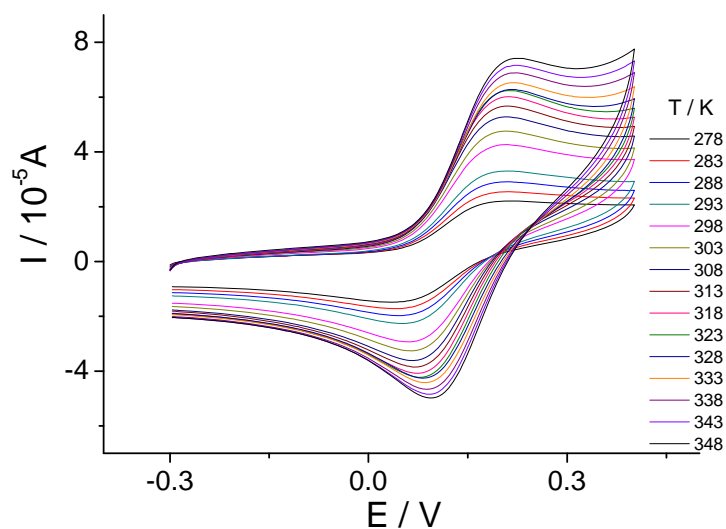


Figure 9.27 Duro TMPPD in undried  $[emim][BF_4]$

Diffusion coefficients and heterogeneous electron transfer rate constant have been calculated by using the same method as described for dried ILs. When diffusion

coefficients have been plotted versus the temperature, two different linear behaviors has been observed.

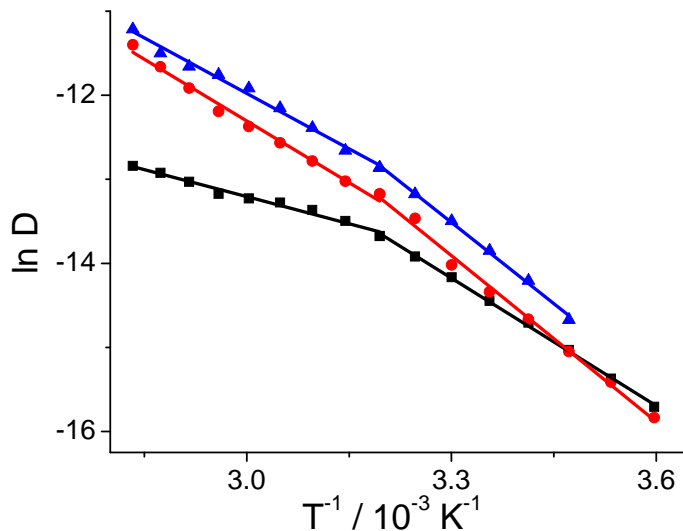


Figure 9.28 Duro-PPD in undried ■ [emim][BF<sub>4</sub>], ● [bmim][OTf], ▲ [bmim][PF<sub>6</sub>]

These two lines are intersecting at 313 K. The similar behaviour has also been observed for the heterogeneous electron transfer rate constants.

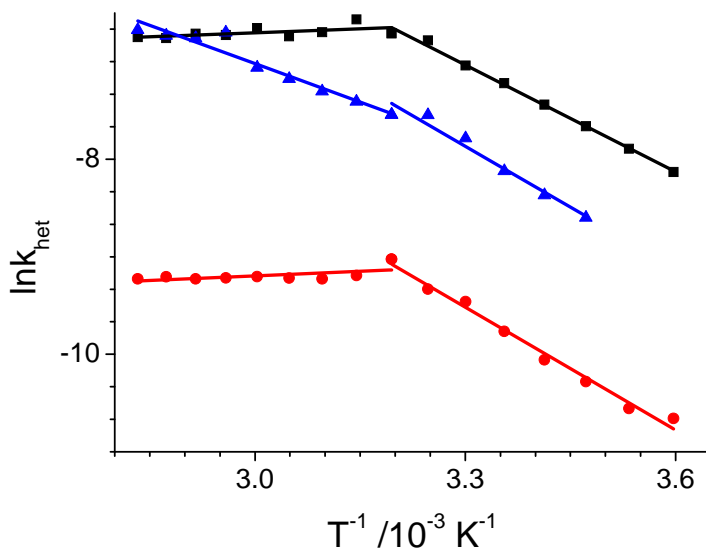


Figure 9.29 Ferrocene in undried ■ [emim][BF<sub>4</sub>], ● [bmim][OTf], ▲ [bmim][PF<sub>6</sub>]

There are two different slopes, leading to two different values for the activation energies.  $\Delta G_{ks1}$  is the activation energy for first slope which is from 278 K to 313 K and



$\Delta G_{ks2}$  for above 313 K.  $\Delta G_{D1}$  is the activation energies for diffusion from 278 K to upto 313 K and  $\Delta G_{D2}$  has been obtained from the slope above 313 K.

**Table 9.8 Activation energies (kJmol<sup>-1</sup>) in undried ionic liquids**

compounds	ILs	$\Delta G_{ks1}$	$\Delta G_{ks2}$	$\Delta G_{D1}$	$\Delta G_{D2}$
Bromanil	[emim]BF <sub>4</sub>	21.31	14.62	39.38	16.47
	[[bmim]][OTf]	20.82	13.57	35.03	
	[bmim][PF <sub>6</sub> ]	29.36	18.13	60.91	37.03
Chloranil	[emim]BF <sub>4</sub>	27.18	14.49	41.09	23.06
	[[bmim]][OTf]	16.03	37.56	44.72	24.88
	[bmim][PF <sub>6</sub> ]	47.36	56.01	74.28	30.92
MV <sup>2+</sup>	[emim]BF <sub>4</sub>	19.35	10.55	40.84	37.72
	[[bmim]][OTf]	29.17		75.45	36.24
	[bmim][PF <sub>6</sub> ]	23.85	36.33	44.60	80.19
Fc	[emim]BF <sub>4</sub>	30.38		42.04	15.01
	[[bmim]][OTf]	34.94		67.74	25.13
	[bmim][PF <sub>6</sub> ]	39.63	20.56	62.02	47.15
PPD	[emim]BF <sub>4</sub>	20.97	24.79	33.00	30.17
	[[bmim]][OTf]	29.85	19.55	27.72	39.09
	[bmim][PF <sub>6</sub> ]	31.14	28.49	46.16	42.44
TMPPD	[emim]BF <sub>4</sub>	17.19	26.37	27.13	12.96
	[[bmim]][OTf]			49.17	23.04
	[bmim][PF <sub>6</sub> ]	31.86		72.06	47.36
Duro-PPD	[emim]BF <sub>4</sub>	26.10	12.30	42.04	17.89
	[[bmim]][OTf]	15.64		54.71	40.19
	[bmim][PF <sub>6</sub> ]	49.01	61.09	46.16	42.44
TTF	[emim]BF <sub>4</sub>	23.10	12.15	49.86	30.33
	[[bmim]][OTf]	13.03		39.66	21.97
	[bmim][PF <sub>6</sub> ]	25.65	54.67	45.05	47.69

Such a behavior in ionic liquids has been observed earlier by Wang et al.<sup>28-29</sup>. They reported that this is due to some phase transition. This is not the correct argument. If any phase transition is going on in ILs then one can also observe the same behaviour in dried ILs. We can suggest here that these changing in slope are due to the presence of water which is forming hydrogen bond with ionic liquids or if possible then with compounds. Due to the presence of hydrogen bond, initially the activation energy is high but after 313 K it drops due to the weakness of the hydrogen bonds.

On comparison of temperature dependent results obtained in dried and undried ionic liquids, it has been observed that value of diffusion coefficient is higher in dried as compare to the undried ionic liquids which is also true for heterogeneous electron transfer reaction. See Figure 9.30

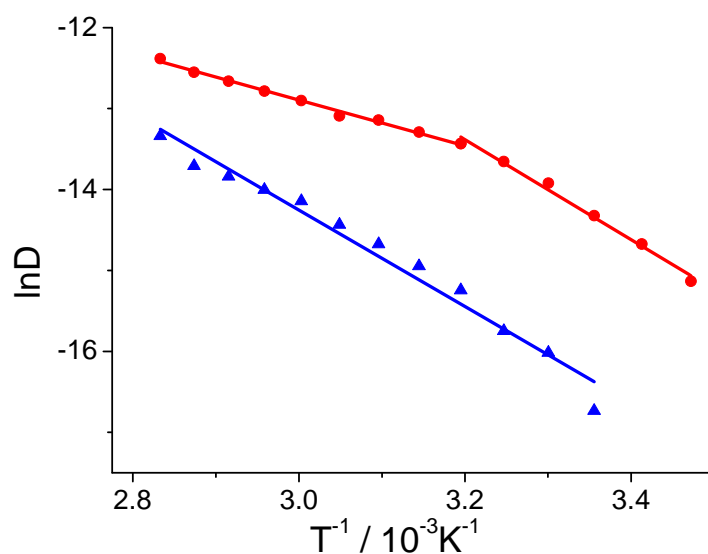


Figure 9.30  $E_{V^{+2}}$  in (●) undried and (▲) dried [bmim][BF<sub>4</sub>]

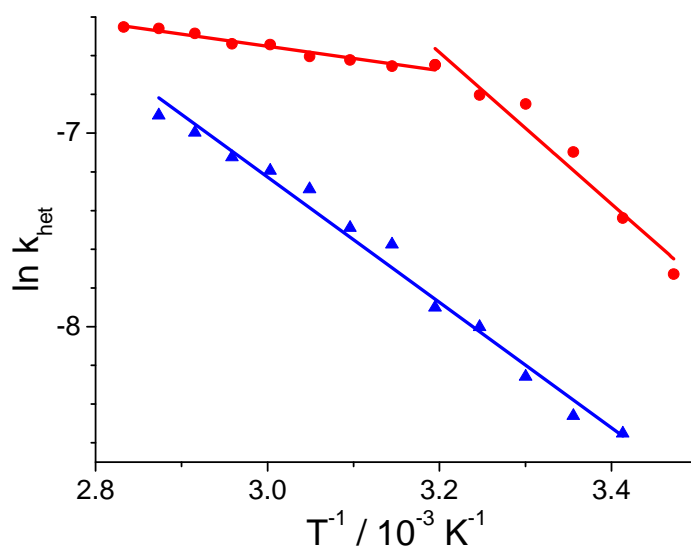


Figure 8.30  $\text{EV}^{2+}$  in (●) undried and (▲) dried [bmim][ $\text{BF}_4$ ]

The measurements above 313K contain water molecule, but the weaker hydrogen bond means water impurity is still in the solution. That is why when the plot of diffusion coefficients versus inverse of temperature in both dried and undried ionic liquids has been compared then it has been observed that in dried ionic liquids values of diffusion coefficients are higher because of the high viscosity of the dried ionic liquids as compare to the undried ionic liquid.

A similar behavior has been observed for the heterogeneous electron transfer rate constant.

1. Huang, X. J.; Rogers, E. I.; Hardacre, C.; Compton, R. G. The Reduction of Oxygen in Various Room Temperature Ionic Liquids in the Temperature Range 293-318 K: Exploring the Applicability of the Stokes-Einstein Relationship in Room Temperature Ionic Liquids. *J. Phys. Chem. B* **2009**, *113*, 8953-8959.

2. Long, J. S.; Silvester, D. S.; Barnes, A. S.; Rees, N. V.; Aldous, L.; Hardacre, C.; Compton, R. G. Oxidation of Several P-Phenylenediamines in Room Temperature Ionic Liquids: Estimation of Transport and Electrode Kinetic Parameters. *J. Phys. Chem. C* **2008**, *112*, 6993-7000.

3. Soriano, A. N.; Doma, B. T., Jr.; Li, M.-H. Density and Refractive Index Measurements of 1-Ethyl-3-Methylimidazolium-Based Ionic Liquids. *J. Taiwan Inst. Chem. Eng.* **2010**, *41*, 115-121.

4. Soriano, A. N.; Doma, B. T.; Li, M.-H. Measurements of the Density and Refractive Index for 1-N-Butyl-3-Methylimidazolium-Based Ionic Liquids. *J. Chem. Thermodyn.* **2009**, *41*, 301-307.
5. Soriano, A. N.; Doma Jr, B. T.; Li, M. H. Measurements of the Density and Refractive Index for 1-N-Butyl-3-Methylimidazolium-Based Ionic Liquids. *J. Chem. Thermodyn.* **2009**, *41*, 301-307.
6. Tariq, M.; Forte, P. A. S.; Gomes, M. F. C.; Lopes, J. N. C.; Rebelo, L. P. N. Densities and Refractive Indices of Imidazolium- and Phosphonium-Based Ionic Liquids: Effect of Temperature, Alkyl Chain Length, and Anion. *J. Chem. Thermodyn.* **2009**, *41*, 790-798.
7. Hunger, J.; Stoppa, A.; Schroedle, S.; Hefter, G.; Buchner, R. Temperature Dependence of the Dielectric Properties and Dynamics of Ionic Liquids. *ChemPhysChem* **2009**, *10*, 723-733.
8. Ohno, K. *Electrochemical Aspects of Ionic Liquids*, 2004.
9. Jacquemin, J.; Husson, P.; Padua, A. A. H.; Majer, V. Density and Viscosity of Several Pure and Water-Saturated Ionic Liquids. *Green Chem.* **2006**, *8*, 172-180.
10. Ghatee, M. H.; Zare, M.; Zolghadr, A. R.; Moosavi, F. Temperature Dependence of Viscosity and Relation with the Surface Tension of Ionic Liquids. *Fluid Phase Equilibria* **2010**, *291*, 188-194.
11. Strehmel, V.; Laschewsky, A.; Stoesser, R.; Zehl, A.; Herrmann, W. Mobility of Spin Probes in Ionic Liquids. *Journal of Physical Organic Chemistry* **2006**, *19*, 318-325.
12. Wachter, P.; Zistler, M.; Schreiner, C.; Fleischmann, M.; Gerhard, D.; Wasserscheid, P.; Barthel, J.; Gores, H. J. Temperature Dependence of the Non-Stokesian Charge Transport in Binary Blends of Ionic Liquids. *Journal of Chemical and Engineering Data* **2009**, *54*, 491-497.
13. Köddermann, T.; Ludwig, R.; Paschek, D. On the Validity of Stokes-Einstein and Stokes-Einstein-Debye Relations in Ionic Liquids and Ionic-Liquid Mixtures. *ChemPhysChem* **2008**, *9*, 1851-1858.
14. Ito, N.; Richert, R. Solvation Dynamics and Electric Field Relaxation in an Imidazolium-Pf<sub>6</sub> Ionic Liquid: From Room Temperature to the Glass Transition. *J. Phys. Chem. B* **2007**, *111*, 5016-5022.
15. Rogers, E. I.; Silvester, D. S.; Poole, D. L.; Aldous, L.; Hardacre, C.; Compton, R. G. Voltammetric Characterization of the Ferrocene|Ferrocenium and Cobaltocenium|Cobaltocene Redox Couples in Rtils. *J. Phys. Chem. C* **2008**, *112*, 2729-2735.
16. Nicholson, R. S. Theory and Application of Cyclic Voltammetry for Measurement of Electrode Reaction Kinetics. *Anal. Chem.* **1965**, *37*, 1351-1355.
17. Rüssel, C., University of Erlangen, 1984.
18. Schmitz, J. E. J.; Van der Linden, J. G. M. Temperature-Dependent Determination of the Standard Heterogeneous Rate Constant with Cyclic Voltammetry. *Anal. Chem.* **1982**, *54*, 1879-1880.
19. Strehmel, V.; Rexhausen, H.; Strauch, P.; Görnitz, E.; Strehmel, B. Temperature Dependence of Interactions between Stable Piperidine-1-Yloxy Derivatives and an Ionic Liquid. *ChemPhysChem* **2008**, *9*, 1294-1302.
20. Dong, K.; Zhang, S.; Wang, D.; Yao, X. Hydrogen Bonds in Imidazolium Ionic Liquids. *J. Phys. Chem. A* **2006**, *110*, 9775-9782.
21. Tokuda, H.; Hayamizu, K.; Ishii, K.; Susan, M. A. B. H.; Watanabe, M. Physicochemical Properties and Structures of Room Temperature Ionic Liquids. 2.

Variation of Alkyl Chain Length in Imidazolium Cation. *J. Phys. Chem. B* **2005**, *109*, 6103-6110.

22. Arzhantsev, S.; Jin, H.; Baker, G. A.; Maroncelli, M. Measurements of the Complete Solvation Response in Ionic Liquids. *J. Phys. Chem. B* **2007**, *111*, 4978-4989.

23. Liu, X.; Zhang, S.; Zhou, G.; Wu, G.; Yuan, X.; Yao, X. New Force Field for Molecular Simulation of Guanidinium-Based Ionic Liquids. *J. Phys. Chem. B* **2006**, *110*, 12062-12071.

24. Arzhantsev, S.; Jin, H.; Baker, G. A.; Maroncelli, M. Measurements of the Complete Solvation Response in Ionic Liquids†. *The Journal of Physical Chemistry B* **2007**, *111*, 4978-4989.

25. Santhosh, K.; Banerjee, S.; Rangaraj, N.; Samanta, A. Fluorescence Response of 4-(N,N'-Dimethylamino)Benzonitrile in Room Temperature Ionic Liquids: Observation of Photobleaching under Mild Excitation Condition and Multiphoton Confocal Microscopic Study of the Fluorescence Recovery Dynamics. *J. Phys. Chem. B* **2010**, *114*, 1967-1974.

26. Tokuda, H.; Tsuzuki, S.; Susan, M. A. B. H.; Hayamizu, K.; Watanabe, M. How Ionic Are Room-Temperature Ionic Liquids? An Indicator of the Physicochemical Properties. *J. Phys. Chem. B* **2006**, *110*, 19593-19600.

27. Grampp, G. Homogeneous Electron-Self Exchange Kinetics of 1,4-Diazine Couples. *Z. Phys. Chem. (Munich)* **1986**, *148*, 53-63.

28. Huang, J. F.; Chen, P. Y.; Sun, I. W.; Wang, S. P. Nmr Evidence of Hydrogen Bond in 1-Ethyl-3-Methylimidazolium-Tetrafluoroborate Room Temperature Ionic Liquid. *Spectroscopy Letters* **2001**, *34*, 591-603.

29. Huang, J. F.; Chen, P. Y.; Sun, I. W.; Wang, S. P. Nmr Evidence of Hydrogen Bonding in 1-Ethyl-3-Methylimidazolium-Tetrafluoroborate Room Temperature Ionic Liquid. *Inorganica Chimica Acta* **2001**, *320*, 7-11.

## CHAPTER 10 CONCLUSIONS

Room temperature ionic liquids (RTILs) are used as electrochemical solvents. Five different RTILs. i.e. [emim][BF<sub>4</sub>], [bmim][OTf], [bmim][BF<sub>4</sub>], [bmim][PF<sub>6</sub>] and [omim][BF<sub>4</sub>] were used in this study. The effect of viscosity on heterogeneous electron transfer reaction and also the effect of different anions and cations in ionic liquids were studied. Cyclic voltammetric experiments were without adding any supporting electrolyte.

Impurities in ionic liquids have been taken into consideration because it affects many physicochemical properties of ionic liquids. Hence, before doing any experiments, the purity of ionic liquids was checked by performing experiments. The water contents were removed by placing ionic liquids under high vacuum ( $5 \times 10^{-5}$  torr) for one day at a constant temperature of 313-323 K. To become confident about the removal of moisture impurities, NIR spectra were recorded for ionic liquids which proved that the ionic liquids were almost dried after placing it to under high vacuum for one day. It was kept in desiccators containing P<sub>4</sub>O<sub>10</sub> to avoid moisture contact with ionic liquids. But it is impossible to remove moisture impurity completely so the ionic liquids were dried every two weeks.

Nine acceptors and six donors systems were studied pertaining to their electrochemical kinetic behaviour in all five different room temperature ionic liquids. Six different derivatives of quinones (four methyl derivatives, MBQ, 2,5-DMBQ, 2,6-DMBQ, and DQ and two halide derivatives such as TBBQ and TCBQ), two viologens (MV<sup>2+</sup> and EV<sup>2+</sup>), and TCNE were studied in ionic liquids as acceptor systems. While as donor systems PPD itself and its derivative TMPPD, TTF, TEMPO and its derivative TEMPOL were used. These systems were selected because of the availability of the data in various organic solvent in different electrolyte. These data were used to compare with the results obtained in ionic liquids.

Cyclic voltammetric experiments were performed at different scan rates to get the value of diffusion coefficients and heterogeneous electron transfer rate constant. All of the donors and acceptor system showed reversible or quasireversible behavior in all five

room temperature ionic liquids. One of the novel things of this work was to design a small electrochemical cell for ionic liquids to avoid the use of larger volume of ionic liquids. This task was achieved by constructing an electrochemical cell consisting of a three electrode assembly and needing only a small amount of solution. The idea of this cell was taken from Compton, but that cell has only a two electrodes arrangements. One can do electrochemical measurements with 0.2 ml of ionic liquids by using this home made special cell. It is essential to place the working electrode in very close proximity to the reference electrode to minimize the  $iR$  drop. That point was taken into consideration during the construction of cell. The quality of the cell in terms of  $iR$  drop was proved by three independent measurements. First, various concentrations of the  $Fc/Fc^+$ -couple were studied and no remarkable change is found in the difference of the peak potentials. Secondly, the  $iR$ -drop was calculated according to a well known relation given in the paper of Oelssner<sup>1</sup> and finally, the uncompensated resistance were measured by recording Bode-plots. The results of all these measurements indicate clearly that the  $iR$ -drop is negligible for the cell construction used.

The results which were obtained for diffusion coefficients and heterogeneous electron transfer rate constants in ionic liquids are compared with the results of conventional organic solvents. It was found that the values of diffusion coefficients are lower by two or three orders of magnitude in ionic liquids as compared to organic solvents. This is because of the high viscosity of the ionic liquids. The diffusion coefficient is inversely proportional to the viscosity of the ionic liquids where anions are constant and only changes of the cation in alkyl chain. Such a Stokes Einstein behaviour was not observed for those ionic liquids where anion are changing while the cations kept constant in all investigated molecule. Some redox systems are not following this behaviour and this is due to the different interaction of the molecules with the different anions of the ionic liquids. Generally it was observed that the diffusion coefficients in  $[bmim][PF_6]$  are lower than the  $[bmimBF_4]$  as the viscosity of  $[bmim][PF_6]$  is higher for  $[bmim][BF_4]$ .  $[bmim][OTf]$  is deviating with this behaviour because only this anion has a dipole moment. The heterogeneous electron transfer rate constants in ionic liquids also show smaller values as compared to organic solvents.

The corresponding rate constants were also investigated in a binary mixture of ionic liquid and acetonitrile. The values of the diffusion coefficients decrease as the content

of ionic liquid increase because the viscosity of the binary mixture increases. The heterogeneous electron transfer rate constants showed a similar trend.

Not only room temperature measurements were done, but also temperature dependent measurements were carried out to get the corresponding values of activation energies. These measurements were done in a different electrochemical cell which was constructed to keep the temperature constant of the analyzing system and it was first designed in our lab. Only a small volume of solution is needed to perform electrochemical measurements. This cell construction is similar to the one for room temperature measurements, but there was an additional line for a water flow which was connected to a thermostat. The  $iR$  drop is also negligible in this cell. The accuracy of the temperature of the solution was in the range of  $\pm 1-2$  K.

The viscosity of ionic liquids is very challenging property. The Vogel-Fulcher-Tamman equation was used to fit the viscosity data at different temperatures. The activation energy of viscosity was determined from the slope of a plot of  $\ln \eta$  versus  $1/T$ . Not only viscosity but also other physicochemical properties were considered at different temperature such as refractive index, and dielectric constant. The values of diffusion coefficients were determined at each temperature. They increase with temperature because the viscosity of the ionic liquids decreases. The plots of  $\ln D$  versus  $1/T$  are linear. Heterogeneous electron transfer rate constants were also investigated at different temperatures. The corresponding values of activation energies are determined from plots of  $\ln k_{\text{het}} T^{-1/2}$  against  $1/T$ .

Temperature dependent measurements were also done in undried ionic liquids. The same calculation was done for diffusion coefficients and heterogeneous electron transfer rate constant. Plots of  $\ln D$  versus  $1/T$  showed two different linear slopes with an intersection at around 313 K. Not surprisingly, this was due to the presence of moisture. The water is involved to form hydrogen bonds with the ionic liquids and above 313 K the strength of these hydrogen bonds became weak. Due to the formation of hydrogen bonds two different linear behaviours were observed. The same trend was also found for undried ionic liquids when plotting  $\ln k_{\text{het}}$  against  $1/T$  using Marcus equation. This behaviour gave two different values of activation energies for the heterogeneous electron transfer reaction. The values of diffusion coefficients and heterogeneous



electron transfer rate constants in undried ionic liquids are smaller than the ones which have been found in dried ionic liquids. This is due to moisture which decreases the viscosity of the ionic liquids.

Quantum mechanical calculations were carried out to determine the values of the inner sphere reorganization energies, according to the method given by Nelsen. All the geometries were visualized before and after electron transfer through the Molden program. ORCA-software was employed for all DFT calculations. A TZVPP with B3LYP basis set was used. The values obtained for the ionization potentials and electron affinities are in good agreement with published data. A temperature correction for the inner reorganization energies was made using Holstein equation. It is difficult to compare the inner sphere reorganization energies values with literature because  $\lambda_i$  was determined by many different methods in literature and some time temperature correction were not taken into account. The values calculated for inner sphere reorganization energies are not comparable with the literature values because different methods were used in literature.

Theoretical calculations of the outer sphere reorganization energy were also done by considering two models for  $d_{\text{het}}$ , the Marcus-model and Hush-model. According to Marcus  $d_{\text{het}}$  should be equal to  $2r$  and in the eyes of Hush,  $d_{\text{het}}$  is taken as infinity. Simply the value for outer sphere reorganization energies obtained by using Marcus equation is half of the value obtained by using Hush approximation. Two different models for the radius (ellipsoidal and spherical) were also taken into account. Interestingly, the results obtained from theoretical calculation of  $\lambda_o$  are not comparable with experimental results. This suggested that the Marcus equation for outer sphere reorganization energy is not applicable for ionic liquids.

No correlation was found when  $1/r$  was plotted against  $4RT\ln(Z_{\text{het}}/k_{\text{het}})-\lambda_i$  for the quinones at constant temperature in an certain ionic liquids. This is in contrast to results obtained in classical organic solvents. This is also an indicates of the failure of the classical Marcus outer sphere reorganization energy concept.

In conclusion, the rates of electron transfer in ionic liquids are slower compared with results obtained in organic solvents because of the slow mass transport in the higher viscous media. Different ionic interactions are present in these media. The Marcus

concept of dielectric polarization of the solvent is not valid for ionic liquids, so the use of dielectric properties for outer sphere reorganization energies calculations is not appropriate.

1. Oelssner, W.; Berthold, F.; Guth, U. The Ir Drop - Well-Known but Often Underestimated in Electrochemical Polarization Measurements and Corrosion Testing. *Mater. Corros.* **2006**, *57*, 455-466.